A Finite Volume Approach for the Numerical Analysis and Solution of the Buckley-Leverett Equation Including Capillary Pressure

by

© Pulok Kanti Deb

A Thesis

submitted to the School of Graduate Studies

in partial fulfillment of the requirements for the degree of

Master of Engineering

Faculty of Engineering and Applied Science

Memorial University of Newfoundland

October 2018

St. John's Newfoundland

ABSTRACT

The study of petroleum recovery is significant for reservoir engineers. Mathematical models of the immiscible displacement process contain various assumptions and parameters, resulting in nonlinear governing equations which are tough to solve. The Buckley-Leverett equation is one such model, where controlling forces like gravity and capillary forces directly act on saturation profiles. These saturation profiles have important features during oil recovery.

In this thesis, the Buckley-Leverett equation is solved through a finite volume scheme, and capillary forces are considered during this calculation. The detailed derivation and calculation are also illustrated here. First, the method of characteristics is used to calculate the shock speed and characteristics curve behaviour of the Buckley-Leverett equation without capillary forces. After that, the local Lax-Friedrichs finite-volume scheme is applied to the governing equation (assuming there are no capillary and gravity forces). This mathematical formulation is used for the next calculation, where the cell-centred finite volume scheme is applied to the Buckley-Leverett equation including capillary forces. All calculations are performed in MATLAB. The fidelity is also checked when the finite-volume scheme is computed in the case where an analytical solution is known. Without capillary pressure, all numerical solutions are calculated using explicit methods and smaller time steps are used for stability. Later, the fixed-point iteration method is followed to enable the stability of the local Lax-Friedrichs and Cell-centred finite volume schemes using an implicit formulation. Here, we capture the number of iterations per time-steps (including maximum and average iterations per time-step) to get the solution of water saturation for a new time-step and obtain the saturation profile. The cumulative oil production is calculated for this study and illustrates capillary effects. The influence of viscosity ratio and permeability in capillary effects is also tested in this study.

Finally, we run a case study with valid field data and check every calculation to highlight that our proposed numerical schemes can capture capillary pressure effects by generating shock waves and providing single-valued saturation at each position. These saturation profiles help find the amount of water needed in an injection well to displace oil through a production well and obtains good recovery using the water flooding technique.

To my Mother & Late Father

Acknowledgements

First of all, I remember almighty God for his blessings and kindness to me for the successful completion of the thesis work.

I express my deep sense of gratitude to my supervisor Dr. Scott MacLachlan for teaching me mathematical applications along with computer applications and guiding me to find out my solutions. I also acknowledged his continuous and overall supervision, valuable suggestions, and providing all kinds of facilities and every possible help throughout the preparation of the thesis.

I convey my immense gratitude and respect to my supervisor Dr. Syed A. Imtiaz for his careful guidance, sincere advice, adequate encouragement and cordial co-operation to complete the thesis work successfully. He gave me the freedom to explore mathematical applications in petroleum engineering and helped me to keep going when the going got tough. I thank him for sending the manuscript of chapter 2 to a high-impact journal, broadening my horizon, and teaching me how to face the anonymous reviewer comments and address those comments in the manuscript before final publication.

I also thank Dr. M. Enamul Hossain, Former Statoil Chair in Reservoir Engineering at Memorial University of Newfoundland (MUN) for absorbing me in his research group and giving me the opportunity to pursue Masters of Engineering degree at Memorial University of Newfoundland.

I would like to thank Dr. Faisal Khan for departmental support, during his tenure and personal suggestions for improving my research skills at many times. I am also thankful to Dr. Lesley James for permitting me to use the simulation lab during my computational work.

Also, my special thanks go to all research mates for their kinds of cordial co-operation and encouragement during this research work. I thank Moya Crocker, Colleen Mahoney, and Tina Dwyer for creating a friendly and enabling atmosphere at the University and providing logistic support and co-operation during this thesis work.

I want to express my deepest sense of gratefulness and gratitude to my parents and my beloved wife “Ms. Joyshree Deb” for their moral support, and my close friends for making cordial help and possible support, at that time.

Finally, I would like to thank the School of Graduate Studies (SGS), Research and Development Corporation (RDC), and Statoil Research Grants for their generous financial support.

Co-Authorship Statement

I, Pulok Kanti Deb, hold primary author status for all the Chapters in this thesis. However, each manuscript is co-authored by my supervisor and co-researchers, whose contributions have facilitated the development of this work as described below:

- *Pulok Kanti Deb, Farhana Akter, Syed Ahmed Imtiaz, M. Enamul Hossain*, (2017), **"Nonlinearity and Solution Techniques in Reservoir Simulation: A Review"**. Journal of Natural Gas Science and Engineering, 46, pp. 845-864.

  Statement: I am the primary author and carried out the literature review and related documents. I drafted the manuscript and incorporated the comments of the co-authors, anonymous reviewers, and journal editors in the manuscript. Co-authors helped in conceiving the idea and writing strategy for a review article, through mentioning all the related information and research gaps.

- *Pulok Kanti Deb, Scott MacLachlan, Syed Ahmed Imtiaz, M. Enamul Hossain,* **"Finite Volume Solution of the Buckley-Leverett Equation".** Preparing for submission to a journal or conference.

  Statement: I am the primary author and carried out all calculations and related literature review. I drafted the manuscript and incorporated the comments of my respected supervisors. Co-authors helped in finding the right mathematical scheme and solution procedure, and with preparing the manuscript and data analysis.

- *Pulok Kanti Deb, Scott MacLachlan, Syed Ahmed Imtiaz, M. Enamul Hossain,* **"Finite Volume Solution of the Buckley-Leverett Equation including Capillary Pressure".** Preparing for submission to a journal or conference.

  Statement: I am the primary author and carried out all calculations and related literature review. I drafted the manuscript and incorporated the comments of my respected supervisors. Co-authors helped in finding the right mathematical scheme and solution procedure, and with preparing the manuscript and data analysis.

Table of Contents

Abstract ii

Acknowledgement iv

Table of Contents vii

List of Tables x

List of Figures xi

Chapter 1: Introduction 1

1.1 Motivation 1

1.2 Objective 2

1.3 Structure of the Thesis 2

Chapter 2: Nonlinearity and solution techniques in reservoir simulation: A review 6

2.1 Introduction 7

2.1.1 Background of the research 8

2.1.2 Technical challenges towards the research 9

2.1.3 Objectives of the research 9

2.2 Critical literature analysis 10

2.2.1 Effect of capillary pressure 11

2.2.2 Effect of memory 16

2.2.3 Effect of viscous fingering for miscible and immiscible displacement 19

2.2.4 Effect of fluid and media properties 20

2.2.5 Effect of time step size 23

2.2.6 Nonlinearity from the modelling of gas flow in reservoir 26

2.2.7 Nonlinearity in EOR applications 26

2.3 Outline of present simulator steps, challenges and solution techniques 27

2.3.1 Present simulator steps 27

2.3.2 Challenges of the present simulator steps 28

2.3.3 Solution techniques for nonlinear algebraic equations 29

2.3.3.1 Techniques for linear equations 29

2.3.3.2 Techniques for nonlinear equations 31

2.3.3.2.1 IMPES and SIM methods 31
2.3.3.2.2 Standard Newton's method 32
2.3.3.2.3 Newton's method with heuristic safeguards 33
2.3.3.2.4 Continuation Newton method 33
2.3.3.2.5 Ordering-based methods 34
2.3.3.2.5.1 Cascade method 35
2.3.3.2.5.2 Natvig's method 35
2.3.3.2.5.3 Phase-based potential ordering 36
2.3.3.2.6 Adomian Decomposition Method 36
2.3.3.2.7 Multilevel nonlinear method 37
2.3.3.2.8 Deflation-nested iteration method 38
2.3.3.2.9 Legendre method 39
2.3.4 Fundamental differences among widely used numerical methods 40
2.4 Discussion and future directions 41
2.5 Conclusions 43

Chapter 3: Finite Volume Solution of the Buckley-Leverett Equation 62
3.1 Introduction 62
3.1.1 Background of the research 63
3.1.2 Literature review 64
3.1.3 Objectives of the research 65
3.2 Research Methodology 65
3.3 Governing Equations 66
3.3.1 Correlation between fractional flow of water (f_w) and water saturation (S_w) 68
3.3.2 Analytical solution using the Method of Characteristics (MOC) 69
3.3.2.1 Determination of characteristic curve for the water saturation 69
3.3.2.2 Flux function of Buckley-Leverett's model equation 72
3.3.2.3 Shock speed calculation from Rankine-Hugoniot relation 74
3.3.3 Numerical solution using Local Lax-Friedrichs method 77
3.3.3.1 Consistency analysis 80
3.4 Results and discussions 81

3.5 Conclusion 87

Chapter 4: Finite Volume Solution of the Buckley-Leverett equation including Capillary Pressure 91

4.1 Introduction 91

4.2 Development of the Buckley-Leverett Equation including capillary pressure 92

4.3 Implicit Scheme using Fixed-Point Iteration 95

4.4 Oil Production Calculation 97

4.5 Results and discussion 98

4.5.1 Effects of Capillary Pressure 105

4.5.2 Impact of Oil Production 106

4.6 Validation of the proposed mathematical scheme 108

4.6.1 Impact of Oil Production 114

4.6.2 Effect by the Viscosity ratio and Permeability 115

4.7 Conclusion 118

Chapter 5: Conclusion 121

5.1 Conclusion 121

5.2 Future Directions 122

Appendix

Appendix - A 124

Appendix - B 127

List of Tables

Chapter 2

Table 2.1 : A few examples of nonlinear equations 10

Table 2.2 : A Critical analysis of different model equations from different researchers 12

Table 2.3 : A comparative and critical study on assumptions and limitations of different model equations 13

Table 2.4 : Summary of the linear equations solution techniques 30

Table 2.5 : Comparisons of different numerical techniques 39

Table 2.6 : Pros and cons of different numerical methods used for solving nonlinear equations 41

Chapter 3

Table 3.1 : Estimation of shock speed and breakthrough time 76

Chapter 4

Table 4.1 : Capillary pressure data 99

Table 4.2 : Capillary pressure data 109

List of Figures

Chapter 1

Figure 1.1 : Summary of the research 03

Chapter 2

Figure 2.1 : Importance of nonlinear solver 09

Figure 2.2 : Major steps of present reservoir simulators 27

Figure 2.3 : Future simulator steps for the reservoir simulation 27

Figure 2.4 : Future research scope in the reservoir simulation 42

Chapter 3

Figure 3.1 : Characteristics curves for the Buckley-Leverett equation for different constant initial and boundary conditions 70

Figure 3.2 : Conservations laws for the Buckley-Leverett equation 73

Figure 3.3 : Shock wave propagation diagram 74

Figure 3.4 : Fluid distributions at initial conditions at 10 days 76

Figure 3.5 : Finite volume discretisation 77

Figure 3.6 : Time-discretisation in finite volume methods 77

Figure 3.7 : Consistency check of the Buckley-Leverett equation 80

Figure 3.8 : Water-oil relative permeability curves 82

Figure 3.9 : The fractional water flow rate with the water saturation 83

Figure 3.10 : Breakthrough time calculation (No capillary) 83

Figure 3.11 : Numerical solution of the Buckley-Leverett equation using local Lax-Friedrichs finite volume method (No capillary) 84

Figure 3.12 : Saturation profile (3-D view) at different days (No capillary) 85

Figure 3.13 : Saturation profile (2-D view) at different days (No capillary) 86

Chapter 4

Figure 4.1 : Computational algorithm for solving the Buckley-Leverett equation using a Fixed-point iteration 96

Figure 4.2 : Variation of capillary pressure with respect to normalized water saturation 100

Figure 4.3 : Saturation profiles including capillary pressure 100

Figure 4.4	:	Breakthrough time calculation (with capillary)	101
Figure 4.5	:	Comparison of breakthrough time with water saturation	102
Figure 4.6	:	Saturation profiles at different days (with capillary)	102
Figure 4.7	:	Development of saturation profiles using fixed-point iteration scheme	103
Figure 4.8	:	Comparison of numerical solutions (with and without capillary) at $S_{wl} = 0.70$	105
Figure 4.9	:	Comparison of oil production (with and without capillary)	106
Figure 4.10	:	The fractional water flow rate with the water saturation	109
Figure 4.11	:	Saturation profiles during simple explicit-form	110
Figure 4.12	:	Saturation profiles during the local Lax-Friedrichs scheme	110
Figure 4.13	:	Saturation profiles during Cell-centered finite volume scheme	111
Figure 4.14		Comparison of breakthrough time with water saturation	111
Figure 4.15	:	Saturation profiles during the Fixed-Point Iteration	112
Figure 4.16	:	Comparison of saturation profiles with and without capillary pressure	113
Figure 4.17	:	Comparison of oil production (with and without capillary)	114
Figure 4.18	:	Effect on saturation profiles by changing the viscosity ratio	116
Figure 4.19	:	Effect on saturation profiles by changing the permeability	117

CHAPTER – 1

INTRODUCTION

1.1 Motivation

Petroleum industries play a vital role in the global economy. In 2016, the global petroleum and other liquid fuel consumption averaged 96.9 million barrels per day and the consumption is expected to increase by 1.5 million barrels per day in 2017 and 1.6 million barrels per day in 2018 (EIA, 2016). Due to high demands and meeting the economic challenges, researchers and engineers are working to increase production with lower costs and stable techniques. In terms of production, recovery is one of the major challenges, minimising all the complexities of the reservoir and reducing the inherent assumptions (Muggeridge et al., 2014). Reservoir simulation models can improve reservoir performance and enhance hydrocarbon recovery mechanisms (Deb et al., 2017). Several mathematical methods have been developed for handling nonlinear problems and to solve critical reservoir simulation models. In field applications, most models assume linearized conditions and ignore the inherent reservoir complexities (Crichlow, 1977; Aziz and Settari, 1979; and, Mustafiz and Islam, 2008; Hossain and Islam, 2010). As a result, mathematical models based on the theory behind fluid flow through porous media mislead the petroleum recovery efficiency. Only numerical solutions of the nonlinear governing equations in reservoir engineering are available to help us to understand, forecast, and manage subsurface fluid migration in a reservoir, especially in complex geometry and highly nonlinear multiphase fluid flow systems. Therefore, an advanced numerical tool is needed to predict the exact solution of a multivariable problem, and yield solutions that are realistic rather than impractical (Deb et al., 2017). Numerical methods discretise the governing differential equations, making a set of algebraic equations, and solving these equations to get an approximate solution (Islam et al., 2016).

Waterflooding is one of the common techniques for petroleum recovery, where water is injected into an injection well for producing oil through a production well. In this context, the Buckley-Leverett equation (Buckley and Leverett, 1942) presents a model for an incompressible, one-dimensional, two-phase flow system (Muggeridge et al., 2014). The model has some limitations, for example, the possibility of multiple-valued water saturation at each position. One of the early efforts to overcome this challenge is shock front theory. Since then, several researchers (Dykstra, 1950; Hiatt, 1958; Fayers and Sheldon 1959; Warren, 1964;

Gottfried, 1966) have tried to solve this issue using various numerical methods, which are discussed by the current authors in Chapter 2 as a literature review.

Based on this issue, the present research considers a single-valued discontinuous solution instead of a multi-valued solution. Shock waves are introduced here through these single-valued solutions. These shock waves help to measure the stability of the solutions and to handle nonlinear hyperbolic PDEs (such as the Buckley-Leverett equation). The differential form of the governing equation is no longer valid, and the integral form of the algebraic equation can be solvable through this phenomenon. Moreover, this wave formation exhibits the physical behaviour of the system and makes the solution discontinuous, rather than giving a multi-valued solution, for any given initial and boundary conditions (De Sterck and Ullrich, 2007). Therefore, finding consistent and stable solutions for multiphase flow from the Buckley-Leverett equation using advanced numerical techniques will be a new contribution from this research.

1.2 Objective

This research aims to solve the nonlinear partial differential equation using a nonlinear solver and find a numerical scheme which can capture all inherent assumptions and explain the nonlinearities. This numerical scheme should be stable and must provide an accurate and consistent solution. In this research, we choose the Buckley-Leverett equation as our model, which arises in waterflooding techniques for petroleum recovery. Here, the researcher tried to resolve the capillary pressure effect by solving that governing equation using a finite volume scheme and, finally, run an iteration method to check the stability and consistency of the numerical results. The overall summary of this research is shown in Figure 1.

1.3 Structure of the thesis

The thesis is organised into five chapters, and the first chapter represents the introduction of the present research. Other sections are organised as follows: Chapter 2 provides the knowledge gap and details the literature of the current research topic, where the authors summarise all nonlinear issues along with their solution techniques and present the various contributions for that field. Chapter 3 considers the shock wave front using the Method of Characteristics and later solves the one-dimensional (1-D) Buckley-Leverett equation (neglecting gravitational forces and capillary pressure gradients) numerically using the local Lax-Friedrichs scheme in explicit form. This chapter also includes the consistency check for the local Lax-Friedrichs

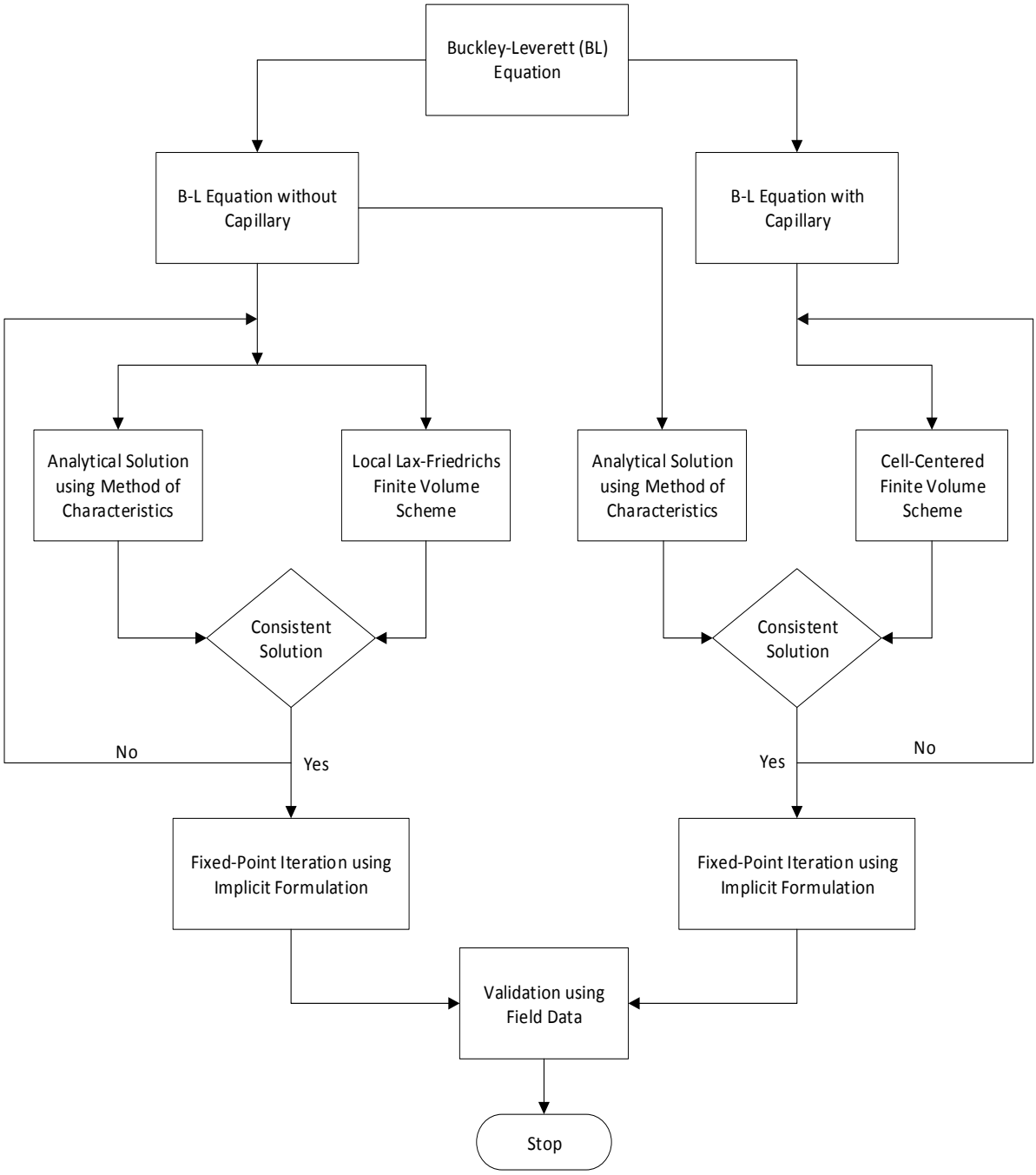

Figure 1.1: Summary of this research.

scheme and presents some observations related to this research. Chapter 4 introduces the numerical solution of the 1-D Buckley-Leverett equation including capillary effects (assuming gravitational force is zero) through a cell-centred finite volume scheme and later validates the stability of the solution by a fixed-point iteration method. This iterative method is also applied to the local Lax-Friedrichs scheme and a simple explicit form calculation to make the solution procedure more stable. A real field case study is also presented in this chapter. Finally, the

results are summarized and highlighting the contributions along with the future recommendations, in Chapter 5.

REFERENCES

Aziz K., and Settari A., (1979), Petroleum Reservoir Simulation, Applied Science Publishers, New York.

Buckley S.E., and Leverett M.C., (1942), Mechanism of Fluid Displacement in Sands, Trans. AIME, 146:187–196.

Crichlow H.B., (1977), Modern Reservoir Engineering: A Simulation Approach, Prentice-Hall, Inc., New Jersey, pp.354.

De Sterck, H., and Ullrich, P., (2007), Introduction to Computational PDEs. Course Notes for Amath, 442.

Deb, P.K., Akter, F., Imtiaz, S.A., and Hossain, M.E., (2017), Nonlinearity and solution techniques in reservoir simulation: A review. Journal of Natural Gas Science and Engineering, 46, 845-864.

Dykstra, H., and Parsons, R.L., (1950), The prediction of oil recovery by waterflood. Secondary recovery of oil in the United States, 2, 160-174.

EIA, (2016), U.S. Energy Information Administration/Monthly Energy Review.

Fayers, F.J., and Sheldon, J.W., (1959), The effect of capillary pressure and gravity on two-phase fluid flow in a porous medium.

Gottfried, B.S., Guilinger, W.H., and Snyder, R.W., (1966), Numerical solutions of the equations for one-dimensional multi-phase flow in porous media. Society of Petroleum Engineers Journal, 6(01), 62-72.

Hiatt, W.N., (1958, January), Injected-fluid coverage of multi-well reservoirs with permeability stratification. In Drilling and Production Practice. American Petroleum Institute.

Hossain M.E., and Islam M.R., (2010), Knowledge-based Reservoir Simulation: A Novel Approach, Intl. J. Eng., 3(6):622–638.

Islam, M.R., Hossain, M.E., Mousavizadeghan, H., Mustafiz, S., and Abou-kassem, J.H., (2016), Advanced Reservoir Simulation: Towards Developing Reservoir Emulators, second ed. Scrivener-Wiley, p. 592.

Muggeridge, A., Cockin, A., Webb, K., Frampton, H., Collins, I., Moulds, T., and Salino, P. (2014). Recovery rates, enhanced oil recovery and technological limits. Phil. Trans. R. Soc. A, 372(2006), 20120320. doi: 10.1098/rsta.2012.0320

Mustafiz S., and Islam M.R., (2008), State of the Art Petroleum Reservoir Simulation, J. Pet. Sci. Technol., Taylor and Francis, 26:1303-1329. doi: 10.1080/10916460701834036

Warren, J.E., (1964), Prediction of waterflood behavior in a stratified system. Society of Petroleum Engineers Journal, 4(02), 149-157.

CHAPTER 2

Nonlinearity and Solution Techniques in Reservoir Simulation: A Review

[1]Pulok Kanti Deb, [1]Farhana Akter, [1]Syed Ahmad Imtiaz and [1]M. Enamul Hossain

[1]Department of Process Engineering, Memorial University of Newfoundland, NL, Canada

PREFACE

This paper was published in the Journal of Natural Gas Science and Engineering as a part of this chapter and its citation link is below. The lead author performed the necessary literature review and wrote the manuscript. The co-authors helped in identifying the gap in research and editing the manuscript.

Deb, P.K., Akter, F., Imtiaz, S.A., & Hossain, M.E. (2017). Nonlinearity and solution techniques in reservoir simulation: A review. Journal of Natural Gas Science and Engineering, 46, 845-864. doi: https://doi.org/10.1016/j.jngse.2017.07.031

ABSTRACT

Reservoir simulation is used to demonstrate the dynamic physical processes of rocks and fluid properties with high-order nonlinear equations. Currently, different types of simulation models are used in the petroleum industry. These models contain several nonlinear complexities and, to get a good solution, researchers have applied different numerical schemes. In this paper, an extensive review is offered on the state-of-the-art literature with a focus on the nonlinearity in partial differential equations related to petroleum reservoir simulation. A critical analysis is done on different techniques for solving nonlinear governing equations in a petroleum reservoir. It also addresses the inherent assumptions, properties, and significance of nonlinear solvers and their technical challenges. Finally, the article discusses the impact of a solution of these nonlinear problems by following different numerical techniques.

Keywords: Nonlinear solver, capillary pressure, nonlinear algebraic equation, numerical technique, partial differential equation.

2.1. INTRODUCTION

The petroleum industry is the primary key to the global economy, and technological advancement moves forward based on this sector. The energy demand is increasing and currently, the crude oil production is some 90 million barrels per day (EIA, 2016). Extracting more oil and gas out of existing reservoirs is therefore of paramount importance if the industry is to meet the future growth of energy consumption. Therefore, there is a need to improve reservoir performance and enhance hydrocarbon recovery mechanisms, which is mostly influenced by proper reservoir simulation models. Crichlow (1977) presented a general overview of the simulation approach for the petroleum industry. However, the physical dimension of a reservoir is always an uncertain issue because every reservoir has different geometrical structure and unique geological characteristics (Mustafiz and Islam, 2008). The prediction of reserves based on the theory behind fluid flow through porous media can mislead petroleum recovery efficiency.

Simulation models capture complex physical phenomena related to the inherent geological complexity of earth models. Due to the nonlinear complexity in the governing equations, the dynamic simulation and solution processes in a petroleum field remain major challenges and an ongoing research topic. The governing equations for fluid flow in porous media are based

on conservation of mass, momentum, and energy equations. Reservoir simulation models can be categorised into two groups, based on standard black-oil models and compositional models (Aziz and Settari, 1979). In compositional models, the conservation equation is written for individual components (Young and Stephenson, 1983). Despite the increase in the use of compositional models, the high computational cost associated with nonlinear complexities remains a major drawback. On the other hand, black oil models are more attractive candidates for most reservoir simulation studies in the industry due to their simplifying assumptions regarding realistic field-scale simulations (Lee et al., 2008).

For solving the simulation models, several analytical and numerical methods were applied to handle nonlinear problems. However, the solutions are not exact due to their use of linearized mathematical schemes and considering various assumptions. Therefore, an advanced numerical tool is needed to predict the exact solution for a multivariable problem, so that the solutions are realistic rather than impractical.

Based on the above issues, the focus of this paper is to review the solution techniques for various nonlinear equations in petroleum reservoir engineering and simulation, technical challenges in solving those governing equations, and future facilitation for reservoir simulation. Here, we review the related literature, summarize the solution techniques and models along with assumptions and properties. Finally, we provide some guidelines for future research and development (R&D).

2.1.1 Background of the Research

In reservoir engineering, many equations express nonlinear behaviour due to effects of the time interval, variation in fluid and formation properties (e.g. porosity, permeability, water saturation, viscosity, etc.), distribution of pressure responses, simplification of the governing equations at formulation stage, or the feasibility of multiple solutions. Islam and Nandakumar (1986, and 1990) showed the nonlinear behaviour of the governing equations in petroleum reservoir engineering and simulation. To avoid the nonlinearity, previous researchers solved the governing equations using linearized methods (e.g., Taylor series expansion, Optimal linearization method, Global linearization method, Perturbation theory, Euler's method, Runge-Kutta method, Newton's Iteration) along with some assumptions (Jordan, 2006). These procedures help the researcher to understand the simulation model and control the system design methods quickly. However, the linearization effects can be significant, and the results may not be accurate due to the wrong prediction of the parameter distribution and number of

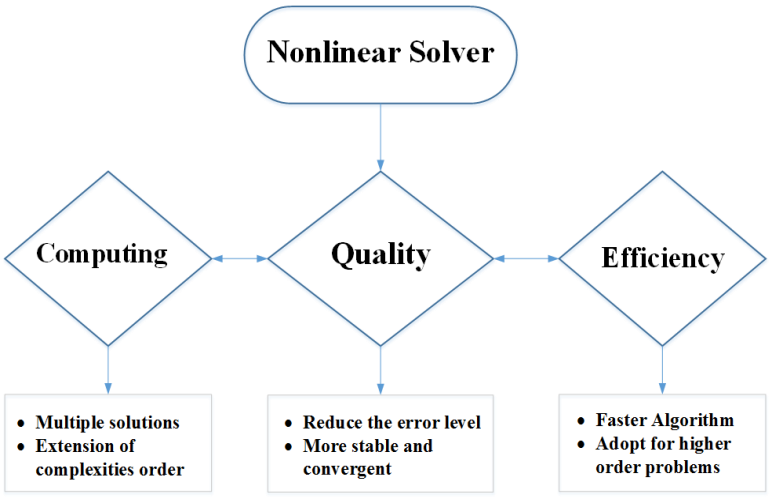

Figure 2.1: Importance of nonlinear solver.

errors. The interpretation of simulation models is also affected by neglecting higher-order roots and other assumptions (Islam et al., 2016). The material balance equation, Navier-Stokes equation, Buckley-Leverett equation, etc., are typical examples of nonlinear behaviour in petroleum reservoir engineering (Table 2.1).

2.1.2 Technical Challenges Towards the Research

All current commercial simulators (e.g. Eclipse, CMG Suite, Tempest MORE, ExcSim, Nexus, FlowSim) in the petroleum industry solve the set of governing equations (including all algebraic equations, PDEs, and ODEs) by linearizing nonlinear equations and adding assumptions. In the majority of cases, the solutions are not ideal due to the nonlinear behaviour of the equations. Islam et al. (2010, 2016) showed that these solutions are varied with the realistic range of most of the petroleum parameters in a single-phase flow. They also found significant errors in the prediction time of petroleum reservoir performance using advanced fuzzy logic. The scenarios are worse for multiphase flow when linearization occurs in governing equations (Islam et al., 2016). Thus, to predict reservoir behaviour and future performance, we need more accurate solutions from nonlinear solvers, which develop a consistent solution scheme by solving nonlinear algebraic equations and helps us to optimize hydrocarbon recovery.

2.1.3 Objectives of the Research

Nonlinearity increases the complexity of reservoir operations and reduces the performance when applying simulation technologies. It also raises the computational cost, requiring more

Table 2.1: A few examples of nonlinear equations

Sl. No.	Equations	Reasons for Nonlinearity	References
1	Material Balance equation	Nonlinear nature of pressure declines with time or distance	Islam et al. (2016)
2	Navier-Stokes equation	Nonlinear stress-rate of strain relationship	Khan and Islam (2006); Zatzman and Islam (2007); Islam et al. (2016)
3	Buckley-Leverett equation	Nonlinear behaviour due to the inclusion of capillary pressure	Mustafiz et al. (2008b); Islam et al. (2016)
4	Darcy's law: Fluid flow through porous medium	Nonlinear nature of pressure-dependent properties	Abou-Kassem et al. (2006); Islam et al. (2016)

time to complete. The numerical solution of the nonlinear governing equations in reservoir engineering helps us to understand, forecast, and manage subsurface fluid migration, especially in complex geometry and highly nonlinear multiphase fluid flow systems. An effective numerical technique can handle nonlinear parameters and enhance productivity. As such, development of techniques has drawn a lot of interest by a diverse group of scientists.

Many models of petroleum properties are not rigorously justified, and approximately 30% deviation occurs due to the linearization of nonlinear algebraic equations for pressure values for single phase flow (Hossain and Islam, 2010a; Islam et al., 2010). This type of error restricts the ability of petroleum reservoir models. The performance further deteriorates when the governing equations for multiphase flow are linearized. The resulting residual equations are also nonlinear, due to various natures of nonlinearity including saturation-dependent nonlinear terms (e.g. relative permeability, and capillary pressure functions), or pressure-dependent nonlinear terms such as viscosities and densities (Shahvali, 2012; Nooruddin et al., 2014). Thus, it is necessary to solve the nonlinear algebraic equations in time and space dimensions. A nonlinear solver reduces the time step and error level with its better algorithm for the equations using the engineering approach. The stability and consistency of a solution are also maintained by a nonlinear solver. However, limited work has been done using this technique to represent the importance of nonlinear solver (Figure 2.1) and resolve the nonlinearity difficulties. Nonlinear solver tasks are more fruitful for enhanced oil recovery (EOR) schemes to optimize oil recovery and improve thermal flooding operations (Hossain et al., 2009; Islam et al., 2010; Al-Mutairi et al., 2014).

2.2. CRITICAL LITERATURE ANALYSIS

The equations used in reservoir engineering and simulation are inherently nonlinear due to the interaction and inclusion of various parameters. These equations may be algebraic,

differential, integral, partial differential equations (PDE), ordinary differential equations (ODE), or integro-differential equations. These equations contain higher-order roots and indicate nonlinear behaviours. Depending on the parameters, nonlinear algebraic equations may yield multiple solutions instead of a single solution. We need to solve such equations to find approximate solutions using Newton's method, Finite Difference Method (FDM), Adomian Decomposition Method (ADM), etc. However, these conventional techniques do not provide multiple solutions for simultaneous nonlinear equations, which has led to diverse groups of scientists working on this question. There are several effects (i.e., pressure-dependent properties, capillary pressure, viscous fingering, memory, gas flow modelling, mixing, phase exchange, absorption and desorption) involved which increase the nonlinearity in the governing equations. A critical analysis of different models is shown in Table 2.2 based on those effects. Here, a summary of the model equations, assumptions, parameters behind these equations, and the limitations for the developed equations are presented in Tables 2.2 and 2.3. These tables represent the last few decades advancement in reservoir simulation models and provide a scope for future research. Furthermore, the identified key features will help researchers improve their ideology and philosophy to develop reservoir emulators considering time and space. In this section, we review this work and sort out the problems from their solution techniques, looking for a research scope in the current area of interest.

2.2.1. Effect of Capillary Pressure

Capillary pressure is the pressure differential between the wetting and non-wetting phase in porous media due to the effects of capillary forces across the fluid interface. Modelling the behaviour of capillary pressure in reservoir engineering and enhanced oil recovery problems is a challenging task. Using capillary pressure, scientists and petroleum engineers evaluate the quality of reservoir rock, the depth of reservoir fluid contacts, seal capacity, pay versus nonpay zones, estimation of recovery efficiency, etc. from petroleum fields (Morrow 1970; Melrose and Brandner, 1974; Wardlaw et al., 1988).

Many researchers tried to solve the governing equations of these areas by considering capillary effects and found significant effects. Based on the Buckley-Leverett equation (1942), Holmgren and Morse (1951) explained capillary effects for removing nonlinearities through the average saturation of water calculation. After that, Welge (1952) found the mean water saturation at a breakthrough point in an oil reservoir and shock effects, described by the Buckley-Leverett equation. Fayers and Sheldon (1959) solved the displacement equation with

Table 2.2: A Critical analysis of different model equations from different researchers.

Researcher	Parameters of the model equations																Solution scheme
	ϕ	k	P	T	S_w	f_w	μ	P_c	x	σ	g	q	α	τ	Reservoir dimension	No. of phases	
Buckley-Leverett (1942)	√	√	-	-	√	√	√	√	√	-	√	√	-	-	1-D	2	Theoretical
Holmgren and Morse (1951)	√	√	-	-	√	-	√	√	√	-	-	√	-	-	1-D	2	Analytical
Welge (1952)	√	√	-	-	√	√	√	√	√	-	-	√	-	-	1-D	2	Analytical
Fayers and Sheldon (1959)	√	√	-	-	√	-	√	√	√	-	√	√	-	-	1-D	2	Analytical
Hovanessian and Fayers (1961)	√	√	-	-	√	√	√	√	√	-	√	√	-	-	1-D	2	Theoretical
Slattery (1967)	-	√	√	-	-	-	√	-	-	√	-	-	√	√	-	1	Theoretical
Bentsen (1978)	√	√	-	-	-	√	√	√	√	-	√	√	-	-	1-D	2	Numerical
Mifflin and Schowalter (1986)	-	√	√	-	-	-	√	-	-	-	-	-	√	√	3-D	1	Analytical
Eringen (1991)	-	-	√	√	-	-	√	-	√	√	-	√	√	√	1-D	1	Theoretical
Nibbi (1994)	-	-	√	√	-	-	√	-	√	-	-	√	√	√	1-D	1	Theoretical
Broszeit (1997)	-	-	√	√	-	-	-	-	-	-	-	-	√	√	1-D	1	Numerical
Caputo (1999)	-	√	√	-	-	-	√	-	√	-	-	√	√	-	-	-	Theoretical
Shin et al. (2003)	-	-	√	√	-	-	√	-	-	-	-	-	√	-	-	1	Theoretical
Liu et al. (2003)	√	√	√	√	-	-	√	-	-	-	√	-	-	√	1-D	1	Numerical
Chen et al. (2005)	√	√	√	√	-	-	√	-	√	-	-	-	√	√	1-D	2	Theoretical
Hossain and Islam (2006)	√	-	√	√	-	-	-	-	-	√	-	-	√	√	-	-	Theoretical
Abou-Kassem (2007)	√	√	√	√	-	-	√	-	√	-	-	√	-	-	1-D	1	Analytical
Hossain et al. (2007)	√	√	-	√	-	-	√	-	-	-	-	-	√	√	1-D	1	Analytical
Mustafiz et al. (2008b)	√	√	-	-	√	√	√	√	√	-	√	√	-	-	1-D	2	Numerical
Hossain et al. (2008)	√	√	√	-	-	-	√	-	√	-	-	√	√	-	1-D	2	Numerical
Hossain et al. (2009b)	-	√	√	√	-	-	√	-	-	-	-	√	√	√	1-D	2	Numerical
Younis et al. (2010)	√	√	-	-	√	√	√	√	√	-	√	√	√	-	1-D	2	Numerical
Hossain (2012)	√	-	√	√	-	-	√	-	√	-	-	√	√	-	1-D	2	Analytical
Wang and Tchelepi (2013)	√	√	-	-	√	-	√	√	√	-	√	-	√	-	1-D	2	Numerical
Li and Tchelepi (2014)	√	√	√	√	-	-	√	√	√	-	-	√	-	-	1-D	2	Numerical
Hossain (2016a)	√	√	√	√	-	-	√	-	√	-	-	√	√	-	1-D	2	Analytical
Hossain (2016b)	√	√	√	√	-	-	√	-	√	-	-	√	√	-	1-D	2	Numerical
Obembe et al. (2016b)	√	√	√	-	-	-	√	-	√	-	-	√	√	-	1-D	2	Numerical

Table 2.3: A comparative and critical study on assumptions and limitations of different model equations.

Investigator	Assumptions	Limitations	Applications
Ciarletta and Scarpetta (1989)	○ Homogeneous, incompressible and viscous fluid ○ Aware of symmetric velocity gradient ○ Defined boundary conditions	○ Not suitable for complex simulation model equations ○ Depends only on fluid viscosity	○ In mathematics field for minimizing viscous-fluids related problems
Eringen (1991)	○ Identified local convergence ○ Applicable only for spherical problems	○ Undefined global convergence ○ Incompetent for thermally active fluid flow systems	○ Developed the suspension mechanism for colloidal problems
Nibbi (1994)	○ Homogeneous, incompressible and viscous fluid ○ Linear and isotropic problems	○ Imprudent for practical problems	○ Fluid related quasi-static problem in Mathematics field
Caputo (1999)	○ Linear isotropic, homogeneous, viscous and incompressible fluid ○ Predicts fluid pressure with time	○ Permeability decreases with time ○ Undefined fluid properties role in a porous media	○ In geothermal areas for studying the pore size of the minerals
Shin et al., (2003)	○ Memory is dependent on the diffusion time scale ○ Homogeneous model ○ Used Taylor series expansion	○ Did not explain the memory impact fully in the media ○ More dependency on time scale	○ Explained particle deposition facts and Non-equilibrium mechanism for fully developed turbulent channel flows
Hossain and Islam (2006)	○ Permeability and fluid compressibility unchanged with time ○ Fluid and media properties have been considered	○ No explanation about nonlinear trends of stress-strain model	○ Visco-elastic fluid flow behavior in a reservoir.
Hossain et al., (2007)	○ No slip conditions ○ No lower contact surface velocity ○ Consider dimensionless parameters ○ Ignored the roles of surface tension on the fluid viscosity, and memory	○ No explanation about matrix heterogeneity, anisotropy, and inelasticity of a reservoir	○ Used in reservoir simulation, rheological study, well test analysis, and EOR surfactant selection
Hossain et al., (2008)	○ Used time-dependent fluid and media properties ○ Used equation of motion and continuity equation ○ Followed fractional order of differentiation	○ Generates only singular form of equations ○ Need to remove singularities using different numerical techniques	○ Used for crude oil flow in porous media, EOR process, and few special case (like decline pressure reservoir condition)
Hossain et al., (2009b)	○ Non-Newtonian and shear thinning fluids ○ Ignored scale-up problems ○ Trapezoidal method used for numerical simulation ○ Porosity, permeability, shape factor and flow velocity considered	○ Captured physical phenomena of a model only ○ Limited works at low shear rates ○ Not showed the effect of apparent viscosity in their model ○ Analytical solution was absent	○ Used in EOR and polymer manufacturing applications
Hossain (2012)	○ Compressible fluids ○ Single phase flow ○ 1-D horizontal reservoir with irregular block size ○ Rectangular coordinates	○ Analytical and numerical solutions were absent	○ Used for the development of petroleum reservoir simulator
Wang and Tchelepi (2013)	○ Newton-based nonlinear solver ○ Large time steps ○ Analysed entire capillary, viscous, and buoyancy parameter spaces of porous media ○ Nonlinear immiscible, incompressible, two-phase flow in	○ Failed to explain time-step based truncation errors ○ Only for single cell problems	○ Developed for coupled multiphase flow and transport in porous media

	porous media		
Li and Tchelepi (2014)	○ Interface of discretized flux function between two cells ○ Guided only Newton iterations for various saturation regions ○ Considered time-truncation errors ○ Oscillation of convergence failure avoided ○ Two-phase flow	○ Undefined many unknown variables in multiple dimensions ○ Unable to explain sharp kinks of relative permeability curves	○ Used for oil/gas recovery, groundwater remediation, and CO_2 geological sequestration
Hossain (2016a)	○ Fluid and rock properties are time-dependent continuous functions ○ Followed engineering approach ○ 1-D Cartesian reservoir considered	○ Have no realistic estimation regarding fractional derivatives ○ Need experimental data set for validation of memory-based diffusivity equation	○ Used in well testing analysis, petroleum reservoir simulation and history matching
Hossain (2016b)	○ Permeability is constant with respect to time and space ○ 1-D model of an oil reservoir ○ Only considered transient phase ○ Asymptotic value is set equal to zero	○ Does not explain about non-local aspects of fluid transport ○ Singularity of the integral formulation with the memory was inherent for integrodifferential equations	○ Determined pressure response in the formation rock and fluid properties for a petroleum reservoir ○ Captured memory in reservoir fluid flow in porous media
Obembe et al., (2016b)	○ Extended the diffusivity equation for multiphase flow system ○ Considered wellbore geometries ○ Defined volumetric flux with time ○ Material balance check per time step	○ R-L fractional operator failed to interpret the initial conditions of a system ○ Time-step must be known for stability check	○ Handled fractional flow problem in porous media

gravity and capillary pressure using a Lagrangian approach. However, they did not obtain saturation values for a required time. Hovanessian and Fayers (1961) also presented capillary pressure effects by avoiding multiple-valued saturation profiles. Hence, Bentsen (1978) explained that fact with separate equations for a particular distance travelled by zero saturation with a numerical investigation. He also showed the incorrect formulation of Fayers and Sheldon (1959) for slow rates of injection at constant normalized saturation conditions. However, Craft and Hawkins (1991) showed the fluid distributions of a single homogeneous formation for different times and detected multiple water saturation values along the formation bed. For simplicity, the authors assumed that the forces generated by gravity and capillary pressures are negligible. Capillary pressure is also significant during fluid injection into confined aquifers. Nordbotten and Celia (2006) predicted the formation zone behavior with semi-analytical solutions for the case of CO_2 injection into deep saline aquifers, considering capillary pressure effects. The authors also attempted to reduce the nonlinearity of PDEs in their modeled system by presenting a couple of solutions through iterative solution techniques and, finally, compared with numerical solutions depicted by Nordbotten et al. (2005). However, to avoid complexity, capillary pressure was neglected in their solution. Later, Schmid et al. (2011) derived semi-analytical solutions for two-phase flow, concerned with the effects of viscous and capillary forces in counter-current and co-current imbibition

processes. Due to the highly nonlinear nature of the problem, they only considered the capillary-free Buckley-Leverett problem.

To minimize the effects of nonlinearity, Mustafiz et al. (2008a, and b) solved the nonlinear Buckley-Leverett equation (1942), considering capillary pressure effects and validated their solution for 1-D, two-phase flow using ADM (Adomian Decomposition Method). Recently, Islam et al. (2016) argued that multiple solutions might come using advanced fuzzy logic and numerical techniques. Therefore, consistently finding multiple solutions for multiphase flow from the Buckley-Leverett equation using advanced numerical techniques will be a new scope of research.

From Buckley-Leverett's theory (1942), the equation can be written as:

$$\frac{\partial S_w}{\partial t} + \frac{q}{A\phi}\frac{\partial f_w}{\partial S_w}\frac{\partial S_w}{\partial x} = 0 \tag{1}$$

where,

$$f_w = \left(\frac{1}{1+\frac{k_{ro}\mu_w}{k_{rw}\mu_o}}\right)\left(1 + \frac{Akk_{ro}}{q\mu_o}\left[\frac{\partial P_c}{\partial x} - (\rho_w - \rho_o)gsin\alpha\right]\right) \tag{2}$$

Here, S_w is water saturation, f_w is the fractional flow rate of water, q is the total flow rate of oil and water, A is the cross-sectional area, φ is porosity, k_{ro} is relative permeability of oil, k_{rw} is relative permeability of water, μ_w is water viscosity, μ_o is oil viscosity, k is absolute permeability, P_c is capillary pressure, ρ_w is water density, ρ_o is oil density, g is gravity, and α is angle of the formation bed.

Equation (1) is a nonlinear PDE. Making assumptions, Craft and Hawkins (1991) presented the following equation by calculating water saturation along the formation bed:

$$x(t, S_{w0}) = \frac{qt}{A\varphi}\frac{\partial}{\partial S_{w0}}\left(\frac{1}{1+\frac{k_{ro}\mu_w}{k_{rw}\mu_o}}\right)_t \tag{3}$$

Equation (3) neglects gravity and capillary forces in the formation, and the flow is horizontal. The results showed multiple saturation values at any point along the bed, which is fully unrealistic in reservoir simulation. Therefore, Mustafiz et al. (2008b) presented the following equation for the case of horizontal flow, considering the capillary pressure effects:

$$S_{w0}(x,t) = S_w(0,x) - \int_0^t \left[\frac{q}{A\varphi}\frac{\partial}{\partial S_{w0}}\left(\frac{1}{1+\frac{k_{ro}\mu_w}{k_{rw}\mu_o}}\right)\frac{\partial S_{w0}}{\partial x}\right] dt \tag{4}$$

$$S_{w1}(x,t) = -\int_0^t \left[\frac{kk_{ro}}{\mu_0\varphi} \frac{\partial}{\partial S_{w0}} \left(\frac{1}{1+\frac{k_{ro}\mu_w}{k_{rw}\mu_o}} \right) \frac{\partial P_c}{\partial S_{w0}} + \frac{k}{\mu_0\varphi} \left(\frac{1}{1+\frac{k_{ro}\mu_w}{k_{rw}\mu_o}} \right) \frac{\partial k_{ro}}{\partial S_{w0}} \frac{\partial P_c}{\partial S_{w0}} + \frac{kk_{ro}}{\mu_0\varphi} \left(\frac{1}{1+\frac{k_{ro}\mu_w}{k_{rw}\mu_o}} \right) \frac{\partial^2 P_c}{\partial {S_{w0}}^2} \right] \left(\frac{\partial S_{w0}}{\partial x} \right)^2 dt \quad (5)$$

Mustafiz et al. (2008b) solved these equations using ADM (Adomian Decomposition Method), which is a powerful technique to solve nonlinear equations. They maintained the capillary pressure and water saturation behaviour and obtained one saturation value for a given time at a point along the formation bed. In fact, the solution converged quickly but failed to produce multiple solutions for the governing Buckley-Leverett's equation. Hence, there is a scope for future researchers to find new schemes and check the feasibility of generating multiple solutions.

On the contrary, capillary effects could be explained by bundle tube and network model concepts. Some researchers had focused only on bundle tube models (Yuster, 1951; Scheidegger, 1953; Bartley and Ruth, 1999; Dong et al., 1998), and other researchers discussed 2-D and 3-D network models (Chatzis and Dullien, 1977, 1982; Chadler et al., 1982; Lapidus et al., 1985; Diaz et al., 1987; Blunt and King, 1991). However, these researchers failed to simulate fluid dynamics in porous media through network modelling. In addition, Dong et al. (2005) analyzed immiscible displacement processes using an interacting capillary bundle model. In this model, capillary pressure was considered, and the fluids used in different capillary pressures were independent of each other. The saturation profiles were calculated using the backward difference approximation, which is a second-order nonlinear equation solved through Newton's method for each time and space step. The stability and convergence were also in good approximation based on experimental, numerical, and analytical results. However, this is a linearized and time-consuming method. Therefore, researchers are looking forward to advance nonlinear solution schemes which will be less time consuming and will provide stable and accurate solutions.

2.2.2 Effect of Memory

Memory is a function of fluid and media properties, and the pressure changes with respect to time in a reservoir, which influence other rock and fluid properties (Caputo 1998a, 1999, 2000; Caputo and Cametti, 2009; Caputo and Fabrizio, 2015). During flow processes, rock and fluid properties alter continuously within the reservoir, and that alteration is directly or indirectly related to time (Hossain et al., 2009; Hossain and Islam, 2009). Research shows that

these properties are inherently nonlinear. Later, Hossain and Abu-Khamsin (2012a, 2012b) presented the notion of memory, which stated the continuous-time functional or history dependency and leads to nonlinearity and multiple solutions.

To incorporate memory effects in petroleum reservoirs, Slattery (1967) defined memory, which represents the deformation rate as a function of extra stresses. He approached this through studying viscoelastic fluid behaviour with the Buckingham-pi theorem and found the nonlinear behaviour in his results. Using the memory function, Mifflin and Schowalter (1986) presented a relationship between the fluid viscosity and stress tensor in non-Newtonian fluids. That research was conducted for solving 3-D steady flows in closed or open flow systems. They divided memory into velocity gradients and continued the calculation until the fluid memory decomposed adequately while the rest of the integral could either be neglected or set to a small constant value. Later, Ciarletta and Scarpetta (1989) focused on the linearized progress of an incompressible fluid flow equation, ignoring the nonlinear convective term of the equation. They were concerned with the symmetric velocity gradient, which helps to observe the immediate stress effects based on memory.

Apart from the above fluids, Eringen (1991) developed a nonlocal theory of micro-polar fluids by considering orientation and memory effects along with stress and fluid viscosity. They showed significant memory effects by measuring the small characteristic length compared with the average gyration radius of the fluid molecular elements. This type of situation arises in the case of thin film lubrications, which exhibit a nonlinear behaviour. However, none of the above researchers explained and solved the nonlinearity. Nibbi (1994); Broszeit (1997); Li et al. (2001); Shin et al. (2003); Chen et al. (2005); and Hossain and Islam (2006) used memory functions based on the characteristic and intermediate diffusion time scales for different fluids and parameters. These authors reviewed memory effects comprehensively, but were unsuccessful at the stage of experimental validation.

After a few years, Hossain et al. (2009a) applied fluid memory to non-Newtonian fluids during an EOR process. Here, the rock compressibility was affected by the pressure decline during the production life of a reservoir. The fluid and formation properties were investigated using space and time derivatives of fractional order, which made it a rigorous model. A significant pressure response was observed due to the increasing production time of the reservoir, which made the fluid memory effects dominant. Recently, a model was solved by

Obembe et al. (2016c) for heterogeneous media which included the memory as a time derivative of fractional order in a diffusion model.

Furthermore, Hossain et al. (2009b) described the characteristics of polymer flooding, reservoir simulation, and the characterization of complex reservoirs with the help of memory effects which could characterize the fluid movement. They were concerned with the characterization of the rheological behaviour along with memory effects for shear-thinning fluids. However, that model did not explain the delay of movement in a viscoelastic fluid. Therefore, Hossain et al. (2009c) presented a mathematical stress-strain model for a complex reservoir considering the effects of memory parameterized by the fractional derivative order, α. For different values of α, they identified the fluid memory effects, considering time and space over the stress-strain relationship. The memory mechanism helps in interpreting the reservoir phenomenology with matrix heterogeneity, anisotropy, and inelasticity. Moreover, the variation of distance and time defines a chaotic behaviour with non-monotone trends of the stress-strain relationship, which was a strong indication of the memory effect. The trapezoidal method was used to solve their proposed model, ignoring the complexity of the nonlinear second order PDEs due to the absence of a nonlinear solver. Recently, memory has been applied appropriately by Hossain (2016a) and Obembe et al. (2016b) to present the modified diffusivity equation where the rock and fluid properties are continuous time-dependent functions. According to Hossain (2016a), the model equation was highly nonlinear due to the application of memory and validated by numerical experiment. Here, the solution of the equation was dependent on memory (α), which was more realistic compared to a conventional Darcy's model. The memory was predominant surrounding the wellbore and diminished toward the outer boundary of the reservoir. However, that model could not provide better predictions due to the inconsistent rate of diffusion and incomplete solution. Here, we show an example where memory is incorporated into a stress-strain relation, making the governing equation nonlinear. The relationship between stress and strain (Hossain and Islam, 2006; Hossain et al., 2007) becomes:

$$\tau_T = \frac{k^2 \Delta p A_{xz} \Gamma(1-\alpha)}{\mu_0^2 \eta \rho_0 \phi y c I} \times \left[\left(\frac{\partial \sigma}{\partial T} \frac{\Delta T}{\alpha_D M_a} \right) \times e^{\left(\frac{E}{RT}\right)} \right] \tag{6}$$

where, $I = \int_0^t (t-\xi)^{-\alpha} \left(\frac{\partial^2 p}{\partial \xi^2} \right) d\xi$ and the permeability of the media and fluid compressibility are unchanged with time.

Here, τ_T is shear stress at temperature T; M_a is Marangoni number; R is universal gas constant; A_{xz} is cross-sectional area of rock perpendicular to the flow of flowing fluid (m^2); E is activation energy for viscous flow $(KJ\ /\ mol)$; T is Temperature (K); ΔT is temperature difference (K); α is fractional order of differentiation, known as Memory; α_D is thermal diffusivity $(m^2\ /\ sec)$; Γ is Euler gamma function; ξ is a dummy variable for time, i.e., real part in the plane of the integral; p is pressure of the system $(N\ /\ m^2)$; Δp is pressure difference; η is ratio of the pseudo-permeability of the medium with memory to fluid viscosity $(m^3 s^{1+\alpha}\ /kg)$; y is distance from the boundary plan (m); ρ_0 is density of the fluid at reference temperature T_0; c is fluid compressibility; ϕ is porosity of fluid media; k is permeability and μ_o is oil viscosity.

The above equation is the simplified form of a mathematical model (Lu and Hanyga, 2005; Hossain et al., 2007) which consists of all fluid and media properties:

$$\tau_T = \frac{k^2 \Delta p A_{xz} \Gamma(1-\alpha)}{\mu_0^2 \eta \rho_0 \phi y c \int_0^t (t-\xi)^{-\alpha} \left(\frac{\partial c}{\partial \xi}\frac{\partial p}{\partial \xi} - \frac{c}{k}\frac{\partial k}{\partial \xi}\frac{\partial p}{\partial \xi} + c\frac{\partial^2 p}{\partial \xi^2}\right) d\xi} \times \left[\left(\frac{\partial \sigma}{\partial T}\frac{\Delta T}{\alpha_D M_a}\right) \times e^{\left(\frac{E}{RT}\right)}\right] \frac{du_x}{dy} \qquad (7)$$

In equation 7, memory is a function of all fluid and media properties over time. When we consider memory and other properties simultaneously, the equation behaves nonlinearly rather than as a linear function. A proper nonlinear solver or a new numerical scheme could handle that type of equation and minimize the challenges of memory-induced rock and fluid properties in porous media.

2.2.3. Effect of Viscous Fingering for Miscible and Immiscible Displacement

To enhance secondary and tertiary oil recovery, modelling viscous fingering is important in both miscible and immiscible displacement. Though this task is formidable, some researchers have attempted to establish a suitable model using few chaos theory. The biggest problem was generating higher-order equations with respect to time and space, and researchers faced complexity to solve those types of governing equations. Naami et al. (1999) conducted an experiment on modelling viscous fingering in a 2-D system and interpreted the model using a numerical method. A similar approach was taken by Saghir et al. (2000) where the governing equations of a viscous fingering model were solved using a finite difference scheme. Both research groups explained the PDEs of the model by propagation of fingers in the system. Some advanced numerical techniques have also been applied to modelling viscous fingering by other researchers (Aboudheir et al., 1999; and Bokhari and Islam, 2005). Bokhari and

Islam (2005) showed their advancements to the order of Δt^4 in time and Δx^2 in space and presented some reasonable agreement to the Barakat-Clark scheme and experimental work. To date, the solution is undefined due to a lack of nonlinear solvers that will work on such higher order roots and solve viscous fingering models accurately.

A 2-D convection-diffusion equation is written as (Islam et al., 2016):

$$\frac{\partial C}{\partial t} = D_x \frac{\partial^2 C}{\partial x^2} + D_y \frac{\partial^2 C}{\partial x^2} - u \frac{\partial C}{\partial x} - v \frac{\partial C}{\partial x} \tag{8}$$

where, D_x and D_y denote lateral and transfer diffusion terms, u and v are the velocity terms in the X and Y directions, and C denotes the concentration term.

A modified Barakat-Clark scheme with central time difference was used (Islam et al. 2016), and the initial and boundary conditions were considered from Aboudheir et al. (1999). The discretization of equation (8) is:

$$\frac{Ca_{i,j}^{n+1} - Ca_{i,j}^{n-1}}{2\Delta t} = D_x \frac{Ca_{i+1,j}^{n} - Ca_{i,j}^{n} - Ca_{i,j}^{n+1} + Ca_{i-1,j}^{n+1}}{\Delta x^2} + D_y \frac{Ca_{i,j+1}^{n} - Ca_{i,j}^{n} - Ca_{i,j}^{n+1} + Ca_{i,j-1}^{n+1}}{\Delta y^2} - u \frac{Ca_{i+1,j}^{n} - Ca_{i-1,j}^{n}}{2\Delta x} - v \frac{Ca_{i,j+1}^{n} - Ca_{i,j-1}^{n}}{2\Delta y} \tag{9}$$

Here, the central time difference (CTD) scheme created artificial oscillations, and the solution was only accurate to first order and introduced a second order truncation error (Mathews, 1992). The Barakat-Clark scheme gave stability for the time term and showed the accuracy of the order of Δt^4, while the Barakat-Clark forward time difference (FTD) scheme showed accuracy approximately of the order of Δt^2. If the memory term is added into the equations, it leads to higher-order nonlinearity, which is a very hard task for the linear solver to solve. One should take the initiative to continue research for better time and space accuracy in the convection-diffusion equation. Finally, an advanced nonlinear solver can tackle this situation, which is another research scope in the area.

2.2.4. Effect of Fluid and Media Properties

In petroleum reservoirs, the most basic fluid and media properties include permeability, density, viscosity, temperature, pressure, diffusivity, compressibility, surface tension, specific gravity and so on. These parameters are interconnected with each other, and small changes in any one lead to significant changes in reservoir estimation and performance. For any governing equation, the equation must show nonlinear behaviours without considering

assumptions and then follow linearization techniques. From that point of view, a nonlinear solver should be able to handle higher complexities and higher roots of nonlinear governing equations.

Memory is a term in reservoir simulation which is well described by Islam et al. (2010, and 2016), Hossain et al. (2006, 2007, 2008, 2009c, and 2010a), and a few other research groups (Slattery, 1967; Caputo, 1999, 2000, 2015; Mustafiz et al., 2005, 2008; and Obembe et al., 2016 a, b, c). Earlier, the present authors tried to highlight memory effects concisely and show their independency. On the other hand, several parameters (i.e., permeability, density, viscosity, temperature, pressure, diffusivity, compressibility, surface tension, specific gravity, etc.) are discussed here. The basic difference is that sometimes memory will influence reservoir simulation independently while the rest of the time, it will act with other parameters. From last few decades, several researchers tried to deal with nonlinear equations along with those properties. Slattery (1967) explained the viscoelastic behaviour of Newtonian and incompressible fluids and presented a fluid behaviour model, which was unrealistic due to permeability effects. Based on previous research findings, Nibbi (1994) discussed the relationship between viscous fluids and free energies of linear viscoelastic fluids extensively for the quasi-static problem. Later, Brosszeit (1997) showed fluid deformation via simulation and attempted to describe and solve stress-related fluid problems. They applied a single integral constitutive law, where the fluid kinematics were known, and dealt with the numerical simulation of steady-state isothermal flow for Newtonian fluids. However, the exact solution was not clearly present in their numerical simulation approach. Liu et al. (2003) also verified analytical solutions of the Navier-Stokes equation for fractured reservoirs by numerical simulation, but failed to define the boundary conditions between the porous medium and the fracture. Later, Hossain et al. (2007) explained viscoelastic fluid flow behaviour in porous media, which is an important variable for predicting oil flow and helps to understand reservoir performance. They worked on existing fluid flow models considering time and other fluid (e.g. viscosity, density, diffusivity, compressibility) and media (e.g. surface tension, porosity, permeability) properties (Hossain et al., 2009c). Further, some researchers showed intangible problems of memory and recognized the need for considering memory and other rock/fluid properties (e.g. stress, viscosity, surface tension, temperature, etc.) (Hossain et al., 2009c). After that, Hossain and co-authors were able to describe the effects of fluid variation and formation properties over time and proposed a model for describing the flow of fluid in porous media (Hossain et al., 2008; Hossain, 2016a). Besides, Hassan and Hossain (2016) and

Obembe et al. (2016a) reviewed the thermal displacement processes for an oil reservoir and presented the rock and fluid property alteration with time. The authors (Hossain et al., 2008, Hossain, 2016a) modified the equations of motion by applying the memory concept in mathematical and computational models. The new form of the equations referred to the memory based diffusivity equation, is a fully nonlinear integrodifferential equation. Here, an implicit-explicit finite difference method was used to obtain a mathematical formulation, where the researchers tried to avoid the singular form of the equation. The only significant feature was the properties of rock and fluid as a function of time. The solutions of the model equations was still incomplete due to lack of nonlinear solver.

In addition, the modified momentum balance equation was presented by Hossain (2016b) for a 1-D oil reservoir, which helps to establish the memory contribution in reservoir fluid flow through porous media. This equation was solved numerically using spline functions, and the trapezoidal rule was applied to crosscheck the stability and accuracy of the solution. The time-domain and space-domain fractional-order derivatives solutions were obtained from that numerical solution. Yet the spline function and trapezoidal rule are not suitable for such equations, and researchers are looking for a nonlinear solver to solve the equation with better accuracy.

For single phase, 1-D (one-dimension) linear flow, the pressure gradient is predicted from the Darcy's diffusivity equation (Hossain et al., 2008; Islam et al., 2016):

$$\frac{\partial^2 p}{\partial x^2} = \frac{\phi \mu_o c_t}{k} \frac{\partial p}{\partial t} \tag{10}$$

where, c_t is the total compressibility, ϕ is the porosity, k is the rock permeability, and μ_o is the oil viscosity.

With the inclusion of rock and fluid memory, Hossain et al. (2008) considered the modified Darcy's law in 1-D reservoir:

$$u_x = -\beta_c \eta \left\{ \left[\frac{1}{\Gamma(1-\alpha)} \right] \int_0^t (t-\xi)^{-\alpha} \frac{\partial}{\partial \xi} \left(\frac{\partial \phi}{\partial x} \right) \partial \xi \right\} \tag{11}$$

where, β_c is the transmissibility unit conversion factor (dimensionless); α is the fractional order of differentiation, known as memory (dimensionless); ξ is a dummy variable for time, i.e., real part in the plane of the integral, u_x is the fluid velocity in porous media in the direction of x-axis (m/s); η is the ratio of the pseudo-permeability of the medium with

memory to fluid viscosity ($m^3 s^{1+\alpha}/kg$); Γ is the Euler gamma function and ϕ is the porosity of fluid media.

They took the range of α from 0 to 1, giving equation (11) a nonlinear form. Later, Hossain (2016a) applied the engineering approach for the development of a memory-based diffusivity equation and expressed the rock and fluid properties as a function of time as giving

$$T_{x_{i+\frac{1}{2}}} p_{i+1}^{n+1} - \left\{ T_{x_{i+\frac{1}{2}}} + T_{x_{i-\frac{1}{2}}} + \frac{V_{b_i}}{\alpha_c \Delta t} \left(\frac{\phi c_t}{B} \right)_i \right\} p_i^{n+1} + T_{x_{i-\frac{1}{2}}} p_{i-1}^{n+1} = T_{x_{i+\frac{1}{2}}} p_{i+1}^{n} - \left\{ T_{x_{i+\frac{1}{2}}} + T_{x_{i-\frac{1}{2}}} + \frac{V_{b_i}}{\alpha_c \Delta t} \left(\frac{\phi c_t}{B} \right)_i \right\} p_i^{n} + T_{x_{i-\frac{1}{2}}} p_{i-1}^{n} - q_{sc_i} - T_{x_{i+\frac{1}{2}}} \sum_{k=1}^{n} b_k^{(1-\alpha)} \left\{ \left(p_{i+1}^{n+1-k} - p_{i+1}^{n-k} \right) - \left(p_i^{n+1-k} - p_i^{n-k} \right) \right\} - T_{x_{i-\frac{1}{2}}} \sum_{k=1}^{n} b_k^{(1-\alpha)} \left\{ \left(p_{i-1}^{n+1-k} - p_{i-1}^{n-k} \right) - \left(p_i^{n+1-k} - p_i^{n-k} \right) \right\} \quad (12)$$

which is the final form

$$\left[\frac{\beta_c \eta A_x}{B} \left\{ \frac{\partial^\alpha}{\partial t^\alpha} \left(\frac{\partial P}{\partial x} \right) \right\} \right]_{x_{i+\frac{1}{2}}} - \left[\frac{\beta_c \eta A_x}{B} \left\{ \frac{\partial^\alpha}{\partial t^\alpha} \left(\frac{\partial P}{\partial x} \right) \right\} \right]_{x_{i-\frac{1}{2}}} + q_{sc_i} = \frac{V_{b_i}}{\alpha_c \Delta t} \left(\frac{\phi c_t}{B} \right)_i \left(p_i^{n+1} - p_i^{n} \right) \quad (13)$$

Equation (12) is the discretized form of the diffusivity equation, where the boundary conditions are applied to reduce nonlinearity, and a numerical experiment was performed to validate the model equation. Here, the author provides only the outline of the solution of model equation instead of an exact solution.

2.2.5. Effect of Time Step Size

The effects of the time step on computational accuracy are generated by the use of different time steps on the simulation system. The calculation of time step effects starts from the formulation and continues to solution. The results of relative percentage error are one way to express the time-interval implications in reservoir simulation, where the relative error is calculated based on pressure, temperature, or water saturation values at different time steps. To validate the models, time steps must be considered for long-term simulation (Islam, 2008). In addition, Newton's method is not always guaranteed to converge for large time steps, due to the nonlinearity of conservation equations (Aziz and Settari, 1979).

Ertekin et al. (2001) found significant changes in the percentage of relative error due to the implementation of time steps in the simulation system. The gradual reduction of error made the convergence rate slower. After that observation, Mustafiz et al. (2008a) investigated the time effects for a compressible fluid in a single-phase flow problem. They conducted their

experiment using Darcy's law, which was described earlier by Abou-Kassem et al. (2006). These researchers collected pressure responses for different time intervals using the interpolation of cubic spline functions and continuous functions. The time effect was more sensitive for the results with continuous functions rather than spline functions, and the pressure drop also increased with increasing time steps. In fact, for short time intervals, the relative error percentage accuracy was less in a single-phase flow system.

Based on the iteration process from Ertekin et al. (2001), Younis et al. (2010) presented a nonlinear iteration process with a converging time step and developed ideas to address nonlinear solver issues in reservoir simulation. The researchers demonstrated the robustness and computational efficiency of their proposed iteration method and the solutions were more attainable than with standard Newton's method. Also, they interpreted an algorithm for the examples of single-phase implicit residual system at different time steps by following Newton's method. Later, Li (2014) solved the nonlinear equations which arise from the fully implicit discretization of fluid flow in porous media using the standard Newton's method. They formulated, verified, and analyzed the computational efficiency of a new nonlinear solution technique for a given time step size, compared with the Sequential-Implicit Method and Newton-based iterative methods. That solution scheme had a lower computational cost without compromising the allowable time step size in each iteration. However, the proposed algorithm was based on rigorous analysis, and only nonlinear solvers could solve the order arbitrarily.

After that, Wang and Tchelepi (2013) described the time step effects for immiscible two-phase transport in porous media by a nonlinear trust-region solver, where viscous, buoyancy, and capillary forces were deemed significant. They highlighted the flux function as a nonlinear function of saturation, which was the primary source of complexity for nonlinear solvers of coupled multiphase flow and transport in porous media. The authors also described a modified Newton method, showing that two successive iterations cannot cross any trust region boundary, and demonstrating significant extensions of the inflection-point strategy for viscous dominated flows. They analyzed the discrete nonlinear transport equation using a finite-volume discretization with a phase-based upstream weighting system. Later, convergence was numerically shown for the trust region Newton method irrespective of the time step size for single-cell problems. However, they tried to overcome the limitations by

analyzing larger heterogeneous reservoir models with proper time step size and developed performance by reducing overall computational cost.

Consequently, Li and Tchelepi (2014) developed a convergent nonlinear solution technique for immiscible multiphase flow and transport in heterogeneous porous media where numerical performance was much superior to previous nonlinear solution methods and bypassed the convergence failure effectively. They also highlighted convergences difficulties (i.e. erratic time stepping, greater number of Newton steps and time steps interval), and achieved solutions for arbitrary time step sizes using Newton's method. They studied their proposed solution technique for oil/gas recovery, groundwater remediation, and carbon-dioxide sequestration related to large-scale problems in the presence of viscous, buoyancy, and capillary forces. In addition, Li and Tchelepi (2015) developed another convergent nonlinear solution technique to analyze the discrete nonlinear transport (i.e. mass conservation) equations for immiscible, incompressible, multiphase flow and transport in porous media, considered with time step size and improved the computational speed of numerical simulations. They analyzed the nonlinearities in heterogeneous domains across the viscous, buoyancy, and capillary forces in detail, which dominate the transport dynamics. The authors also pointed out heterogeneities in the capillary pressure–saturation relationship extensively using their proposed numerical solution scheme. Recently, Hamon and Tchelepi (2016) presented nonlinear ordering based solution techniques to reduce the number of iterations significantly, which lead to improvements in the entire computational cost and promoted the potential based ordering method in the presence of gravity. They introduced the Fully Implicit Method (FIM) for the temporal discretization for multiphase flow in porous media and solving large coupled systems of nonlinear algebraic equations instead of Newton-based iterations (Ortega and Rheinboldt, 1970; Deuflhard, 2004). The researchers also extended their nonlinear approach to interphase (i.e. between liquid and gas) mass transfer as a function of pressure and composition, with which the algorithm deals accurately. The detailed comparisons of the robustness and efficiency of the potential nonlinear and linear solvers for immiscible two-phase (dead oil), black oil, and compositional problems also presented. Still, researchers are working on efficient solution techniques where they utilize the time step size for each grid block in a microscopic way and save computational time in modern reservoir simulation systems.

2.2.6. Nonlinearity from the Modelling of Gas Flow in Reservoir

In gas reservoirs, modeling of pore-size distribution and understanding the pore structure of the formation are necessary for fluid-flow measurement and hydrocarbon estimation. The recovery of most reservoirs is highly dependent on the pore structure characteristics (Clarkson et al., 2013; Hu et al., 2012; Josh et al.,2012; Kuila and Prasad, 2013; Wang et al., 2014; Lin et al., 2015). To explain this issue, many researchers have investigated the pore characteristics of the formation, but failed due to the lack of proper mathematical models (Clarkson et al., 2012, 2013; Hu et al., 2012; Josh et al., 2012; Kuila and Prasad, 2013; Wang et al., 2014). Lin et al. (2015) proposed a numerical fitting model for estimating the pore volume of a shale formation under reservoir conditions and analyzed samples in qualitative and quantitative ways. Still, researchers are working continuously to represent a complete scenario of pore volume structure and its suitability in gas flow modelling.

The residual natural gas saturation also affects multiphase flow behavior in gas reservoirs and is challenging during the modelling of multiphase flow characteristics (Caudle et al., 1951; Holmgren and Morse, 1951; Gonzalez et al., 2007; Idem and Ibrahim, 2002; Roman et al., 2008, 2009). Sometimes, the pressure responses in fractured (e.g., symmetric, asymmetric, longitudinal, transverse, vertical, inclined) gas reservoirs affect the fluid flow models (i.e., analytical, semi-analytical or numerical) and exhibit nonlinear behavior (Crosby et al., 2002; Wan and Aziz, 2002; Al-Kobaisi et al., 2006; Zhu et al., 2007; Lin and Zhu, 2010; Rbeawi and Tiab, 2013; Huang et al., 2015). The situation would be more complicated with shale gas moved from tight gas reservoirs using various fracture network models (Bustin et al., 2008; Gong et al., 2011; Firoozabadi, 2012; Swami et al., 2013; Kudapa et al., 2017). Therefore, researchers and engineers need to solve highly nonlinear models. They need to obtain the fluid flow rate from the matrix to the wellbore before proceeding to model production.

2.2.7. Nonlinearity in EOR Applications

The exact flow regime in EOR applications should be determined through accurate mathematical or numerical models. A well-designed EOR method, such as miscible gas injection, also provides the exact phase behavior for multi-component fluid systems (Islam et al., 2016). The solution of the nonlinear governing equations for an unstable flow regime will carry significant value. The chances of numerical errors would be increased without any rigorous solution techniques. Moreover, the governing equations could become more and more nonlinear because of carbon-di-oxide (CO_2) sequestration, the presence of non-

Newtonian fluid flow, injecting gas and fluids for recovery, thermal-flooding, fractal permeability and porosity, phase changes during the measurement of rock and fluid properties, absorption and desorption during flooding mechanism, etc. (Mungan, 1992; Özkılıç, and Gumrah, 2009; Farajzadeh, 2009; Gogoi, 2011; Ju et al., 2012; Sheng, 2010, 2015; Jang et al., 2014; Patacchini et al., 2014; Wang et al., 2015; Sun et al., 2017). Sometimes, researcher have found semi-analytical solutions for those governing equations, which may be solved by a nonlinear solver using advanced numerical simulations (Wentao et al., 2012; Cossio et al., 2013; Wang et al., 2015).

2.3. Outline of Present Simulator Steps, Challenges and Solution Techniques

2.3.1. Present Simulator Steps

In petroleum reservoir simulation, several numerical techniques are used to find the exact and approximate solutions of the governing equations. Most of them end up with unique solutions. However, due to computational advancement, it is time to look forward to algorithms for multiple solutions and/or a cloud of solutions with high computational efficiency. This target

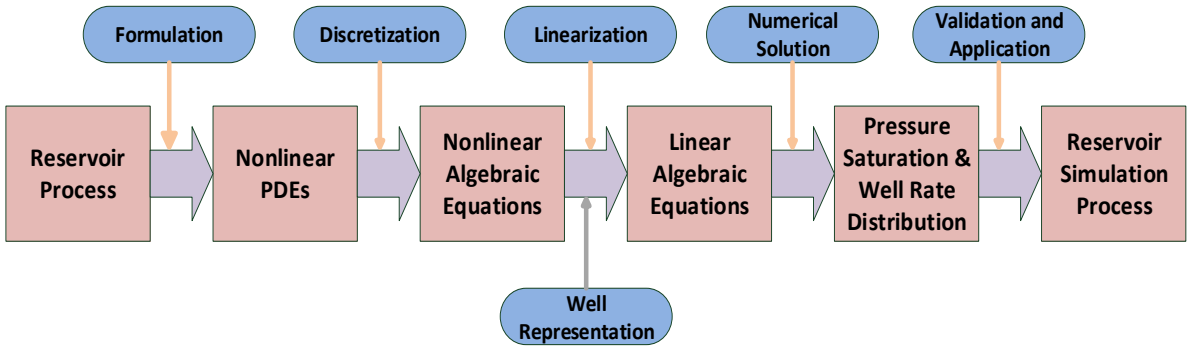

Figure 2.2: Major steps of present reservoir simulators (modified after Hossain 2012)

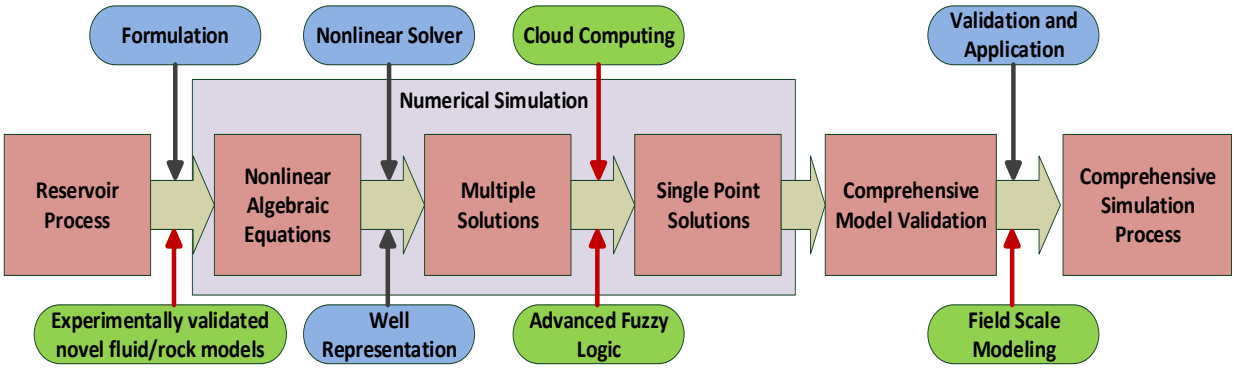

Figure 2.3: Future simulator steps for the reservoir simulation (modified after Islam et al., 2016)

may be achieved through an efficient nonlinear solver or a new scheme. According to Islam et al. (2016), the ADM (Adomian Decomposition Method) was successfully used to solve nonlinear PDEs (e.g., the Buckley-Leverett equation) and generated solutions in single-phase flow systems.

Based on Ertekin et al. (2001) and Hossain (2012), the outlook of current simulator steps is shown in Figure 2.2. In the formulation stage, the simulator describes the governing nonlinear PDEs along with the underlying assumptions and mathematical terms. The equations are discretized by following time discretization and generate a set of nonlinear algebraic equations for the choice of different schemes (e.g., old-time step, intermediate time step or new time step). Using Newton's method, the nonlinear algebraic equations are turned into linear algebraic equations, and production and injection wells for a petroleum field are defined. To get the solutions, different numerical techniques are applied to these equations. Finally, an experiment needs to be run for the validation of the model equations.

2.3.2. Challenges of the Present Simulator Steps

Most of the governing equations are in nonlinear form and need to be solved to predict reservoir performance. The current commercial computer simulators (e.g. Eclipse, CMG Suite, Tempest MORE, ExcSim, Nexus, FlowSim) use linear solvers that produce solutions by linearizing the nonlinear governing equations. Using mathematical approaches, mathematicians have provided solutions of the nonlinear equations by linearizing the governing equations and simplifying them with initial and boundary conditions (Ertekin et al., 2001). Apart from the previous approach, Abou-Kassem et al. (2006); and Abou-Kassem (2007) presented an outline of the engineering approach for solving the governing nonlinear equations. This approach showed the nonlinear equations in an integral form instead of the nonlinear algebraic equations using time and space discretization, which made the solution simpler than what mathematicians had done earlier (Figure 2.3). Besides, Mousavizadegan et al. (2006) proposed Adomian Decomposition Method (ADM) for solving nonlinear equations through computing the governing equations via the engineering approach formulation. Hence, several researchers claimed that multiple solutions are achievable for the nonlinear governing equations without linearization using the ADM (Adomian Decomposition Method) (Mustafiz and Islam, 2008; Mustafiz et al., 2008a; Islam et al., 2010, and 2016). In addition, Islam et al. (2016) raised concerns about the single point solution because cloud computing solutions for reservoirs can be achieved by advanced fuzzy logic theory. This theory will maximise the

accuracy of the unique solution using an artificial intelligence system. The comprehensive validation of the future simulator is also possible by following this theory. Here, the comprehensive term is used to consider all parameters calculation and their solution in the reservoir for a specific time and space. The approximate solutions are close to exact solutions but are not achievable due to the lack of nonlinear solvers. As further elaborated by Islam et al. (2016), these solutions without linearization revealed a number of key observations, such as (i) a broad range of operating parameters for which the nonlinear solvers predict results remarkably different from those predicted by linear solvers; (ii) the possibility of multiple solutions inherent to reservoir simulation problems; and (iii) linearization of governing equations likely to divert subsequent results, hence biasing the decision-making process irreversibly.

2.3.3. Solution Techniques for Nonlinear Algebraic Equations

From the beginning of the simulation, researchers have used different numerical methods for solving nonlinear algebraic equations in fluid flow systems. Most of those techniques consist of various assumptions, which influence the governing equations directly and make simple linear equations. Some of them are iterative, based on linearizing the governing equations, and the remainder are phase-based solution approaches. Only a few researchers have tried to apply advanced numerical techniques (e.g. ADM (Adomian Decomposition Method), Implicit Pressure Explicit Saturation (IMPES), Multilevel Nonlinear Method (MNM), Nested Iteration, etc.) without eliminating assumptions, which give reliable results rather than linear and nonlinear solver techniques and discretization approaches (e.g. Newton's Method, Secant Method, Finite Element Method (FEM), Jacobi method, Relaxation method, Gauss-Seidel method, Alternating-Direction Implicit Procedure (ADIP), Iterative ADIP, Linearized-Implicit method) (Crichlow, 1977). Here, we briefly narrate some standard techniques to solve nonlinear equations in reservoir simulation.

2.3.3.1 Techniques for Linear Equations

From the very beginning of petroleum reservoir simulation, several numerical methods have been applied to get accurate solutions, which influence the operations, forecasting performance, and computational costs of petroleum fields. These numerical methods applied to the linear algebraic equations by following two ways: (i) Direct processes (e.g., Matrix inversion, Cramer's rule, Gaussian Elimination, Gauss-Jordan method, Matrix decomposition); and (ii) Iterative Processes (e.g., the Jacobi method, Relaxation methods, and

Table 2.4: Summary of the linear equations solution techniques.

Methods	Features	Limitations	References
Matrix inversion	○ Straight forward process ○ Better elimination quality ○ Real-time simulation method	○ Very cumbersome method ○ Usable for finding unique solution	Crichlow (1977); Nash (1990); Lipschutz (1991)
Cramer's rule	○ Explicit type solution method ○ Systemic and rapid solution ○ Determinants of the matrices will never zero value ○ Only applicable when coefficient of the matrices is square	○ Numerically unstable ○ Not appropriate in Computational process ○ Concern with trivial parameters	Hoffman and Frankel (2001); Higham (2002); Shores (2007); Habgood and Arel (2012)
Gaussian elimination	○ Two-step calculation and unknown parameters are obtained from second step algorithm ○ Determine coefficient of the matrices sequentially	○ Non-efficient algorithm ○ Handle only band matrices problem ○ Do not find approximate solution ○ Numerically unstable for large number of equations and unknowns	Gentle (1998); Marc and Seymour (2001); Higham (2002); Grcar (2011)
Gauss-Jordan method	○ Directly obtain identity matrix ○ Reduced order elimination method ○ Results obtain from the matrix without back substitution	○ Increases the chance of round-off errors	Crichlow (1977); Seymour (2001); Higham (2002); Grcar (2011)
Matrix decomposition	○ Transform larger matrix problems into smaller matrix ○ Helpful for singularities in a problem ○ Better solution comes from linear algebraic equations	○ Only follows the back-substitution rules ○ Generate erroneous solutions	Choudhury and Horn (1987); Meyer (2000); Townsend and Trefethen (2015)
Jacobi method	○ Determine the solutions from diagonal systems of linear equations ○ Iterations continue until it converges.	○ Requires well-conditioned linear system for fast convergence	Bronshtein and Semendyayev (1997); Saad (2003); Yang and Mittal (2014)
Relaxation method	○ Introduce a relaxation parameter to accelerate the convergence ○ Improve the quality of solution ○ Solve PDEs by splitting and iterating until solution is found	○ Slow convergence ○ High computational cost	Jeffreys and Jeffreys (1988); Ortega and Rheinboldt (2000); Goffin (1980); Richard (2002)
Gauss-Seidel method	○ Stable method ○ Faster convergence than Jacobi method ○ Requires current approximation for unknown vector	○ Finds only one solution ○ High computational cost	Crichlow (1977); Jeffreys and Jeffreys (1988); Richard (2002)
Multigrid method	○ Reducing high frequency errors ○ Down sampling the residual error to a coarser grid ○ Interpolating on a coarser grid into finer grid ○ Number of operations is proportional to the number of unknowns for a given problem ○ Can be applied in combination with any of the common discretization techniques	○ Requires an underlying PDE problem before constructing the sequence of grids ○ Not efficient for complex geometries problem ○ Only employed to elliptic or parabolic problems	Wesseling (1992); Briggs and McCormick (2000); Shapira (2003)

the Gauss-Seidel method). In direct processes, the solution of the system of equations is obtained after the completion of a fixed number of operations. The methods are also easily compatible with pressure equations in simulation, and the algorithms are reasonably efficient. However, they have a higher possibility of round-off error and require a significant amount of computational labour (Crichlow, 1977). In contrary, the iterative processes are more efficient, with faster convergence, and provide greater levels of accuracy. Here, the solution is

generated after a systematic computation of solution approximations at each iteration step. The important features of both processes are critically analyzed and reported in Table 4. However, both processes increase the complexity and number of errors, time-steps and computational speed for all types of reservoir simulation nowadays (Ertekin et al., 2001). Due to technological advancements and higher demands for petroleum products, simulation models are more complex higher order equations, considering with all rock and fluid properties (e.g., porosity, permeability, water saturation, pressure-temperature distribution, etc.) and the linearized solution techniques are not usable here. Therefore, researchers are looking for more accurate, stable and convergent numerical solution methods or new schemes to solve these higher-order equations.

2.3.3.2 Techniques for Nonlinear Equations

Researchers have studied some techniques (e.g., IMPES (Implicit Pressure Explicit Saturation), Sequential Implicit Method (SIM), Standard Newton's method, Newton's method with heuristic solution, Continuation Newton, Ordering-based methods, ADM (Adomian Decomposition Method), MNM (Multilevel Nonlinear Method), Deflation-Nested Iteration (NI) Methods) to avoid higher-order complexity and gain rapid convergence and savings of computational time by nonlinear solvers. These nonlinear solvers are more reliable, accurate and stable than previous linearized solution techniques (Nordbotten et al., 2005b; Yavneh and Dardyk, 2006; Kwok and Tchelepi, 2007; Mustafiz et al., 2008b; Younis et al., 2010; Younis, 2011; Adler et al., 2016). This challenge can be addressed by numerical techniques along with field data interpretations and validation. The approximate solutions have been improved, reducing the problems of previous linearized solution techniques, considering local and global convergence features, solution accuracy, and stability. Here, we summarise numerical solution techniques concerning the basic principles, advantages, limitations, and significant features related to reservoir simulation.

2.3.3.2.1 IMPES and SIM methods

Aziz and Settari (1979) used SIM (Sequential Implicit Method) to solve the black oil model equations by solving for pressure using the prior time steps and computing a new total velocity field based on the pressure. The solution of pressure equations is conveniently separated in sequential solution, which permits approximation of the saturation equations (Peaceman and Rachford, 1955). After that, they solved the transport problem implicitly considering the total velocity field. Then, the fully implicit method (FIM) made both the

saturation and pressure variables implicit with respect to time and generated a solution of the resulting nonlinear algebraic equations. Later, Coats (2000) introduced the IMPES (Implicit Pressure Explicit Saturation) method where the saturation variables are explicit in time, and the pressure variables are implicit in time. IMPES (Implicit Pressure Explicit Saturation) requires a time-step limit inversely proportional to the largest fluid velocity in the reservoir due to its stability limit, and this limit is often too restrictive in practice. Later, the stability of IMPES (Implicit Pressure Explicit Saturation) was derived by Coats (2001) for multidimensional black oil and compositional models for three-phase flow. The truncation error was smaller in IMPES (Implicit Pressure Explicit Saturation) (Coats, 2001; Coats, 1968; Bansal et al., 1979). On the other side, the SIM (Sequential Implicit Method) did not suffer stability problems like IMPES (Implicit Pressure Explicit Saturation) due to the absence of capillarity. The General Purpose Reservoir Simulator (GPSIM) used SIM (Sequential Implicit Method) (Spillette et al., 1973) for more computational efficiency (Douglas et al., 1959).

2.3.3.2.2 Standard Newton's method

This is an iterative scheme where a sequence of iterations is generated to solve a nonlinear system of equations, obtained from the linearization of the original nonlinear system. At each Newton iteration, this method solves:

$$J^{\nu}\delta x^{\nu} = -R^{\nu}$$

where J denotes the Jacobian matrix, representing the derivatives of the residual with respect to the unknowns, and $\delta x^{\nu}$is the vector of Newton updates. Thus, the sequence of iterations generated starting from the beginning can be written as:

$$x^{n+1,0} = x^{n} \tag{14}$$

$$x^{n+1,\nu+1} = x^{n+1,\nu} - (J^{\nu})^{-1}R(x^{n+1,\nu}; \Delta t, x^{n}), \nu = 0,1, \dots \dots \tag{15}$$

where R denotes the vector of discrete residual equations, and Δt is the time step size. This method can be seen as an explicit first-order time stepping scheme with dynamical system defined by Deuflhard (2004) and Younis (2011) as:

$$x^{n+1,\nu} = x^{n},\ \nu = 0 \tag{16}$$

$$\frac{dx^{n+1}}{d\nu} = -(J^{\nu})^{-1}R(x^{n+1,\nu}; \Delta t, x^{n}), \nu > 0 \tag{17}$$

where the Newton iteration index (v) is considered to be a continuous quantity. A first-order explicit discretization of equation (17) results in the following discrete form representing the dynamical system:

$$x^{n+1,\nu+1} - x^{n+1,\nu} = -\Delta\nu J^{-1} R(x^{n+1,\nu}; \Delta t, x^n) \quad (18)$$

Comparison of equations (15) and (17) shows that Newton's method approximates the derivative of the new state in terms of the embedded time (v) using a first-order finite-difference scheme with a unit step size, $\Delta\nu = 1$ (Deuflhard, 2004; Younis, 2011). Since explicit first-order time stepping may be unstable due to time step restriction, Newton iterations may not converge even though the continuous Newton flows are well-behaved (Shahvali, 2012).

2.3.3.2.3. Newton's method with heuristic safeguards

In commercial simulators (e.g. Eclipse, CMG Suite, Tempest MORE, ExcSim, Nexus, FlowSim), the convergence behaviour of standard Newton's method has been improved by using heuristic solution methods; especially when buoyancy forces are influential in the fluid flow (Naccache, 1997; Nordbotten et al., 2005). In porous media, the modified Appleyard chop algorithm (e.g. used in Eclipse^{TM}) is one of the most common heuristic approaches. It is a cell-based approach, and, for any grid cell, Newton iterates for saturation from old iteration levels are updated to new iteration levels using that algorithm (Geoquest, 2005; Younis, 2011). The Buckley-Leverett 1-D displacement problem is one of the examples, to which the modified Appleyard chop algorithm has been applied. The convergence behaviour improved and the saturation is changed from immobile to mobile for the range between 0 and 1. Here, the problem is discretized implicitly and separated into 100 grid cells. The generated nonlinear problem is solved for one time-step size using standard Newton's method and the Modified Appleyard chop algorithm. The results showed that standard Newton's method converged for time-steps less than 10^{-2} PVI (pore volumes injected), whereas the modified Appleyard chop converged from the beginning of the pore volumes injection time-step sizes (Younis, 2011; Shahvali, 2012).

2.3.3.2.4. Continuation Newton Method

This method was formulated by Younis et al. (2010) and Younis (2011) to handle` the challenges in a reservoir simulator. At the initial iteration step, the time step was zero and the convergence neighbourhood was considered for increasing computational efficiency and

avoiding the iteration solution path (Shahvali, 2012). They developed the existing nonlinear methods by this approach and handled the current and upcoming challenges in physical nonlinearity in a reservoir simulator. The significant finding was removing convergence difficulties by adapting time-step sizes, which increased the computational effort and performed the iteration for small time-steps (Younis, 2011). For the Buckley-Leverett Problem, they calculated time-steps when the fractional flow was horizontal and when the fractional flow was affected by gravity effects. In both cases, time-steps influenced the governing equations and, here, the continuation Newton method converges to the solution with small time-step sizes. The results showed that a better approximation of the solution was generated for smaller time steps instead of larger time steps. In fact, the saturation changed sharply with distances and provided the worst approximation of the governing equation for large time steps (Younis et al., 2010; Younis, 2011).

2.3.3.2.5. Ordering-based methods

Appleyard and Cheshire (1982); and Natvig et al. (2006) proposed an ordering-based method to solve flow and transport equations. The approaches to the solution may be cell-based (Cascade method and Natvig's method) or use a phase-based ordering method. Cell-based approaches are considered when cells are rearranged along the direction of fluid flow and the transport equations are solved on a cell-by-cell basis sequentially. On the other hand, when ordering is performed on phase potentials due to capillarity effects, the method is known as the phase-based method.

Kwok and Tchelepi (2007) and Natvig and Lie (2008) implemented this ordering-based method for a set of multiphase flow equations in porous media, which is in nonlinear form due to gravity and capillarity effects. They also considered the linear solution step and investigated the advantages of potential ordering methods for saturation variables on large heterogeneous problems. They simplified the nonlinear algebraic equations for pressure dependence using the fully implicit method (FIM). Here, the saturation was treated as a function of pressure and was solved for using small time steps. This FIM method speeds up the solution of the nonlinear systems of algebraic equations implicitly. They also achieved real convergence for larger time steps using a reduced-order Newton’s method instead of the standard Newton’s method. Shahvali (2012) used ordering-based methods for solving flow and transport equations and faced the gravitational challenges of the counter-current flow equations efficiently.

2.3.3.2.5.1. Cascade method

Appleyard and Cheshire (1982) proposed a cell-based ordering method, known as the cascade method, which accelerates the standard Newton's method and solves the conservation equations simultaneously for pressure and saturation in a two-phase flow. Kwok (2007) and Shahvali (2012) also applied the cascade method for an incompressible 1-D modelling problem when the counter-current flow was absent.

They applied the cascade method for evaluating the pressure values without saturation iterations from higher-order cells to lower-order cells. This approach performed the sweep activity, and, for each cell phase, this method runs sequentially within each phase. Depending on the phases, the nonlinear equations would be generated for pressure and saturations. This method converges the pressure and saturation solutions in the presence of local minima and countercurrent flow in multiple dimensions. Due to poor initial guesses, the cascade method existence might not converge in real field applications and fails to provide guarantees of the local minima (Kwok, 2007; Shahvali, 2012).

2.3.3.2.5.2. Natvig's method

Natvig et al. (2006), Natvig and Lie (2008), and Shahvali (2012) presented a solution method based on discontinuous Galerkin spatial discretization to solve hyperbolic transport equations when gravity and capillarity were absent. They solved the equations by applying an optimal reordering of grid cells on a cell-by-cell basis from upstream to downstream, using a standard Newton algorithm.

This cell-based ordering method was used to solve the multiphase advection problem, when gravity and capillarity have no influences. Sometimes, this approach can be applied equally for the standard FVM (Finite Volume Method) approach (Shahvali, 2012). The cell problems consist of multiple nonlinear systems and are solved from upstream to downstream order by decoupling the system. Current reservoir simulators are also developed based on this sequential solution scheme, and computational efficiency is achieved for unified cell-based applications. However, the convergence of the solution is no longer linear due to the presence of countercurrent fluid flow, and a robust implementation would be needed at that time. In addition, for higher order nonlinear problems, the solution procedure is solely responsible for time-dependent problems and the sequential solution procedure is still undiscovered (Natvig et al., 2006; Natvig and Lie, 2008).

2.3.3.2.5.3. Phase-based potential ordering

Kwok and Tchelepi (2007) performed a rigorous mathematical analysis of 1-D problems, where the algorithm was always convergent due to the absence of counter-current flow and derived a reduced Newton algorithm for multiphase flow in porous media based on the new phase-based potential ordering. Before that, they presented an order of equations and unknowns based on phase potentials and showed that saturation dependence in the Jacobian method takes a lower-triangular form, allowing solution one unknown at a time. They also extended this approach for counter-current flow due to gravity, using different orderings corresponding to different phases. On the other hand, the reduced Newton algorithm only converges in the presence of counter-current flow with satisfaction of backward CFL conditions. This algorithm may cycle or diverge when the backward CFL number is greater than one (Kwok, 2007; Shahvali, 2012). However, this phase-based potential ordering might not be necessary in simulation for computing time-steps when the fluid flow directions are unchanged. At that time, this approach was used only for beginning time-steps counts when they could validate that ordering easily (Kwok and Tchelepi, 2007).

For the Buckley-Leverett equation, the phase-based potential ordering method only works in the presence of capillarity due to the downstream water saturation. From that governing nonlinear equation, the pressure of one phase is evaluated for another pressure phase. Therefore, they considered some preprocessing steps to avoid the downstream dependency of water saturation. Also, the gas equations are solved in the last step of the phase ordering due to the presence of countercurrent fluid flow and the gas components are mixed in the oil and gas phases (Kwok, 2007; Shahvali, 2012).

2.3.3.2.6. Adomian Decomposition Method

The ADM (Adomian Decomposition Method) is one of the potential methods to solve nonlinear equations without considering any linearization steps or inherent assumptions and provides a way for generating multiple solutions (Adomian, 1984, 1986, 1991; Wazwaz, 2001; Wazwaz and El-Sayed, 2001, Gu and Li, 2007). For reservoir engineering, ADM (Adomian Decomposition Method) is a very robust solution method for solving various equations, including algebraic, integral, differential, integrodifferential, higher-order PDEs and ODEs. This technique determines the roots of a nonlinear parameter in the governing equations and solves the nonlinearity without considering linearization or unjustified assumptions on a problem. This method provides more analytic, verifiable and rapidly

convergent approximations than other numerical methods (Wazwaz, 2001; Wazwaz and El-Sayed, 2001; El-Sayed and Abdel-Aziz, 2003). ADM (Adomian Decomposition Method) handles nonlinear problems with full strength, saving computational time (Biazar and Ebrahimi, 2005). Following this technique, Mustafiz et al. (2008b) could demonstrate the real scenario of the 1-D governing equations for single-phase flow reservoir problems. The ADM solution profile is also validated through numerous experimental studies in petroleum reservoir simulation (Whitaker, 1986 (a, b); Mustafiz et al., 2005; Mustafiz and Islam, 2005; Mustafiz et al., 2008b; Islam et al., 2010).

In the field of physics, mathematics, and medical research, ADM (Adomian Decomposition Method) attracted scientists and researchers for its deterministic and stochastic problem-solving capability, and for improved computational time (Adomian, 1986). Using ADM (Adomian Decomposition Method), the governing equations are replaced by a recursive relationship and the solution comes in a power series form. For a smaller region or grid block, the solutions converge rapidly and are more exact than any approximate solution. The accuracy of ADM (Adomian Decomposition Method) solutions also depends on the boundary conditions of the problem and interval lengths of the governing equation variables (Islam et al., 2016). However, for the Buckley-Leverett equation, ADM (Adomian Decomposition Method) solved the nonlinear part of this governing equation by using an Adomian polynomial, obtaining saturation values in terms of distance. Still, there is scope to find multiple solutions from the nonlinear Buckley-Leverett equation, and ADM (Adomian Decomposition Method) is not more feasible in that case (Mustafiz et al., 2008b; Islam et al., 2016).

2.3.3.2.7. Multilevel Nonlinear Method (MNM)

The MNM (Multilevel Nonlinear Method) is another technique for solving nonlinear problems in engineering, mathematics, physics, or other branches of science (Yavneh and Dardyk, 2006). The MNM (Multilevel Nonlinear Method) technique is less dependent on the variables in a nonlinear problem and provides a good initial approximation when Newton's methods are limited. The procedure was successfully implemented for 2-D complex phase problems and avoided the distinct behaviours which were found earlier from Newton's method and the Full Approximation Scheme (FAS). That technique eliminates the differences between global and local linearization, provides consistency through scaling analysis, and increases computational efficiency. Sometimes coefficients are non-smooth in coarse grid

approximations, and only MNM (Multilevel Nonlinear Method) solves this by direct discretization (Hackbusch, 1985; Brandt, 1977, 1982; Yavneh and Dardyk, 2006). MNM (Multilevel Nonlinear Method) is able to solve nonlinear equations by taking smaller nonlinear parts of the governing equation and providing better convergence than Newton's method and FAS (Full Approximation Scheme) (Yavneh and Dardyk, 2006). This technique is less effective for nonlinear problems in the presence of discontinuous coefficients and irregular boundary values, which indicates a significant disadvantage of this approach. By examining the nature of the problem, the MNM (Multilevel Nonlinear Method) is more capable of representing important conceptual and statistical limitations related to the problem (Brandt, 1982; Yavneh and Dardyk, 2006).

2.3.3.2.8. Deflation-Nested Iteration Method

To solve nonlinear governing equations in an efficient way, Nested Iteration (NI) is an excellent choice for nonlinear solvers. Solvers use this technique to improve computational efficiency and adopt exact solutions for specific problems by using the deflation methodology (Farrell et al., 2015). The Deflation method is an unsystematic approach, and the algorithm employed here for providing multiple solutions is obtained by modifying the nonlinear problems (Adler et al., 2016). Adler et al. (2016) presented the combined deflation NI (Nested Iteration) method for computing multiple solutions of nonlinear PDEs efficiently. They performed numerical simulations with the combined deflation NI (Nested Iteration) algorithm on liquid crystals and found multiple solutions for the nonlinear governing equations. They also investigated and demonstrated the algorithm's performance and its accuracy for different physical phenomena (i.e., bifurcation and disclination behaviours). This powerful technique reduced the overall computational cost for the solution of nonlinear PDEs. In addition, this technique works sequentially for a nonlinear problem and obtains distinct solutions from previous stages of the algorithm by eliminating the previous solutions from the nonlinear residual using a deflection projection. Here, the nonlinear solvers integrate the deflation technique with an NI (Nested Iteration) approach, improving the efficiency of the solution. This technique has mostly been applied in the branch of physics, particularly for liquid crystal problems, where the NI (Nested Iteration) approach solved coarse and fine-grid problems even with mild complexity. Using Dirichlet boundary conditions, multiple solutions are revealed sequentially, including stable and unstable local extrema and increasing the scope of solution for global minima. By blending the deflation and NI (Nested Iteration) approach, the solutions are easily detectable for both coarser and fine mesh grids, and the set of initial

Table 2.5: Comparisons of different numerical techniques.

Schemes	Why is the scheme used?	How is the scheme used?	Strength of the scheme	Accuracy level of the scheme	Limitations
FEM (Schnipke, 1986; Chaskalovic, 2008; Zienkiewicz et al., 2005)	Extensively applicable for computational fluid dynamics, structural mechanics problems	Inclusion of dissimilar material properties	Extremely powerful and useful for more complex problems	Quickly evaluate the PDEs solution at any point with high accuracy	Hard to follow calculation steps
	Smooth representation of the solution	Subdivide large problem into smaller problems	Local effects adoption	Accurate representation of complex geometry	Longer time needed
	Approximate solutions of PDEs are achievable		Faster and less expensive scheme	Visualisation is possible in detail	Less physical significance
FDM (Schnipke, 1986; Chaskalovic, 2008; Zienkiewicz et al., 2005)	Used to find the values and the problem derivatives at discrete points	Boundary conditions required	Intuitive and easy to implement into PDEs	High accuracy	Solves simple PDEs and fails to interpolate the solution
	Very easy to implement	Problem discretizes into large number of cell /grid points	Lower order approximation within each cell	Observe better formulation	Increases round-off errors
	Solutions are more accurate due to multiple parameters	Solutions are achievable by Taylor series expansion	Less expensive		Only for rectangular geometry shapes
FVM (Schnipke, 1986; Versteeg and Malalasekera, 1995; Toro, 1999; LeVeque, 2002)	Calculate the average values of the conserved variables across the volume	Boundary conditions applied to PDEs	Structured mesh is not required	Especially influential on non-uniform grids	Need more effort to solve irregular shapes
	Represent PDEs into algebraic equations	Values calculated at discrete point on each small volume mesh	Simply formulated for unstructured meshes	Strongly applicable for discrete places on a meshed geometry	Need to be aware of flux calculation
	Piece-wise linear variation may be helpful for accuracy	Need to balance the fluxes across the boundaries of individual volumes	Flux calculation at neighbouring domains provides accuracy		
EA (Islam et al., 2010, 2016; Mustafiz et al., 2008 a, b)	New technique to solve PDEs with boundary conditions	Avoid formulations step	Solve nonlinear PDEs comprehensively	Provide accurate multiple solutions	Lack of nonlinear solver
	Provides physical interpretation of forward, central and backward differences for time derivatives	Nonlinear algebraic equations come from discretized nonlinear PDEs	Reduce the time steps and inherent assumptions of a model	Solutions are convergent, stable, and consistent	Selection of efficient numerical methods
	Algebraic equations are easily attainable	Solve PDEs through bypassing linearization	Solve higher order complex nonlinearities equation	Enhance the production and recovery of oil and gas fields	Field applications

guesses for the deflation method are closer for each grid. This combination technique is still working on smaller grid problems and is challenging for higher order grid problems.

2.3.3.2.9. Legendre Method

This method is used to solve nonlinear first- and second-order PDE using separation of variables. The singularities of a problem are defined using Legendre polynomials, and the

solutions will be generated for each domain point through symmetric or antisymmetric ways. This technique is mostly used for fractional derivative calculations, multiple expansions in physics, and trigonometry from where we get many eigenvalues (Beylkin et al., 1991). Especially, the Legendre Wavelet method has presented a solution for linear and nonlinear fractional and partial differential equations which is more accurate, stable, reliable, and requires less computational effort. The convergence and boundary conditions also verified through this technique. This method was rapidly adopted within diverse fields of science and engineering and transformed boundary value problems into algebraic systems of equations (Razzaghi and Yousefi, 2001). They considered only calculus of variations for mathematic as fields and showed the validation of their proposed technique for the Brachistochrone problem. The results were excellent due to the smooth implementation of that technique and reduced the system of nonlinear algebraic equations (Razzaghi and Yousefi, 2001). Later, Ablaoui-Lahmar et al. (2014) solved PDEs using the Legendre wavelet decomposition method by considering spatial and temporal variables and reduced the time-dependent solutions into a set of ODEs. They also highlighted the resolution of differential, linear integrodifferential and fractional differential equations; and optimal control problems.

2.3.4. Fundamental Differences among Widely Used Numerical Methods

In reservoir simulation, the governing equations come from mathematical models that are solvable by various numerical and analytical methods. The solutions came from numerical methods that are understandable, and the models are used to optimise complex reservoir fluid flow processes. These applications have greatly expanded due to computational capabilities and provide a set of solutions for large problems (Chen et al., 2006). There are several methods incorporated into reservoir simulation to predict multiple solutions of nonlinear governing equations of a complex reservoir (Peaceman, 1977B; Aziz and Settari, 1979). Here, we summarised the fundamental methods (such as FDM, Finite Element Method (FEM), Finite Volume Method (FVM), Engineering Approach (EA), etc.) which are using to solve the nonlinear governing equations of the petroleum reservoirs in Table 2.5. Further, the pros and cons of different numerical methods used for solving nonlinear algebraic equations are presented in tabular form in Table 2.6. Both of these tables influence the researcher to investigate more regarding selection of numerical techniques and the solution of nonlinear algebraic equations in reservoir simulation.

2.4. DISCUSSION AND FUTURE DIRECTIONS

Nonlinearity is a challenging issue for science and engineering fields. Most researchers aim to reduce computational cost and increase the accuracy by reducing nonlinear behaviours. To mitigate these problems, they utilize several numerical techniques by considering different parameters and inherent assumptions. Based on the previous review of numerical techniques and problem descriptions, they have worked on this issue until now and tried to find more

Table 2.6: Pros and cons of different numerical methods used for solving nonlinear equations.

Techniques		Opportunities	Limitations
Newton–Raphson Method (Kelley, 2003; Lu, 2008)		○ Used in heterogeneous reservoir properties simulation ○ Count small time steps ○ Explain nonlinearities in linearizing and iterative ways ○ Produces local convergence ○ More stable than IMPES method	○ Time-consuming ○ Less accurate solver ○ Less robust technique ○ Not applicable for large time step simulation ○ Fails to obtain global convergence
IMPES (Snyder and Ramey, 1967; Chen et al., 2006)		○ Better stability ○ Require less computation time ○ Best fitted only for two-phase incompressible flow problems ○ Efficient for countercurrent problems	○ Inefficient for more nonlinear problems ○ Applicable up to two-phase fluid flows
ADM (Adomian, 1991; Holmquist, 2007; Wang and Bajaj, 2006; Waewcharoen et al., 2008)		○ Provide rapid convergent series solutions ○ Solutions are more realistic, which come from differential, delay-differential, integrodifferential, and partial differential equations. ○ A powerful method to obtain explicit and numerical solutions at a time. ○ Analytical solutions are achievable from deterministic and stochastic ODEs and PDEs. ○ Linearization is not required	○ Exhibits small region of convergence ○ Uncertain to apply to boundary value problems ○ Accuracy is dependent on the interval of the independent variable lengths (For example time)
Ordering-based methods (Appleyard and Cheshire, 1982; Shahvali, 2012; Natvig et al., 2006; Natvig and Lie, 2008; Kwok and Tchelepi, 2007; Kwok, 2007)	Cascade method	○ Pressure and saturation equations are solving for two-phase flow ○ Used individually for each phase	○ Not applicable in the presence of counter-current flow
	Natvig's method	○ Solve equations when gravity and capillary pressure are absent	○ Only solve hyperbolic equations ○ Time-consuming
	Phase-based potential ordering	○ Applicable for counter-current flow problems ○ Reduce order Newton's method follows	○ Only solved convergent problems
MNM (Yavneh and Dardyk, 2006)		○ Suitable for 1D and 2D PDE problems ○ Problem has been broken into steps or grids ○ Helpful for discontinuous and noisy problems	○ Operation cost is more expensive than other methods ○ Need another simplify model for calculation
Deflation-NI (Adler et al., 2016; Gambolati et al., 2008)		○ Useful iterative technique ○ Exhibit more inner properties and behaviour ○ Applicable for Symmetric Eigenproblems ○ Used for regular and irregular finite element grids	○ Less stability

Implicit methods (Duffy, 2004; Chen et al., 2006; Lu, 2008)	FIM	○ Accurate method for linear solver ○ Stable method ○ Used for fractured reservoirs	○ Implementation is hard ○ Higher computational cost
	SIM	○ Used for complex reservoir simulation problems ○ Solving equations implicitly without coupling ○ Suitable for compositional and chemical compositional flow problems includes chemical components	○ Less stable but more computationally effective than the SS scheme, and more stable but less efficient than the IMPES scheme ○ Can't solve the rapid change of capillary pressure problems
	Adaptive Implicit Scheme	○ Efficient at the mid-level of IMPES and SS schemes ○ The resulting equations are more efficient and stable	○ Used linearize and iterative equations ○ Time-consuming
Simultaneous Solution Method (SS) (Chen et al., 2006)		○ Solves all coupled nonlinear equations simultaneously and implicitly ○ Stable technique and can handle enormous time steps with excellent stability ○ Suitable for the black oil and thermal models	○ Analyse only a few components in the black oil and thermal models ○ Not appropriate for the compositional and chemical compositional flow problems
Legendre Wavelet Method (Beylkin et al., 1991; Razzaghi and Yousefi, 2001)		○ Analyse orthogonality properties of a reservoir ○ Exact polynomials representation up to certain degree ○ Represents the functions with different resolution levels ○ Build fast connection with numerical algorithms	○ Fail to provide analytical Solutions ○ Time sensitive with flow rate changes

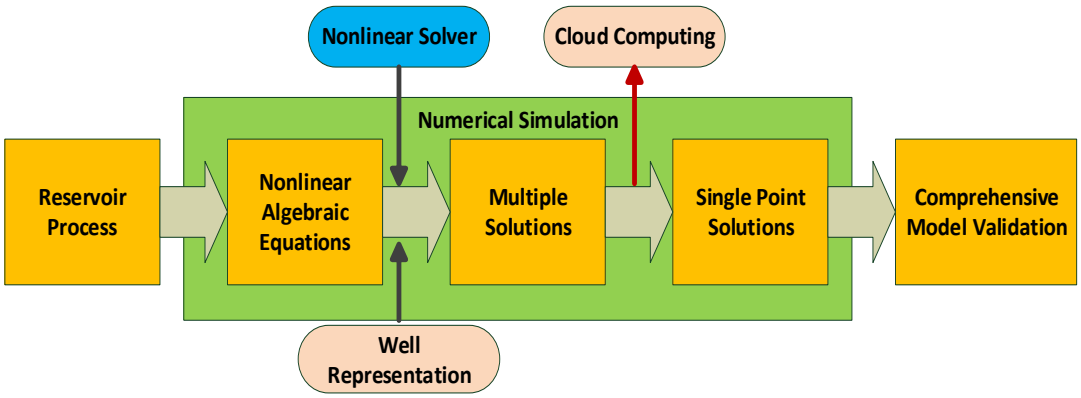

Figure 2.4: Future research scope in reservoir simulation.

accurate and efficient solutions. Among all the numerical techniques, the engineering approach and finite volume method will be adapted to solve nonlinear algebraic equations, following by time and space discretization and the eventual solution. Specifically, ordering-based methods, deflation-nested iteration, and multilevel nonlinear methods provided a clear solution for a set of nonlinear algebraic equations. The ADM (Adomian Decomposition Method) technique also tried to solve nonlinear equations, but after some steps, that method failed to provide multiple solutions. Thus, researchers are looking for stable, consistent, and accurate solutions, which raises the task for the nonlinear solver. The challenges for future

reservoir simulation steps are shown in Figure 2.4. From this figure, researchers pick nonlinear algebraic equations, which are discretized using time functions. The nonlinearity starts from that point and, using efficient numerical schemes, the solver will solve the equations and provide a set of multiple solutions. The principle focus of this research is to bypass the linearization of nonlinear algebraic equations and reduce assumptions on the governing equations. Later, the solutions will be stored in the reservoir cloud system and validated comprehensively by future researchers. Moreover, the solver will check the stability, convergence, and accuracy of the solutions, and will find single solutions for the governing equations. Finally, this solution will work for developing a reservoir emulator and predicting future reservoir performance in the petroleum industry.

2.5. CONCLUSIONS

This article presents critical reviews on nonlinearity problems and solution techniques in petroleum reservoir simulation. This study also accumulates the significance of nonlinearity by discussing stepwise nonlinear equation development, solution strategies and the pros and cons for various solution schemes. The authors also point out the scope of research in terms of governing equation parameters and solution scheme variables. Finally, the authors show future research directions by sequential analysis of current reservoir simulator steps and addressing their challenges.

NOMENCLATURE

1-D	One-dimensional
2-D	Two-dimensional
3-D	Three-dimensional
A_{xz}	Cross-sectional area of rock perpendicular to the flow of flowing fluid, m^2
A	Area of the cross-section for a sample volume
a	Parameter in Carreau–Yasuda model, dimensionless
B_o	Oil formation volume factor, $m^3(std.m)^{-3}$
C	Total compressibility of the system, $1/Pa$
c_f	$c_0 + c_w =$ total fluid compressibility of the system, $1/Pa$
c_t	$c_f + c_s =$ total compressibility of the system, $1/Pa$
c_s	Formation rock compressibility of the system, $1/Pa$
c_w	Formation water compressibility of the system, $1/Pa$

$\frac{du_x}{dy}$	Velocity gradient along *y*-direction, $1/sec$
D_x	Lateral diffusion terms
D_y	Transfer diffusion terms
$D_t^{1-\gamma}$	Grunwald-Letnikov (G-L) operator
E	Activation energy for viscous flow, KJ/mol
F	Wetting phase flux
f_w	Fractional flow rate
g	Gravitational acceleration, ft/sec^2
J	Jacobian matrix
k	Initial reservoir permeability, m^2
k_{ro}	Relative permeability of oil
k_{rw}	Relative permeability of water
M_a	Marangoni number
n	Power-law exponent for Carreau–Yasuda model, dimensionless
p	Pressure of the system, N/m^2
p_{i-1}	Pressure of gridblock i-1, psia [kPa]
p_i	Pressure of grid block i, psia [kPa]
p_{i+1}	Pressure of grid block i+1, psia [kPa]
p_i^n	Pressure of grid block i at time t^n, psi [kPa]
p_i^{n+1}	Pressure of grid block i at time t^{n+1}, psi [kPa]
P_e	Peclet number
p_c	Capillary force: pressure difference between oil phase and water phase
q	Total flow rate of oil and water
R	Universal gas constant, KJ/mole – K
S_w	Wetting phase saturation
T	Temperature, *K*
T	Time, *s*
t	Time, sec
$T_{x_{i+\frac{1}{2}}}$	Transmissibility between block i and i + 1
$T_{x_{i-\frac{1}{2}}}$	Transmissibility between block i and i - 1
u_x	Fluid velocity in porous media in the direction of x-axis, *m/s*

V_{b_i} Bulk volume of grid block i, ft^3

y Distance from the boundary plan, m

Greek alphabet

α Fractional order of differentiation, known as Memory

α_c Volume conversion factor = 5.614583 for customary units or 1 for SPE preferred SI units

α_d Thermal diffusivity, m^2/sec

α_{SF} Shape factor which is medium-dependent

β_c Transmissibility unit conversion factor (dimensionless)

Γ Euler gamma function

Δp Pressure difference

ΔT $T_T - T_0 =$ Temperature difference, K

Δt Time step, s

Δx Grid block size, m

δx^v Vector of Newton updates

η Ratio of the pseudo-permeability of the medium with memory to fluid viscosity, $m^3 s^{1+\alpha}/kg$

λ Time constant in Carreau–Yasuda model, s

μ_0 Fluid dynamic viscosity at reference temperature, $T_0, Pa - sec$

μ_w Water viscosity

μ_∞ Fluid dynamic viscosity at infinite shear rate, pa-s

ξ A dummy variable for time, i.e., real part in the plane of the integral, s

$\Delta\xi$ Dummy time step, s

ρ_0 Density of the fluid at reference temperature T_0, kg/m^3

ρ_w Water density

σ Surface tension, N/m

$\left|\frac{d\sigma}{dT}\right|$ The derivative of surface tension α with temperature; can be positive or negative, depending on the substance, $N/m - K$

τ_T Shear stress at temperature T, Pa

ϕ Porosity of fluid media, m^3/m^3

v Newton iteration index

ACKNOWLEDGEMENTS

The authors would like to thank the Natural Sciences and Engineering Research Council of Canada (NSERC); Research & Development Corporation of Newfoundland and Labrador (RDC), funding no. 210992; and Statoil Canada Ltd., funding no. 211162 for providing financial support to accomplish this research under the Statoil Chair in Reservoir Engineering at the Memorial University of Newfoundland, St. John's, NL, Canada.

DECLARATIONS OF INTEREST

All authors have seen and approved the final version of the manuscript submitted. We warrant that the article is original work, has not received prior publication and is not under consideration for publication elsewhere. Finally, the authors have no conflict of interest.

REFERENCES

Ablaoui-Lahmar, N., Belhamiti O., and Bahri S.M., 2014. A new Legendre wavelets decomposition method for solving PDEs. Int. J. Math. Sci. Comp. App. 1(1), 72 – 81.

Aboudheir, A., Kocabas, I., and Islam, M.R., 1999. Improvement of numerical methods in petroleum engineering problems. Proc. IASTED Int. Conf., Applied Modelling and Simulation, Cairns, Australia.

Abou-Kassem, J., 2007. Engineering approach vs the mathematical approach in developing reservoir simulators. J. Nat. Sci. Sust. Tech. 1(1), 35 – 68.

Abou-Kassem, J.H., Farouq Ali, S.M., and Islam, M.R., 2006, Petroleum Reservoir Simulation: A Basic Approach, Gulf Publishing Company, Houston, USA.

Adler, J.H., Emerson, D.B., Farrell, P.E., and Maclachlan, S.P., 2016. Combining deflation and nested iteration for computing multiple solutions of nonlinear variational problems. (**In Press**)

Adomian, G., 1984. A new approach to nonlinear partial differential equations. J. Math. Anal. Appl. 102, 420 – 434.

Adomian, G., 1986. Nonlinear Stochastic Operator Equations. San Francisco: Academic Press.

Adomian, G., 1991. A review of the decomposition method and some recent results for nonlinear equations. Computers Math. Applic. 21(5), 101 – 127.

Al-Kobaisi, M., Ozkan, E., Kazemi, H., 2006. A hybrid numerical-analytical model of finite-conductivity vertical fractures intercepted by a horizontal well. SPE Reserv. Eval. Eng. (Aug.), 345.

Al-Mutairi, S.M., Sidqi, A.A., and Hossain, M.E., 2014. A new rigorous mathematical model to describe immiscible CO_2 oil flow in porous media. J. Porous Media. 17(5), 421 – 429.

Appleyard, J.R., and Cheshire, I.M., 1982. The cascade method for accelerated convergence in implicit simulators. In European Petroleum Conference. Society of Petroleum Engineers.

Aziz, K., and Settari, A., 1979. Petroleum Reservoir Simulation. Applied Science Publishers, New York.

Bansal, P.P., McDonald, A.E., Moreland, E.E., and Trimble, R.H., 1979. A strongly coupled, fully implicit three-dimensional, three phase reservoir simulators. SPE-8329-MS, SPE Annual Technical Conference and Exhibition, 23-26 September, Las Vegas, Nevada.

Bartley, J.T., and Ruth, D.W., 1999. Relative permeability analysis of tube bundle models, Transport Porous Med. 36, 161–187.

Bentsen, R.G., 1978. Conditions under which the capillary term may be neglected. J. Canadian Pet. Tech. 17(04).

Beylkin, G., Coifman, R., and Rokhlin, V., 1991. Fast wavelet transforms and numerical algorithms – I. Communications on Pure and Applied Mathematics. 44(2), 141–183.

Biazar, J., and Ebrahimi, H., 2005. An approximation to the solution of hyperbolic equations by Adomian decomposition method and comparison with characteristics method. Applied mathematics and computation, 163(2), 633 – 638.

Blunt, M., and King, P., 1991. Relative permeabilities from two- and three-dimensional pore-scale network modeling, Transport Porous Med. 6, 407–433.

Bokhari, K., and Islam, M.R., 2005. Improvement in the time accuracy of numerical methods in petroleum engineering problems: A new combination. Energy Sources, 27(1-2), 45 – 60.

Brandt, A., 1977. Multi-level Adaptive solutions to boundary-value problems. Math. Comp., 31, 333 – 390.

Brandt, A., 1982. Guide to Multigrid Development, in Multigrid Methods. W. Hackbusch and U. Trottenberg, eds., Springer-Verlag, Berlin. pp. 220 – 312.

Briggs, W.L., and McCormick, S.F., (2000), A multigrid tutorial. Vol. 72. Siam.

Bronshtein, I.N., and Semendyayev, K.A., 1997. Handbook of Mathematics, third ed. Springer-Verlag, New York. 892.

Broszeit, J., 1997. Finite element simulation of circulating steady flow for fluids of the memory-integral type: Flow in a single-screw extruder. J. Non-Newtonian Fluid Mech. 70(1-2), 35 – 58.

Buckley, S.E., and Leverett, M.C., 1942. Mechanism of fluid displacement in sands. Trans. AIME, 146, 187 – 196.

Bustin, R.M., Bustin, A.M.M., Cui, X., Ross, D.J.K., Pathi, V.S.M., 2008. Impact of shale properties on pore structure and storage characteristics. SPE – 119892, SPE Shale Gas Production Conference, Ft. Worth, TX, USA, 16–18.

Caputo, M., 1998a. 3-Dimensional physically consistent diffusion in anisotropic media with memory. Rend. Mat. Acc. Lincei. 9(9), 131 – 1443.

Caputo, M., 1999. Diffusion of fluids in porous media with memory. Geothermics, 23, 113 – 130.

Caputo, M., 2000. Models of flux in porous media with memory. Water Resour. Res., 36(3), 693 – 705.

Caputo, M., and Cametti, C., 2009. The memory formalism in the diffusion of drugs through skin membrane. J. Phys. D Appl. Phys. 42, 125505 – 125512. doi: 10.1088/0022-3727/42/12/125505

Caputo, M., and Fabrizio, M., 2015. A new definition of fractional derivative without singular Kernel, Progr. Fract. Differ. Appl. 1(2), 73 – 85.

Caudle, B.H., Slobod, R.L., and Brownscombe, E.R., 1951. Further developments in the laboratory determination of relative permeability. Trans. AIME 192, 145.

Chandler, R., Koplik, J., Lerman, K., and Willemsen, J.F., 1982. Capillary displacement and percolation in porous media, J. Fluid Mech. 119, 249–267.

Chaskalovic, J., 2008. Finite Elements Methods for Engineering Sciences. Springer-Verlag.

Chatzis, I., and Dullien, F.A.L., 1977. Modelling pore structure by 2-D and 3-D networks with application to sandstones, J. Can. Petrol. Tech. 16(1), 97–108.

Chatzis, I., and Dullien, F.A.L., 1982. Mise en oeuvre de la the´orie de la Percolation pour mode´ liser le drainage des milieux de la perme´abilite´ relative au liquide non mouillant injecte´, Revue del' Institut Franc¸ais duPetrole, 37, 183–205.

Chen, M., Rossen, W., and Yortsos, Y.C., 2005. The flow and displacement in porous media of fluids with yield stress. J. Chem. Engg. Sci. 60, 4183 – 4202.

Chen, Z., Huan, G., and Ma, Y., 2006. Computational Methods for Multiphase Flows in Porous Media. SIAM, Philadelphia, PA 19104-2688, USA.

Choudhury, D., and Horn, R.A., 1987. A complex orthogonal-symmetric analog of the polar decomposition. SIAM, J. Algebraic Discrete Methods. 8(2). doi: 10.1137/0608019.

Ciarletta, M., and Scarpetta, E., 1989. Minimum problems in the dynamics of viscous fluids with memory. Int. J. Engg. Sci. 27(12), 1563 – 1567.

Clarkson, C.R., Solano, N., Bustin, R.M., Bustin, A.M.M., Chalmers, G.R.L., He, L., Melnichenko, Y.B., Radlinski, A.P., and Blach, T.P., 2013. Pore structure characterization of North American shale gas reservoirs using USANS/SANS, gas adsorption, and mercury intrusion. Fuel 103, 606-616.

Coats, K.H., 1968. Computer Simulation of Three-Phase Flow in Reservoirs. University of Texas, Austin, USA.

Coats, K.H., 2000. A note on IMPES and some IMPES-based simulation models. SPE-65092-PA, SPE Journal, 5(3), 245 – 251.

Coats, K.H., 2001. IMPES stability: The stable step. SPE-69225-MS, SPE Reservoir Simulation Symposium, 11-14 February, Houston, Texas.

Cossio, Manuel, Moridis, George, Blasingame, Thomas A., 2013. A semi-analytic solution for flow in finite-conductivity vertical fractures by use of fractal theory. SPE J. 18 (1), 83-96. SPE 153715-PA.

Craft, B.C., and Hawkins, M.F., 1991. Applied Petroleum Reservoir Engineering, second ed. Prentice Hall Inc., USA.

Crichlow, H.B., 1977. Modern Reservoir Engineering: A Simulation Approach. Prentice-Hall, Inc., New Jersey, 354.

Crosby, D.G., Rahman, M.M., Rahman, M.K., et al., 2002. Single and multiple transverse fracture initiation from horizontal wells. J. Pet. Sci. Eng 35 (3-4), 191-204.

Deuflhard, P., 2004. Newton Methods for Nonlinear Problems: Affine Invariance and Adaptive Algorithms. No. 35. Berlin: Series in Computational Mathematics, Springer-Verlag.

Diaz, C.E., Chatzis, I.,and Dullien, F.A.L., 1987. Simulation of capillary pressure curves using bond correlated site correlated site percolation on a simple cubic network, Transport Porous Med. 2, 215–240.

Dong, M., Dullien, F.A.L., and Zhou, J., 1998. Characterization of waterflood saturation profiles history by the 'complete' capillary number, Transport Porous Med. 31, 213–237.

Dong, M., Dullien, F.A.L., Dai, L., and D. Li, 2005. Immiscible displacement in the interacting capillary bundle model, Part I. Development of interacting capillary bundle model. Transport in Porous Media, 59, 1 – 18.

Duffy, D.J., 2004. A Critique of the Crank-Nicolson Scheme Strengths and Weaknesses for Financial Instrument Pricing. Wilmott Magazine, 68 – 76.

Douglas, J., Jr., Peaceman, D.W., and Rachford, H.H., Jr., 1959. A method for calculating multi-dimensional immiscible displacement. Trans. AIME, 216, 297 – 308.

EIA, 2016. U.S. Energy Information Administration/Monthly Energy Review.

Eringen, A.C., 1991. Memory dependent orientable nonlocal micropolar fluids. Int. J. Engg. Sci. 29(12), 1515 – 1529.

Ertekin, T., Abou-Kassem, J.H., and King, G.R., 2001. Basic Applied Reservoir Simulation. SPE Textbook Series, vol. 7. Richardson, TX: SPE.

Farajzadeh, R., Andrianov, A., and Zitha, P.L.J., 2009) Investigation of immiscible and miscible foam for enhancing oil recovery. Industrial & Engineering Chemistry Research, 49(4), 1910-1919.

Farrell, P.E., Birkisson, A., and Funke, S.W., 2015. Deflation techniques for finding distinct solutions of nonlinear partial differential equations. SIAM J. Sci. Comput. 37, 2026 – 2045.

Fayers, F.J., and Sheldon, J.W., 1959. The effect of capillary pressure and gravity on two-phase fluid flow in a porous medium.

Firoozabadi, A., 2012. Nano-particles and nano-pores in hydrocarbon energy production. Research talk delivered at University of Calgary, December 07.

Gambolati, G., Pini, G., and Putti, M., 1995. Nested iterations for symmetric eigen problems. SIAM J. Sci. Comput. 16(1), 173 – 191. doi:10.1137/0916012

Gentle, J.E., 1998. Gaussian Elimination in Numerical Linear Algebra for Applications in Statistics. Berlin: Springer-Verlag. 87 – 91.

Geoquest, S., 2005. Eclipse technical description. Multi-Segment Wells.

Goffin, J.L., 1980. The relaxation method for solving systems of linear inequalities. Math. Oper. Res., 5(3), 388 – 414. doi:10.1287/moor.5.3.388.

Gogoi, S.B., 2011) Adsorption–desorption of surfactant for enhanced oil recovery. Transport in porous media, 90(2), 589-604. DOI 10.1007/s11242-011-9805-y

Gong, B., Qin, G., L, Bi., X, Wu., 2011. Multiscale and multi physics methods for numerical modeling of fluid flow in fractured formations. SPE 143590. SPE EUROPEC Annual Technical Conference and Exhibition, Vienna, Austria, USA, 23-26.

Gonzalez, D.L., Vargas, F.M., Hirasaki, G.J., and Chapman, W.G., 2007. Modeling study of CO_2 induced Asphaltene precipitation. Energy Fuel 22 (2), 757–762.

Grcar, J.F., 2011. Mathematicians of Gaussian elimination. Notices of the American Mathematical Society. 58(6), 782 – 792.

Gu, H., and Li, Z., 2007. A modified Adomian method for system of nonlinear differential equations. Appl. Math. Comput. 187, 748 – 755.

Habgood, K., and Arel, I., 2012. A condensation-based application of Cramer's rule for solving large-scale linear systems. J. Discrete Algorithms. 10, 98–109. doi: 10.1016/j.jda.2011.06.007.

Hackbusch, W., 1985. Multi-grid Methods and Applications. Springer-Verlag, Berlin.

Hamon, F.P., and Tchelepi, H.A., 2016. Ordering-based nonlinear solver for fully implicit simulation of three-phase flow. J. Comp. Geosci. Springer, 20(3), 475 – 493. doi: 10.1007/s1059601595058

Hassan, A.M., and Hossain, M.E., 2016. A numerical study of temperature profile by coupling memory-based diffusivity model with energy balance during thermal flooding. J. Pet. Environ. Biotech. 7(5), 1 – 7. doi: 10.4172/2157-7463.1000300

Higham, N.J., 2002. Accuracy and Stability of Numerical Algorithms, second ed. SIAM. 13.

Hoffman, J.D., and Frankel, S., 2001. Numerical Methods for Engineers and Scientists, second ed. CRC Press, 30.

Holmgren, C.R., and Morse, R.A., 1951. Effect of free gas saturation on oil recovery by water flooding. J. Pet. Tech. 3(05), 135 – 140.

Holmgren, C.R., and Morse, R.A., 1951. Effect of free gas saturation on oil recovery by waterflooding. Trans AIME 192, 135.

Holmquist, S., 2007. An Examination of the Effectiveness of the Adomian Decomposition Method in Fluid Dynamic Applications. Ph.D. Dissertation, University of Central Florida, USA. **[Unpublished]**

Hossain, M.E., 2012. Comprehensive modeling of complex petroleum phenomena with an engineering approach. J. Porous Media. 15(2), 173 – 186.

Hossain, M.E., 2016a. Modified engineering approach toward the development and solution of memory-based diffusivity equation. J. Comp. Math. App., Elsevier (**In press**).

Hossain, M.E., 2016b. Numerical investigation of memory-based diffusivity equation: the integro-differential equation. Arabian J. Sci. and Engg. 41(7), 2715 – 2729. doi: 10.1007/s13369-016-2170-y.

Hossain, M.E., and Abu-Khamsin, S.A., 2012a. Utilization of memory concept to develop heat transfer dimensionless numbers for porous media undergoing thermal flooding with equal rock-fluid temperatures. J. Porous Media. 15(10), 937 – 953.

Hossain, M.E., and Abu-Khamsin, S.A., 2012b. Development of dimensionless numbers for heat transfer in porous media using memory concept. J. Porous Media. 15(10), 957 – 973.

Hossain, M.E., and Islam, M.R., 2006. Fluid Properties with memory: A critical review and some additions. Proc. 36th Int. Conf. Computers and Industrial Engg. CIE–00778, Taipei, Taiwan, 20 – 23.

Hossain, M.E., and Islam, M.R., 2009. A comprehensive material balance equation with the inclusion of memory during rock-fluid deformation. Adv. Sustai Pet. Eng. Sci., 1(2):141-162.

Hossain, M.E., and Islam, M.R., 2010a. Knowledge-based reservoir simulation: A novel approach. Intl. J. Eng. 3(6), 622 – 638.

Hossain, M.E., Liu, L., and Islam, M.R., 2009b. Inclusion of the memory function in describing the flow of shear-thinning fluids in porous media. Int. J. Engg., 3(5), 458 – 477.

Hossain, M.E., Mousavizadegan, S.H. Ketata, C., and Islam, M.R., 2007. A novel memory-based stress-strain model for reservoir characterization. J. Nat. Sci. Sust. Tech. 1(4), 653-678.

Hossain, M.E., Mousavizadegan, S.H., and Islam M.R., 2009. Variation of rock and fluid temperature during thermal operations in porous media. J. Pet. Sci. Tech. 27, 597 – 611.

Hossain, M.E., Mousavizadegan, S.H., and Islam, M.R., 2008. A new porous media diffusivity equation with the inclusion of rock and fluid memories. SPE–114287-MS, SPE.

Hossain, M.E., Mousavizadegan, S.H., and Islam, M.R., 2009a. Modified engineering approach with the variation of permeability over time using the memory concept. Proc. 3rd Intl. Conf. on Modeling, Simulation, and Applied Optimization, Paper no. 41-77246, UAE.

Hossain, M.E., Mousavizadegan, S.H., and Islam, M.R., 2009c. Effects of memory on the complex rock-fluid properties of a reservoir stress-strain model. J. Pet. Sci. Technol. 27(10), 1109 – 1123.

Hovanessian, S.A., and Fayers, F.J., 1961. Linear water flood with gravity and capillary effects. Society of Petroleum Engineers Journal, 1(01), 32 – 36.

Hu, Q., Ewing, R.P., and Dultz, S., 2012. Low pore connectivity in natural rock. J. Contam. Hydrol. 133, 76-83.

Huang, T., Guo, X., and Chen, F., 2015. Modeling transient pressure behavior of a fractured well for shale gas reservoirs based on the properties of nanopores. J. Nat. Gas Sci. Engg., 23, 387-398.

Idem, R.O., and Ibrahim, H.H., 2002. Kinetics of CO_2 induced Asphaltene precipitation from various Saskatchewan crude oils during CO_2 miscible flooding. J. Pet. Sci. Eng. 35 (3–4), 233–246.

Islam, M.R., 2008. Without the science of intangibles: The Earth is still flat. J. Physics: Conference Series. 96, 12 – 19. doi:10.1088/1742-6596/96/1/012019

Islam, M.R., and Nandakumar, K., 1986. Multiple solution for buoyancy-induced flow in saturated porous media for large Peclet numbers. Trans. ASME, Ser. C: J. Heat Transfer. 108(4), 866 – 871.

Islam, M.R., and Nandakumar, K., 1990. Transient convection in saturated porous layers with internal heat sources. Intl. J. Heat Mass Transfer. 33(1), 151 – 161.

Islam, M.R., Moussavizadegan, S.H., Mustafiz, S., and Abou-Kassem, J.H., 2010. Advanced Petroleum Reservoir Simulation, Scrivener Publishing, Wiley, USA.

Islam, M.R., Hossain, M.E., Mousavizadeghan, H., Mustafiz, S., and Abou-kassem, J.H., 2016. Advanced Reservoir Simulation: Towards Developing Reservoir Emulators, second ed. Scrivener-Wiley, 592.

Jang, S.H., Liyanage, P.J., Lu, J., Kim, D.H., Arachchilage, G.W., Britton, C., Weerasooriya, U., and Pope, G.A., 2014. Microemulsion phase behavior measurements using live oils at high temperature and pressure. In SPE Improved Oil Recovery Symposium.

Jeffreys, H., and Jeffreys, B.S., 1988. Relaxation Methods, Methods of Mathematical Physics, third ed. Cambridge, England: Cambridge University Press, pp. 307 – 312.

Jordan, A.J., 2006. Linearization of non-linear state equation. Bull. Pol. Ac. Sci.: Tech. Sci., 54(1), 63 – 73.

Josh, M., Esteban, L., Delle Piane, C., Sarout, J., Dewhurst, D.N., and Clennell, M.B., 2012. Laboratory characterization of shale properties. J. Petrol. Sci. Eng. 88-89, 107-124.

Ju, B., Wu, Y. S., Qin, J., Fan, T., and Li, Z., 2012. Modeling CO2 miscible flooding for enhanced oil recovery. Petroleum Science, 9(2), 192-198.

Kelley, C.T., 2003. Solving nonlinear equations with Newton's method. Fundamentals of Algorithms, SIAM. doi: 10.1137/1.9780898718898

Kudapa, V.K., Sharma, P., Kunal, V., and Gupta, D.K., 2017. Modeling and simulation of gas flow behavior in shale reservoirs. J. Petrol. Explor. Prod. Technol., 1-18. doi 10.1007/s13202-017-0324-4

Kuila, U., and Prasad, M., 2013. Specific surface area and pore-size distribution in clays and shales. Geophys. Prospect. 61, 341-362.

Kumar, A., and Unny, T.E., 2002. Application of Runge-Kutta method for the solution of non-linear partial differential equations. Applied Mathematical Modelling, doi:10.1016/0307-904X(77)90006-3

Kwok, F., 2007. Scalable Linear and Nonlinear Algorithms for Multiphase Flow in Porous Media, Ph.D. Dissertation, Stanford University, Stanford, USA.

Kwok, F., and Tchelepi, H.A., 2007. Potential-based reduced Newton algorithm for nonlinear multiphase flow in porous media. J. Comp. Phy. 227, 706 – 727. doi: 10.1016/j.jcp.2007.08.012

Lapidus, G.R., Lane, A.M., Ng, K.M., and Corner, W.C., 1985. Chem. Eng. Commun. 38, 33.

Lee, S.H., Wolfsteiner, C., and Tchelepi, H.A., 2008. Multiscale finite-volume formulation for multiphase flow in porous media: Black oil formulation of compressible, three-phase flow with gravity. J. Comput. Geosci. 12, 351 – 366. doi: 10.1007/s10596-007-9069-3

LeVeque, R., 2002. Finite Volume Methods for Hyperbolic Problems, Cambridge University Press.

Li, B., and Tchelepi, H.A., 2014. Unconditionally convergent nonlinear solver for multiphase flow in porous media under viscous force, buoyancy, and capillarity. Energy Procedia, 59, 404 – 411.

Li, B., and Tchelepi, H.A., 2015. Nonlinear analysis of multiphase transport in porous media in the presence of viscous, buoyancy, and capillary forces. J. Comp. Phy., 297, 104 – 131. doi: 10.1016/j.jcp.2015.04.057.

Li, H.Z., Frank, X., Funfschilling, D., and Mouline, Y., 2001. Towards the understanding of bubble interactions and coalescence in non-Newtonian fluids: A cognitive approach. J. Chem. Engg. Sci. 56, 6419 – 6425.

Li, Z., 2014. An efficient solver for nonlinear multiphase flow based on adaptive coupling of flow and transport, 14th European Conference on the Mathematics of Oil Recovery (ECMOR), Italy.

Lin, B., Chen, M., Jin, Y., and Pang, H., 2015. Modeling pore size distribution of southern Sichuan shale gas reservoirs. J. Nat. Gas Sci. Engg., 26, 883-894.

Lin, J., Zhu, D., 2010. Modeling well performance for fractured horizontal gas wells. In: Paper Presented at the International Oil and Gas Conference and Exhibition in China, Beijing, China. http://dx.doi.org/10.2118/130794-ms. SPE 130794.

Lipschutz S., (1991), Invertible Matrices, Schaum's Outline of Theory and Problems of Linear Algebra, second ed. New York: McGraw-Hill, pp. 44 – 45.

Liu, J., Bodvarsson, G.S., and Wu, Y., 2003. Analysis of flow behavior in fractured lithophysical reservoirs. J. Contaminant Hydrology, 62-63, 189 – 211.

Lu, B., 2008. Iteratively Coupled Reservoir Simulation for Multiphase Flow in Porous Media, Ph.D. Dissertation, The University of Texas at Austin, USA.

Lu, J., and Hanyga, A., 2005. Wave field simulation for heterogeneous porous media with singular memory drag force. J. Compu. Phy. 208, 651 – 674.

Marc, L., and Seymour, L., 2001. Schaum's Outline of Theory and Problems of Linear Algebra, New York: McGraw-Hill, pp. 69 – 80.

Mathews, J.H., 1992. Numerical Methods for Mathematics, Science, and Engineering, second ed. New Jersey: Prentice Hall.

Melrose, J.C., and Brandner, C.F., 1974. Role of capillary forces in determining microscopic displacement efficiency for oil recovery by waterflooding. J. Canadian Pet. Tech. 13, 54 – 62.

Meyer, C.D., 2000. Matrix Analysis and Applied Linear Algebra, SIAM.

Mifflin, R.T., and Schowalter, W.R., 1986. A numerical technique for three-dimensional steady flow of fluids of the memory-integral type. J. Non-Newtonian Fluid Mech. 20, 323 – 337.

Morrow, N.R., 1970. Irreducible wetting phase saturations in porous media. J. Chem. Engg. Sci. 25, 1799 – 1815.

Mousavizadegan, S.H., Mustafiz, S., and Rahman, M., 2006. The Adomian decomposition method on solution of non-linear partial differential equations. J. Nat. Sci. Sust. Tech. 115 – 131.

Mungan, N., 1992. Carbon dioxide flooding as an enhanced oil recovery process. J. Can. Petro. Tech., 31(09).

Mustafiz, S., and Islam, M.R., 2005. Adomian decomposition of two-phase, two-dimensional non-linear PDEs as applied in well testing, Proc. 4th Int. Conf. Comp. Heat and Mass Trans. Paris-Cachan, May 17–20.

Mustafiz, S., and Islam, M.R., 2008. State of the art petroleum reservoir simulation. J. Pet. Sci. Technol. Taylor and Francis, 26, 1303 – 1329. doi: 10.1080/10916460701834036

Mustafiz, S., Biazar, J., and Islam, M.R., 2005. An Adomian decomposition solution to the modified Brinkman model (MBM) for a two-dimensional, one-phase flow of petroleum fluids, Proc. CSCE 33rd Annual Conf., Toronto, ON, Canada, June 02–04.

Mustafiz, S., Moussavizadeghan, H., and Islam, M.R., 2008b. Adomian decomposition of Buckley-Leverett equation with capillary effects. J. Pet. Sci. Technol., Taylor and Francis, 26(15), 1796 – 1810. doi:10.1080/10916460701426049

Mustafiz, S., Moussavizadeghan, S.H., and Islam, M.R., 2008a. The effects of linearization on solutions of reservoir engineering problems. J. Pet. Sci. Technol., Taylor and Francis, 26, 1224 – 1246. doi: 10.1080/10916460701833905

Naami, A.M., Catania, P., and Islam, M.R., 1999. Numerical and experimental modelling of viscous fingering in two-dimensional consolidated porous medium. Paper – 118, CIM Conference, Regina.

Naccache, P.F., 1997. A fully-implicit thermal reservoir simulator. In SPE Reservoir Simulation Symposium. Society of Petroleum Engineers.

Nash, J.C., 1990. Compact Numerical Methods for Computers: Linear Algebra and Function Minimisation, second ed. Bristol, England: Adam Hilger, pp. 24 – 26.

Natvig, J.R., and Lie, K.A., 2008. Fast computation of multiphase flow in porous media by implicit discontinuous Galerkin schemes with optimal ordering of elements. J. Comp. Phy. 227(24), 10108 – 10124.

Natvig, J.R., Lie, K.A., and Eikemo, B., 2006. Fast solvers for flow in porous media based on discontinuous Galerkin methods and optimal reordering. Proc. XVI Int. Conf. Comp. Meth. Water Re., Copenhagen, Denmark (Vol. 2).

Nibbi, R., 1994. Some properties for viscous fluids with memory. Int. J. Engg. Sci. 32(6), 1029 – 1036.

Nooruddin, H.A., Hossain, M.E., Al-Yousef, H., and Okasha, T., 2014. Comparison of permeability models using mercury injection capillary pressure data on carbonate rock samples. J. Pet. Sci. Engg. 121, 9 – 22.

Nordbotten, J.M., and Celia, M.A., 2006. Similarity solutions for fluid injection into confined aquifers. J. Fluid Mech. 561, 307 – 327.

Nordbotten, J.M., Celia, M.A., and Bachu, S., 2005. Injection and storage of CO_2 in deep saline aquifers: analytical solution for CO_2 plume evolution during injection. Transp. Porous Media, 55, 339 – 360.

Obembe, A.D., Abu-Khamsin, S.A., and Hossain, M.E., 2016a. A review of modeling thermal displacement processes in porous media, Arab. J. Sci. Eng. 41, 4719 – 4741. doi: 10.1007/s13369-016-2265-5

Obembe, A.D., Hossain, M.E., and Abu-Khamsin, S.A., 2016c. Variable-order derivative time fractional diffusion model for heterogeneous porous media. J. Pet. Sci. Engg. (**In press**).

Obembe, A.D., Hossain, M.E., Mustapha, K., and Abu-Khamsin, S.A., 2016b. A modified memory-based mathematical model describing fluid flow in porous media. J. Comp. Math. App. doi: 10/1016/j.camwa.2016.11.022

Ortega, J.M., and Rheinboldt, W.C., 1970. Iterative Solution of Nonlinear Equations in Several Variables, New York: Academic Press.

Ortega, J.M., and Rheinboldt, W.C., 2000. Iterative Solution of Nonlinear Equations in Several Variables, Classics in Applied Mathematics, Philadelphia, SIAM.

Özkılıç, Ö.İ., and Gumrah, F., 2009. Simulating CO2 sequestration in a depleted gas reservoir. Energy Sources, Part A, 31(13), 1174-1185.

Patacchini, L., De Loubens, R., Moncorge, A., and Trouillaud, A., 2014. Four-fluid-phase, fully implicit simulation of surfactant flooding. SPE Reservoir Evaluation & Engineering, 17(02), 271-285.

Peaceman, D.W., 1977B. Fundamentals of Numerical Reservoir Simulation, Elsevier, New York.

Peaceman, D.W., and Rachford, H.H.Jr., 1955. The numerical solution of parabolic and elliptic differential equations. SIAM. 3(1), 28 – 41.

Razzaghi, M., and Yousefi, S., 2001. Legendre wavelets method for the solution of nonlinear problems in the calculus of variations. J. Math. Comp. Model. Elsevier, 34, 45 – 54.

Rbeawi, S.A., Tiab, D., 2013. Pressure behaviours and flow regimes of a horizontal well with multiple inclined hydraulic fractures. Int. J. Oil. Gas Coal Technol. 6 (1/2), 207-241.

Richard, S.V., 2002. Matrix Iterative Analysis, second ed., Prentice Hall, Springer-Verlag.

Roman, B., Guillermo Ramon, C., Lars, K., and Leonid, M.S., 2008. Modelling CO2 Injection: IOR Potential After Waterflooding. SPE/DOE Symposium on Improved Oil Recovery. Society of Petroleum Engineers, Tulsa, Oklahoma, USA.

Roman, B., Guillermo, R.C.-G., and Leonid, M.S., 2009. Simulating CO2 EOR process: Numerical investigation based on the experimental results. SPE International Conference on CO2 Capture, Storage, and Utilization. San Diego, California, USA.

Saad, Y., 2003. Iterative Methods for Sparse Linear Systems, second ed., SIAM. p. 414.

Saghir, Z., Chaalal, O., and Islam, M.R., 2000. Experimental and numerical modeling of viscous fingering. J. Pet. Sci. Eng. 26(1-4), 253 – 262.

Scheidegger, A.E., 1953. Theoretical models of porous matter, Producers Monthly, 17–23.

Schmid, K.S., Geiger, S., and Sorbie, K.S., 2011. Semianalytical solutions for cocurrent and countercurrent imbibition and dispersion of solutes in immiscible two-phase flow. Water Resources Research, 47(2).

Schnipke, R.J., 1986. A Streamline Upwind Finite Element Method for Laminar and Turbulent Flow, Ph.D. Dissertation, University of Virginia, USA.

Shahvali, M., 2012. Ordering-based Nonlinear Solver with Adaptive Coupling for Multiphase Flow and Transport, Ph.D. Dissertation, Stanford University, USA.

Shapira, Y., (2003), Matrix-Based Multigrid for Locally Refined Meshes. In Matrix-Based Multigrid. Springer, Boston, MA, 133-166.

Sheng, J. J. (2010). Optimum phase type and optimum salinity profile in surfactant flooding. Journal of Petroleum Science and Engineering, 75(1), 143-153.

Sheng, J. J. (2015). Status of surfactant EOR technology. Petroleum, 1(2), 97-105.

Shin, M., Kim, D.S., and Lee, J.W., 2003. Deposition of inertia-dominated particles inside a turbulent boundary layer. Int. J. Multiphase Flow. 29, 893 – 926.

Shores, T.S., 2007. Applied Linear Algebra and Matrix Analysis, Springer Science & Business Media, p. 132.

Slattery, J.C., 1967. Flow of viscoelastic fluids through porous media, J. AIChE. 1066 – 1077.

Snyder, R.W., and Ramey, Jr.H.J., 1967. Application of Buckley-Leverett displacement theory to non-communicating layered systems, SPE-1645-PA, J. Petro. Tech. 19(11). doi: 10.2118/1645-PA

Spillette, A.G., Hillestad, J.G., and Stone, H.L., 1973. A high stability sequential solution approach to reservoir simulation, SPE-4542-MS, SPE of AIME, 30 September-03 October, Las Vegas, Nevada.

Sun, X., Zhang, Y., Chen, G., and Gai, Z., 2017. Application of Nanoparticles in Enhanced Oil Recovery: A Critical Review of Recent Progress. Energies, 10(3), 345.

Swami, V., Settari, A., and Aguilera, R., 2013. Modeling of stress dependent permeability tensor with pressure depletion/injection for fractured reservoirs. SPE-164839-MS, SPE EUROPEC, London, UK. doi:10.2118/164839-MS

Toro, E.F., 1999. Riemann Solvers and Numerical Methods for Fluid Dynamics, Springer-Verlag.

Townsend, A., and Trefethen, L.N., 2015. Continuous analogues of matrix factorizations, Proc. R. Soc. A, 471 (2173). doi: 10.1098/rspa.2014.0585

Versteeg, H.K., and Malalasekera, W., 1995. An Introduction to Computational Fluid Dynamics: The Finite Volume Method. Reading, MA: Addison-Wesley.

Waewcharoen, S., Boonyapibanwong, S., and Koonpraserf, S., 2008. Applications of 2-D nonlinear shallow water model of tsunami by using Adomian decomposition method. CP1048, Int. Conf. Numerical Analysis and Applied Mathematics, American Institute of Physics.

Wan, J., Aziz, K., 2002. Semi-analytical well model of horizontal wells with multiple hydraulic fractures. SPE J. 7 (4), 437-445.

Wang, F., and Bajaj, A.K., 2006. Adomian decomposition method applied to nonlinear normal modes of an inertially coupled conservative system. J. Vibration and Control, 14(1-2), 107 – 134. doi: 10.1177/1077546307079401

Wang, W., Su, Y., Sheng, G., Cossio, M., and Shang, Y., 2015. A mathematical model considering complex fractures and fractal flow for pressure transient analysis of fractured horizontal wells in unconventional reservoirs. J. Nat. Gas Sci. Engg., 23, 139-147.

Wang, X., and Tchelepi, H.A., 2013. Trust-region based solver for nonlinear transport in heterogeneous porous media. J. Comp. Phy. 253, 114 – 137. doi: 10.1016/j.jcp.2013.06.041

Wang, Y., Zhu, Y., Chen, S., and Li, W., 2014. Characteristics of the nanoscale pore structure in northwestern Hunan shale gas reservoirs using field emission scanning electron microscopy, high-pressure mercury intrusion, and gas adsorption. Energy Fuels 28, 945-955.

Wardlaw, N.C., McKellar, M., and Li, Y., 1988. Pore and throat size distribution determined by mercury porosimetry and by direct observation, J. Carbonates and Evaporites, 3, 1 – 15.

Wazwaz, A., 2001. A new algorithm for calculating Adomian polynomials for nonlinear operators. J. App. Math. Comp. 111(1), 33 – 51.

Wazwaz, A.M., and El-Sayed, S.M., 2001. A new modification of Adomian decomposition method for linear and nonlinear operators. J. App. Math. Comp. 122(3), 393 – 405.

Welge, H.J., 1952. A simplified method for computing oil recovery by gas or water drive. J. Pet. Tech. 4(04), 91 – 98.

Wentao, Zhou, Banerjee, Raj, Dale Poe, Bobby, Spath, Jeff, Thambynayagam, Michael, 2012. Semi-analytical production simulation of complex hydraulic fracture network. Presented at International Production and Operations Conference & Exhibition. Doha, Qatar. 157367-MS

Wesseling, P., (1992), An introduction to multigrid methods. sl Wiley. New York.

Whitaker, S., 1986a. Flow in porous media I: A theoretical derivation of Darcy's law. J. Transp. Porous Media, 1, 3 – 25.

Whitaker, S., 1986b. Flow in porous media II: The governing equations for immiscible two–phase flow. J. Transp. Porous Media, 1, 105 – 125.

Yang, X., and Mittal, R., 2014. Acceleration of the Jacobi iterative method by factors exceeding 100 using scheduled relaxation. J. Comp. Phy. doi: 10.1016/j.jcp.2014.06.010.

Yavneh, I., and Dardyk, G., 2006. A multilevel nonlinear method. SIAM, J. Sci. Comp., 28(1), 24 – 46. doi: 10.1137/040613809

Young, L.C., and Stephenson, R.E., 1983. A generalized compositional approach for reservoir simulation. SPE J., 23(5), 727 – 742.

Younis, R., Tchelepi, H.A., and Aziz, K., 2010. Adaptively localized continuation Newton method: Nonlinear solvers that converge all the time. SPE-119147, USA, 15(02), 526 – 544.

Younis, R.M., 2011. Modern advances in software and solution algorithms for reservoir simulation, Ph.D. Dissertation, Stanford University, USA.

Yuster, S.T., 1951. Theoretical considerations of multiphase flow in idealized capillary systems, In: Proceedings of the 3rd World Petroleum Congress, Section II, The Hague, pp. 437 – 445.

Zhu, D., Magalhaes, F.V., Valko, P., 2007. Predicting the productivity of multiple fractured horizontal gas wells. In: Paper Presented at the SPE Hydraulic Fracturing Technology Conference, College Station, Texas USA. SPE 106280-MS.

Zienkiewicz, O.C., Taylor, R.L., and Zhu, J.Z., 2005. The Finite Element Method: Its Basis and Fundamentals, Butterworth-Heinemann.

CHAPTER 3

Finite-Volume Solution of the Buckley-Leverett Equation

[1]Pulok Kanti Deb, [2]Scott MacLachlan, [1]Syed Ahmad Imtiaz and [1]M. Enamul Hossain

[1]Department of Process Engineering, Memorial University of Newfoundland, NL, Canada
[2]Department of Mathematics and Statistics, Memorial University of Newfoundland, NL, Canada

Abstract

The Buckley-Leverett equation is an important model of displacement mechanisms for efficient petroleum recovery. This mechanism follows the relative permeability concept through an immiscible process. Many researchers have studied this equation by neglecting the complexity of parameters, utilising them in calculating recovery factors and improvement of efficiency in the form of linearised solution techniques. The present research aims to represent all salient features that are complex in nature and solve the governing equation using advanced numerical methods. Here, an analytical solution is generated through the method of characteristics, where the saturation curves are observed for the governing equation (assuming zero capillary pressure gradient and gravitational forces). Later, the Lax-Friedrichs finite volume scheme is applied to solve the model equation numerically. This finite volume scheme is checked by a simple explicit calculation, demonstrating that the local Lax-Friedrichs scheme is consistent with the governing equation. Based on both computational techniques, a single-valued solution is achievable for the Buckley-Leverett equation, and we present the propagation of saturation profiles during the displacement of oil by water in a petroleum reservoir. This saturation profile also indicates the shock position, from where the displacement of oil will decrease and, the results can be used to optimise water injection in order to good recovery from petroleum reservoir.

Keywords: The Buckley-Leverett equation, method of characteristics, Lax-Friedrichs scheme, reservoir simulation.

3.1. INTRODUCTION

The Buckley-Leverett equation is one of the more popular models for fluid flow displacement in porous media. This model equation can simulate waterflooding injection processes under various reservoir conditions. Many numerical schemes can handle waterflooding modelled in this way when the nonlinear capillary pressure term is negligible (Yortsos and Fokas, 1983). This nonlinear term leads to numerical instabilities in many mathematical models. Further, the saturation calculated using the Buckley-Leverett equation may be a multiple-valued function

for each position in the fluid flow direction with the progression of time. The interpretation of multiple-valued saturation indicates that the saturation-distance curve had become discontinuous in the displacement process. In addition, capillary forces have significant influences on fluid distribution in the macroscopic flow behaviour (Singh, 1970). We consider a nonlinear solver and try to solve the Buckley-Leverett equation for a single-valued discontinuous solution of the immiscible oil displacement. For validation, an analytical solution is needed for the Buckley-Leverett equation with given initial and boundary conditions. Finding an exact solution (including the capillary pressure term) through analytical methods is closely related to numerical schemes and their resolution (Deb et al., 2017). The analytical result will help to identify numerical tools for solving the Buckley-Leverett equation, reducing the capillary effects during the solution stage.

3.1.1. Background of the Research

In reservoir engineering, many equations express nonlinear behaviors due to effects of the time interval, variation in fluid and formation properties (e.g., porosity, permeability, water saturation, viscosity), distribution of pressure responses, and simplification of the governing equations at formulation stage or the feasibility of multiple solutions. Islam and Nandakumar (1986, 1990) showed the nonlinear behaviour of the governing equations in petroleum reservoir engineering and simulation. To avoid nonlinearity, engineers and researchers have solved the governing equations using linearised methods (e.g., Taylor series expansion, Optimal linearization method, Global linearization method, Perturbation theory, Newton's Iteration) along with some assumptions (Jordan, 2006). These procedures help researchers to understand the simulation model and control system design methods quickly. However, linearization effects can be significant, and results may not be accurate due to the wrong prediction of the parameter distribution and other errors. The interpretation of simulation models is also affected by neglecting higher order roots and other assumptions (Islam et al., 2016, and Deb et al., 2017).

Based on this, the present study offers analytical and numerical solutions for the Buckley-Leverett equation in immiscible displacement. This work contains capillary pressure effects, finding consistent solutions, which is state-of-the-art in modelling oil/water displacement processes. Therefore, a suitable mathematical method for solving the Buckley-Leverett equation and generating approximate solutions are the new scope of research which are addressed in this study.

3.1.2. Literature Review

Immiscible fluid flow and displacement in porous media have a significant role during natural resources recovery (especially for petroleum products), waste disposal and contamination transport evaluation (Wu et al., 1993). Due to the presence of multiple parameters, the fluid phases show complexities during these processes, and it is more challenging for multiphase flow rather than single phase flow. Since the 1940's, several researchers have made some contributions on this issue. Until today, however, researchers face the problem of solving the nonlinear complexities of the Buckley-Leverett equation. This theory was first introduced by Buckley and Leverett (1942) to fractional flow, where the solution gives a sharp front saturation profile along the fluid flow direction. Capillary pressure and gravitational forces were neglected. They found multiple-valued saturation as time progresses. A few years later, Holmgren and Morse (1951) presented the average water saturation calculation, explaining the nonlinear parameters in the Buckley-Leverett equation. After that, Welge (1952) developed a simple graphical approach by considering the uniform initial saturation and determining the saturation front. After that, Sheldon and Cardwell (1959) used the method of characteristics for solving the water saturation problem, as previously described by Buckley-Leverett. At the same time, Fayers and Sheldon (1959) addressed the Buckley-Leverett equation by including the effects of gravity and capillary pressure on a linear waterflood driven reservoir, but detailed steps were not presented. Hovanessian and Fayers (1961) also considered capillary pressure effects in their applied numerical models. Codreanu et al. (1966) presented the solution of non-capillary immiscible displacement for heterogeneous media. Other researchers (Chen, 1988; Yortsos and Fokas, 1983; McWhorter and Sunada, 1990, Wu et al., 1993) also presented analytical solutions by incorporating capillary pressure effects. Moreover, Craft and Hawkins (1991) introduced fluid distributions in a single homogeneous porous medium for various time intervals and found multiple values for water saturation along the fluid flow directions. These authors neglected gravity and the capillary pressure terms in their calculations. Due to the effects of linearization, Mustafiz et al. (2008a, 2008b) solved the nonlinear Buckley-Leverett equation (1942), considering capillary pressure effects and presented their solution for 1-D, two-phase flow using the Adomian decomposition method (ADM). However, they did not show any stability analysis for their proposed solution. Arabzai and Honma (2013) demonstrated Buckley-Leverett's theory in quantitative ways, avoiding capillary pressure effects during the numerical solution, both in finite difference (FDM) and finite element (FEM)

methods. Later, Helvig (2013 - Unpublished) also investigated capillary pressure effects in a fractured reservoir, but could not present details of the solution procedure.

Therefore, it is a challenge for researchers to analyse the governing equations in analytical and numerical methods simultaneously. The present research is trying to address capillary pressure effects along the fluid flow directions and solve the governing equation through simplified analytical and numerical solution methods. The authors also discuss the correlations between the fractional flow of water and water saturation and define the flux function for the Buckley-Leverett equation.

3.1.3. Objectives of the Research

Nonlinearity increases the complexity of reservoir operations and reduces performance when applying simulation technologies. It also raises computational costs, taking more time to complete. An efficient numerical technique can handle nonlinear parameters and enhance petroleum recovery.

In the Buckley-Leverett equation, the effects of capillary pressure were not extensively covered in the existing literature. Even solution procedures are not presented in detail. Therefore, the present author aims to solve the model equation using numerical methods, showing the steps in detail. In this research, the primary objective is to find analytical solutions for the Buckley-Leverett equation and, later, to develop an efficient numerical method, which will give a stable, consistent and more accurate solution. It is also necessary to solve the resulting nonlinear algebraic equations in time and space dimensions. A nonlinear solver reduces the time step and error level with better algorithms for the equations. A nonlinear solver should also maintain the stability and consistency of a solution process.

3.2. RESEARCH METHODOLOGY

The Buckley-Leverett equation (1942) gives hyperbolic and parabolic partial differential equation (PDE) characteristics for two-phase flow in porous media when the capillary forces are neglected and considered respectively (Koch, 1992). Here, both hyperbolic and parabolic equations are first order in time and in the spatial variables (White and Subramanian, 2010). Therefore, the method of characteristics and the local Lax-Friedrichs finite volume technique are used to solve the differential equation in finite domains.

Here, the method of characteristics is used to solve PDEs that are hyperbolic in nature and mostly applies to first-order equations, though it is valid for any hyperbolic type PDEs. The curves that are generated by this method are known as characteristics curves along which the PDEs are transformed into a family of ordinary differential equations (ODEs). These curves help to find the solutions of the ODEs and, subsequently, the solutions of the PDEs. In this research, the characteristics curves show the saturation profiles in the (x, t) plane for the Buckley-Leverett equation.

Further, we apply the local Lax-Friedrichs finite volume scheme for computing saturation values, explicitly discretizing the Buckley-Leverett equation considering a one-dimensional horizontal reservoir where there are no capillary and gravitational forces. We neglect implicit schemes for their programming complexity, requiring more computational effort in each time step, although they allow for large time steps. The stability and accuracy are of concern for explicit schemes, requiring the time- and space step sizes to be (roughly) equivalent to ensure stability and accuracy. Finally, we compare the analytical and numerical solutions for different saturation values by presenting graphical plots.

3.3. GOVERNING EQUATIONS

The Buckley-Leverett equation can be written as:

$$\frac{\partial S_w}{\partial t} + \frac{q}{A\phi}\frac{\partial f_w}{\partial S_w}\frac{\partial S_w}{\partial x} = 0 \tag{1}$$

where f_w is defined as the fractional flow of water, given by:

$$f_w = \left(\frac{1}{1+\frac{k_{ro}\mu_w}{k_{rw}\mu_o}}\right)\left(1 + \frac{Akk_{ro}}{q\mu_o}\left[\frac{\partial P_c}{\partial x} - (\rho_w - \rho_o)gsin\alpha\right]\right) \tag{2}$$

where α is the angle of the fluid flow direction.

The ratio of effective permeability to viscosity is defined as the mobility (λ), which is given for water and oil, respectively:

$$\lambda_w = \frac{kk_{rw}}{\mu_w} \tag{3}$$

$$\lambda_o = \frac{kk_{ro}}{\mu_o} \tag{4}$$

The mobility ratio (M) for oil and water is defined by:

$$M = \frac{\lambda_o}{\lambda_w} = \frac{k_{ro}\mu_w}{k_{rw}\mu_o} \quad (5)$$

According to Islam et al. (2016), the assumptions associated with the Buckley-Leverett equation are as follows: (i) two-phase flow; (ii) incompressible porous medium; (iii) oil and water phases are incompressible; (iv) constant porosity; (v) constant cross-sectional area; (vi) no external sources or sinks in the porous medium; and (vii) fractional flow of water is fully dependent on the water saturation.

Eq. [2] can be written as:

$$f_w = \frac{1}{1+M} \quad (6)$$

when the flow is horizontal $(sin\alpha = 0)$ and the effects of capillary pressure are negligible $\left(\frac{\partial P_c}{\partial x} = 0\right)$.

The relative permeability of water and oil are related to the water saturation in the following form (Islam et al., 2016):

$$k_{rw} = a_1 S_{wn}^{n1} \quad (7)$$

$$k_{ro} = a_2(1 - S_{wn})^{n2} \quad (8)$$

where the normalised water saturation (Al-Mutairi et al., 2012; Islam et al., 2016) is defined as:

$$S_{wn} = \frac{S_w - S_{w\,initial}}{1 - S_{w\,initial} - S_{or}} \quad (9)$$

If we consider the effects of capillary pressure in a horizontal reservoir $(sin\alpha = 0)$, Eq. [2] can be written as:

$$f_w = \left(\frac{1}{1+\frac{k_{ro}\mu_w}{k_{rw}\mu_o}}\right)\left(1 + \frac{Akk_{ro}}{q\mu_o}\frac{\partial P_c}{\partial x}\right) \quad (10)$$

For immiscible displacement, capillary pressure is a function of water saturation (Leverett, 1941). The relationship is written in the following form:

$$P_c = f(S_w) \quad (11)$$

Differentiating both sides of Eq. [11] with respect to displacement distance, x, the equation takes the form as:

$$\frac{\partial P_c}{\partial x} = \frac{\partial P_c}{\partial S_w}\frac{\partial S_w}{\partial x} = f'(S_w)\frac{\partial S_w}{\partial x} \quad (12)$$

To solve Eq. [1] analytically with f_w given as in Eqns. [10] and [11], is very complicated and time-consuming. Systematic solutions for higher-order nonlinear differential equations are usually not possible. Therefore, researchers are always looking for numerical techniques that are less time-consuming and offer a complete approximate solution. In this research, we apply the method of characteristics (MOC) to determine the shock wave location and speed for a simplified equation (assuming there is no capillary pressure gradient and zero gravitational force) and, later, solve the equation numerically using the local Lax-Friedrichs scheme. The main reason to avoid Eq. [10] is that the method of characteristics works only for first-order equations to get the analytical solution. In addition, the local Lax-Friedrichs technique is also conservative and provides an accurate result for first-order PDEs.

3.3.1. Correlation between Fractional Flow of Water (f_w) and Water Saturation (S_w)

Using Eqs. [5], [7] and [8], the mobility ratio can be written as:

$$M = \frac{k_{ro}\mu_w}{k_{rw}\mu_o} = \frac{a_2(1-S_{wn})^{n2}\mu_w}{a_1 S_{wn}^{n1}\mu_o} \quad (13)$$

Differentiating Eq. [9] with respect to water saturation gives –

$$\frac{\partial S_{wn}}{\partial S_w} = \frac{1}{1-S_{w_{initial}}-S_{or}} \quad (14)$$

Again, differentiating both sides of Eq. [6] with respect to water saturation and incorporating Eq. [14] yields –

$$\frac{\partial f_w}{\partial S_w} = \frac{\partial}{\partial S_w}\left(\frac{1}{1+M}\right)$$

$$\Rightarrow \frac{\partial f_w}{\partial S_w} = -\frac{1}{(1+M)^2}\frac{\partial M}{\partial S_w}$$

$$\Rightarrow \frac{\partial f_w}{\partial S_w} = -\frac{1}{(1+M)^2}\frac{\partial M}{\partial S_{wn}}\frac{\partial S_{wn}}{\partial S_w}$$

$$\Rightarrow \frac{\partial f_w}{\partial S_w} = -\frac{1}{(1+M)^2}\frac{1}{\left(1-S_{w_{initial}}-S_{or}\right)}\frac{\partial M}{\partial S_{wn}} \quad (15)$$

Differentiating both sides of Eq. [13] with respect to normalized water saturation gives:

$$\frac{\partial M}{\partial S_{wn}} = -\frac{\left(\mu_o a_1 n1 (S_{wn})^{n1-1}\right)\left(\mu_w a_2 (1-S_{wn})^{n2}\right)+\left(\mu_o a_1 (S_{wn})^{n1}\right)\left(n2\mu_w a_2 (1-S_{wn})^{n2-1}\right)}{\left(\mu_o a_1 S_{wn}^{n1}\right)^2} \quad (16)$$

Based on the Corey model (Johansen, 2008 (Unpublished)), $n1$ and $n2$ are called the Corey indices. Values between 1.5 and 2.5 are commonly used. In this case, Eq. [16] is simplified while taking $n1 = 0$ and $n2 = 1$

$$\frac{\partial M}{\partial S_{wn}} = -\frac{(\mu_o a_1)(\mu_w a_2)}{(\mu_o a_1)^2} = -\frac{\mu_w a_2}{\mu_o a_1} \tag{17}$$

From Eqs. [15] and [17],

$$\frac{\partial f_w}{\partial S_w} = \frac{1}{(1+M)^2}\frac{1}{(1-S_{w_{initial}}-S_{or})}\frac{\mu_w a_2}{\mu_o a_1} = \frac{\mu_w a_2}{(1+M)^2(1-S_{w_{initial}}-S_{or})\mu_o a_1} \tag{18}$$

Eq. [18] indicates that there is no relationship between the fractional flow of water (f_w) and water saturation (S_w) for these values of $n1$ and $n2$. To solve this issue, we consider the mobility ratio along with oil and water viscosities for different saturation values, while the remaining parameters are treated as constant values. This correlation is used during the solution of the discretisation scheme and for finding the shock speed along with breakthrough time.

3.3.2. Analytical Solution using the Method of Characteristics (MOC)

3.3.2.1. Determination of Characteristic Curve for the Water Saturation

To calculate the petroleum recovery efficiency for an immiscible displacement process, the Buckley-Leverett equation is:

$$\frac{\partial S_w}{\partial t} + \frac{q}{A\phi}\frac{\partial f_w}{\partial x} = 0 \tag{19}$$

For a simple waterflood model, the water injects into the reservoir and Eq. [19] becomes

$$\frac{\partial S_w}{\partial t} + \frac{q}{A\phi}\frac{\partial f_w}{\partial S_w}\frac{\partial S_w}{\partial x} = 0 \tag{20}$$

Here, we take q, A, and ϕ to be constant.

Let,

$$a = \frac{q}{A\phi}\frac{\partial f_w}{\partial S_w} \tag{21}$$

From Eq. (20),

$$\frac{\partial S_w}{\partial t} + a\frac{\partial S_w}{\partial x} = 0 \tag{22}$$

This equation is a one-dimensional (1-D) linear equation. From Eq. [22], the right moving wave solution is given by

$$S_w(x,t) = f(x - at) \tag{23}$$

Using the chain rule, the exact solution of $S_w(x(t),t)$ changes along a curve in the xt-plane by following equation,

$$\frac{d}{dt}S_w(x(t),t) = \frac{\partial S_w}{\partial x(t)}\frac{dx(t)}{dt} + \frac{\partial S_w}{\partial t} \tag{24}$$

Comparing Eqs. [22] and [24], the slope of this curve is defined by

$$\frac{dx(t)}{dt} = a \tag{25}$$

If the saturation of water has travelled the distance from x_0 to x over the time t, then Eq. [25] can be written in the following form

$$x = x_0 + at \tag{26}$$

where the slope is a. These curves are depicted in Figure 3.1(a-c). This figure does not represent any rarefaction or shock wave solution, but simply, the characteristics along which the solution is constant. The solution moves faster at larger slope value and moves slowly at lower slope values. Those are illustrated in Figure 3.1(a-c). Both cases, the slope is uniform along these curves, and the governing PDE equation changes into ODE form along these curves in the xt plane (Figure 3.1(a-c)).

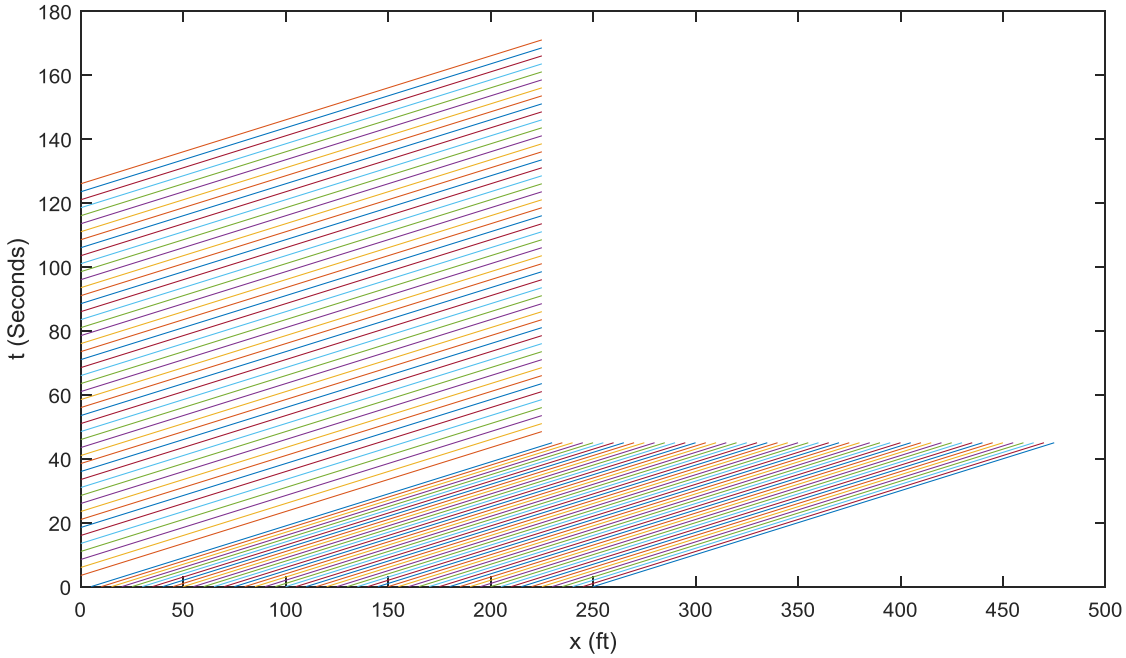

(a) For slope, $a = 5$

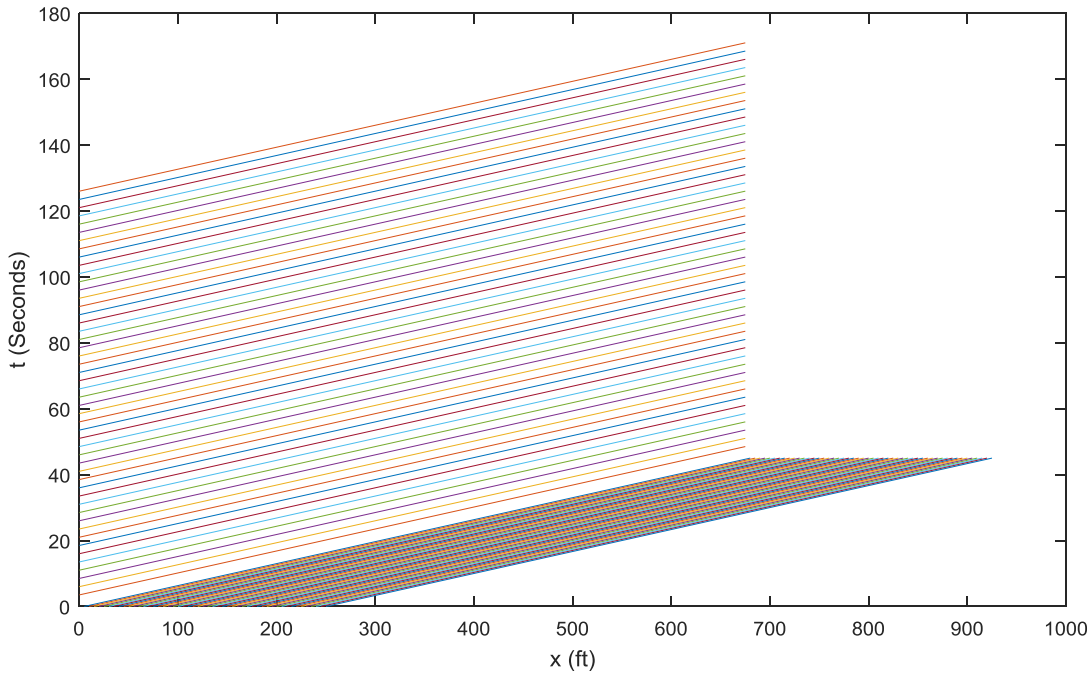

(b) For slope, $a = 10$

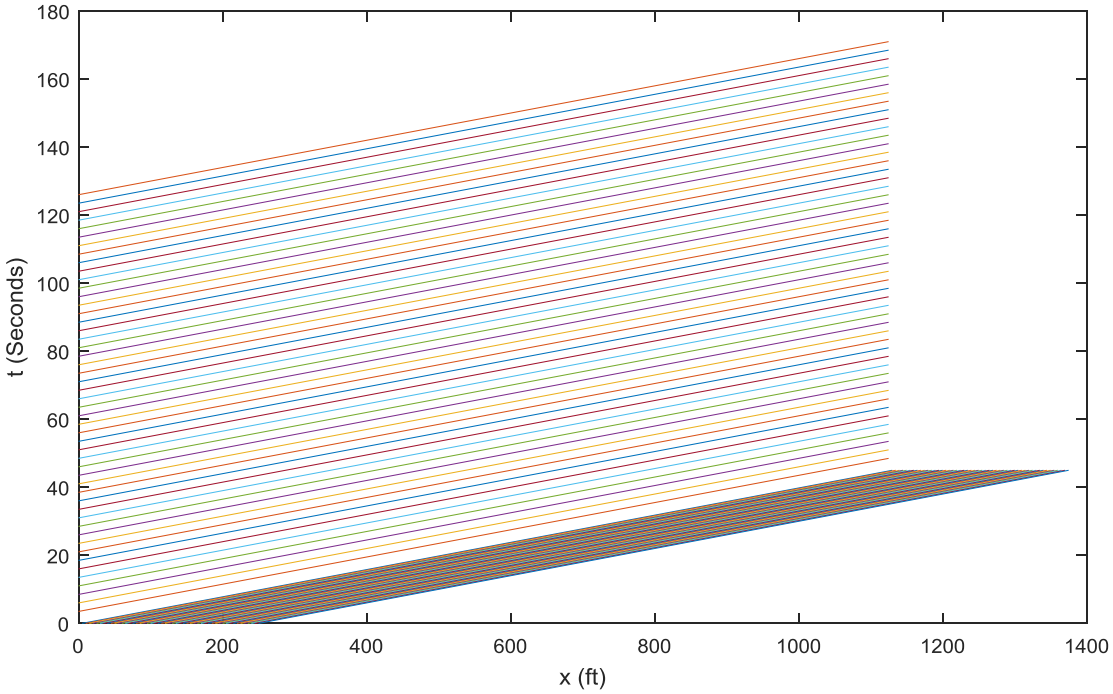

(c) For slope, $a = 25$

Figure 3.1 (a-c): Characteristics curves for the Buckley-Leverett equation for different constant initial and boundary conditions.

Substituting Eq. [25] into Eq. [24], we see that, along this special curve,

$$\frac{d}{dt}S_w(x(t),t) = a\frac{\partial S_w}{\partial x} + \frac{\partial S_w}{\partial t} = 0 \tag{27}$$

as in Eq. [22]. The curves generated from Eq. [25] are called the characteristic curves of the Buckley-Leverett equation. Since S_w is constant along the characteristic curves, it follows that the slope of each line must be given by Eq. [21]. Further, the characteristic curves are allowed to enter into a shock wave but cannot emerge from the shock wave. Therefore, we need to find the shock position, where information is lost in the shock wave.

3.3.2.2. Flux Function of Buckley-Leverett's Model Equation

According to the Buckley-Leverett equation, the differential form of the conservation law in 1-D for state variable $S_w(x,t)$ is given by:

$$\frac{\partial S_w}{\partial t} + \frac{q}{A\phi}\frac{\partial}{\partial x}(f_w) = 0 \tag{28}$$

$$\frac{\partial S_w}{\partial t} + \frac{\partial f_n}{\partial x} = 0 \tag{29}$$

where f_n is called the flux function. From Eq. [28], we write:

$$f_n = f_n\big(S_w(x,t)\big) = \frac{q}{A\phi}f_w = \frac{q}{A\phi}\left(\frac{1}{1+\frac{k_{ro}\mu_w}{k_{rw}\mu_o}}\right) \tag{30}$$

Applying the second fundamental theorem of calculus for an arbitrary interval $[a,b]$ in 1-D, and integrating Eq. [29] within this interval, we can interchange the integral and derivative operations, giving

$$\frac{\partial S_w}{\partial t} + \frac{\partial}{\partial x}f_n(S_w) = 0$$

$$\Rightarrow \frac{d}{dt}\int_a^b S_w dx + \int_a^b \frac{\partial}{\partial x}f_n(S_w)dx = 0$$

$$\Rightarrow \frac{d}{dt}\int_a^b S_w dx + f_n\big(S_w(b,t)\big) - f_n\big(S_w(a,t)\big) = 0 \tag{31}$$

$$\Rightarrow \frac{d}{dt}\int_a^b S_w dx = f_n\big(S_w(a,t)\big) - f_n\big(S_w(b,t)\big) \tag{32}$$

From Eq. [31], if we define

$$Q(t) = \int_a^b S_w(x)dx \tag{33}$$

Then $Q(t)$ is a conserved quantity in $[a, b]$, i.e., $Q(t)$ will only change in time when there is a net inflow or outflow of flux through the domain boundaries. From Eq. [31], we write the first integral form of a conservation law

$$\frac{d}{dt}Q(t) - \left(f_n\left(S_w(a,t)\right) - f_n\left(S_w(b,t)\right)\right) = 0 \tag{34}$$

Now, integrate Eq. [34] over some time interval $t \in [0, T]$, obtaining

$$\int_0^T \frac{d}{dt}Q(t)dt - \int_0^T \left[f_n\left(S_w(a,t)\right) - f_n\left(S_w(b,t)\right)\right]dt = 0 \tag{35}$$

From Eq. [35], the second integral form of a conservation law is given by

$$Q(T) - Q(0) - \int_0^T \left[f_n\left(S_w(a,t)\right) - f_n\left(S_w(b,t)\right)\right]dt = 0 \tag{36}$$

In terms of a mathematical interpretation for Figure 3.2, we obtain

$$Q(T) - Q(0) = \int_0^T \left[f_n\left(S_w(a,t)\right) - f_n\left(S_w(b,t)\right)\right]dt \tag{37}$$

In terms of a physical interpretation, Eq. [36] states that the difference in the total amount of the state variable S_w in $[a, b]$ between time 0 and T is equal to the difference in the total flux through the boundaries integrated from time 0 and T (Figure 3.2). From the reservoir engineering view, when water is injected into an injection well located by a, oil is displaced through a production well at point b. The changing of water saturation between these wells indicates the flux difference for time, T.

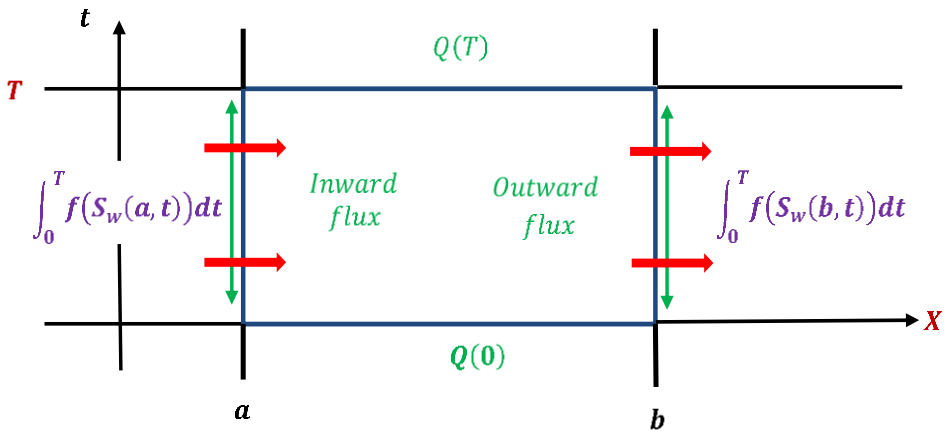

Figure 3.2: Conservations laws for the Buckley-Leverett equation (modified after De Sterck and Ullrich, 2009).

3.3.2.3. Shock Speed Calculation from Rankine-Hugoniot Relation

The shock speed calculation provides a discontinuous feature of the governing equation where the differential form of the PDEs is no longer valid. This speed can give the pre- and post-shock states of the water saturation in a simple waterflood model. The integral form of conservation law describes the behaviour of the shock wave under a few assumptions. Assume that after $t = 0$ there is a single shock wave propagating rightward with a constant speed (s) and the application is governed by a conservation law form (Eq. 37). Consider a region, Ω, in the xt-plane given by

$$\Omega = [a, b] \times [0, T] \tag{38}$$

and ensure that it is sufficiently large to contain the shock for all times $t \in [0, T]$ (Figure 3.3). In Figure 3.3, we use S_{w_l} and S_{w_r} to denote the state of the system to the left and right of the shock wave, respectively. We use $Q(t)$ to denote the amount of material in the interval $[a, b]$ at time (t), defined as in Eq. [33]. By inspection, $Q(t)$ must satisfy

$$Q(T) - Q(0) = sT\left(S_{w_l} - S_{w_r}\right) \tag{39}$$

Using Eq. [36], we also have that

$$Q(T) - Q(0) - \int_0^T \left[f_n\left(S_w(a,t)\right) - f_n\left(S_w(b,t)\right)\right]dt = 0$$

$$\Rightarrow Q(T) - Q(0) = T\left[f_n\left(S_{w_l}\right) - f_n\left(S_{w_r}\right)\right] \tag{40}$$

since $S_w(a,t) = S_{w_l}$ and $S_w(b,t) = S_{w_r}$ for all $t \in [0, T]$. Equating (39) and (40) and solving for s then leads to the Rankine-Hugoniot Relation for the shock speed (s),

$$sT\left(S_{w_l} - S_{w_r}\right) = T\left[f_n\left(S_{w_l}\right) - f_n\left(S_{w_r}\right)\right]$$

$$\Rightarrow s = \frac{f_n(S_{w_l}) - f_n(S_{w_r})}{S_{w_l} - S_{w_r}} \tag{41}$$

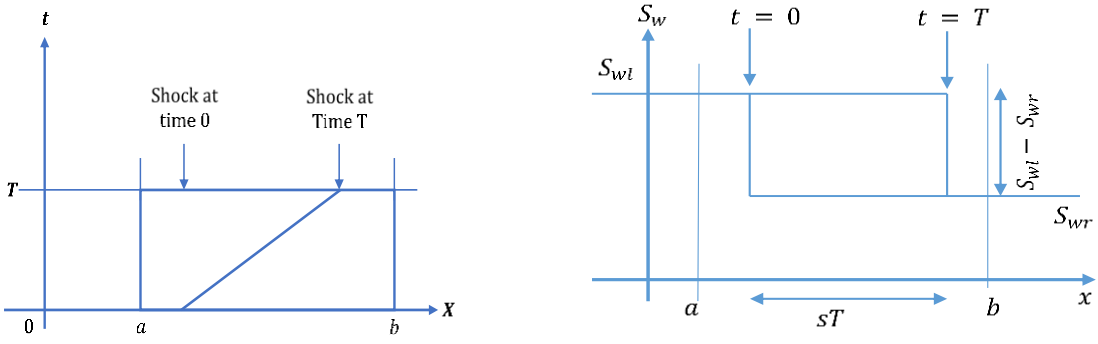

Figure 3.3: Shock wave propagation diagram (modified after De Sterck and Ullrich, 2009).

Thus, the shock propagates rightward with constant speed (s) depending on the different water saturation values.

Consider a reservoir with initial water saturation of 15%, where water is injected into the reservoir with a linear flow rate of $1 ft/day$. The water and oil viscosities are $0.52\ cp$ and $1.73\ cp$, respectively. The residual oil saturation is assumed to be 10% along with an absolute permeability of $10\ mD$ and porosity of 25%. Using some correlations and the flux function definition, the following procedure can be used to calculate the shock speed for a given injected water saturation value.

Step i: The normalised water saturation (Al-Mutairi et al., 2012; Islam et al., 2016) is calculated using the following definition,

$$S_{w_n} = \frac{S_w - S_{w\,initial}}{1 - S_{w\,initial} - S_{or}} \tag{42}$$

Step ii: The relative permeability of water and oil are computed through the following correlations, where we take $n1 = 4$ and $n2 = 2$, as we do for all calculations in this study.

$$k_{rw} = 0.59439 {S_{w_n}}^4 \tag{43}$$

$$k_{ro} = \left(1 - S_{w_n}\right)^2 \tag{44}$$

Step iii: The flux function of the Buckley-Leverett equation is calculated from

$$f_n(S_w) = \frac{q}{A\phi} f_w = \frac{q}{A\phi}\left(\frac{1}{1 + \frac{k_{ro}\mu_w}{k_{rw}\mu_o}}\right) \tag{45}$$

Step iv: Finally, the shock speed is found from

$$s = \frac{f_n(S_{w_l}) - f_n(S_{w_r})}{S_{w_l} - S_{w_r}} \tag{46}$$

The distance travelled by the shock is given by multiplying the shock speed by the time elapsed. Table 3.1 represents the resulting values for different values of the injection water saturation. Based on the initial condition, the distribution of fluid (water and oil) in the reservoir formation is shown in Figure 3.4 (assuming the capillary pressure gradient is zero, and gravitational effects are neglected). This figure exhibits a double-valued saturation for some positions, which is unrealistic. For example, the water saturation after ten days at $50\ ft$ is 60 and 90%

respectively (Figure 3.4). The saturation can be only one value at any place and time. To resolve these difficulties, the shock wave characteristics would be a good choice and could provide single-valued saturation at any position and time.

Table 3.1: Estimation of shock speed and breakthrough time.

$S_{w_l} \approx S_w$	S_{w_r} (Residual water)	$f_n(S_{w_l})$	$f_n(S_{w_r})$	Shock speed (s) ft/day	Distance (x), ft (10 days)
0.3	0.1	0.01	0.001	0.04	0.39
0.4	0.1	0.14	0.001	0.46	4.57
0.5	0.1	0.80	0.001	2.00	19.98
0.6	0.1	2.28	0.001	4.55	45.48
0.7	0.1	3.50	0.001	5.83	58.29
0.8	0.1	3.93	0.001	5.61	56.13
0.9	0.1	4.00	0.001	5.00	50.00
1.0	0.1	3.98	0.001	4.42	44.20

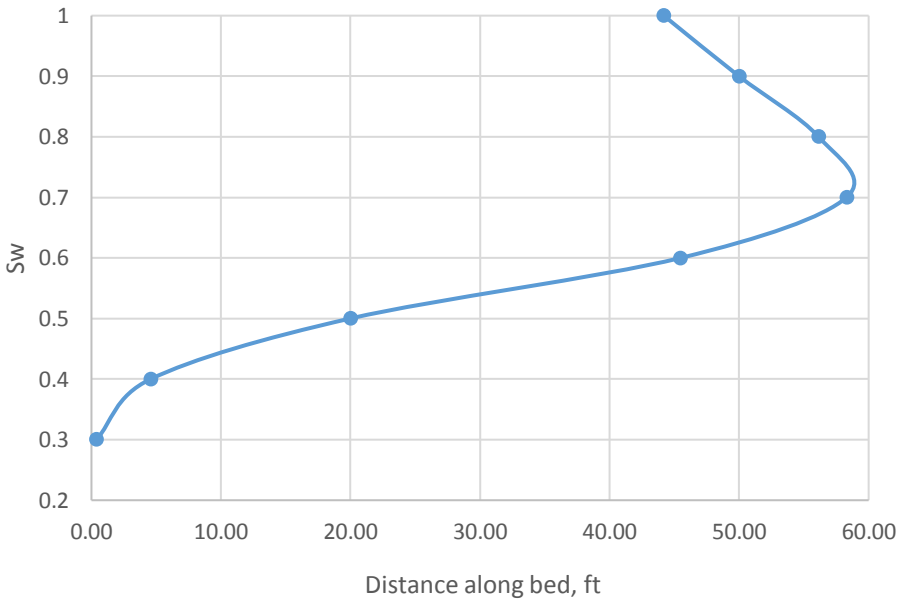

Figure 3.4: Fluid distributions at initial conditions at 10 days.

3.3.3. Numerical Solution using Local Lax-Friedrichs Method

To solve the Buckley-Leverett equation numerically, we introduce the local Lax-Friedrichs method. This method can address the hyperbolic nature of the partial differential equation and exhibits favorable dissipation and dispersion characteristics. In this method, the spatial domain is divided into equal size cells (Δx) of finite volume (Figure 3.5), and later time discretisation leads to the subdivision of the domain (Figure 3.6). Here, cell interfaces are denoted by half-integer indices, such as $\left(i+\frac{1}{2}\right)$ or $\left(i-\frac{1}{2}\right)$. The Buckley-Leverett equation can written as the following form

$$\int_{t_n}^{t_{n+1}} \int_{x_{i-\frac{1}{2}}}^{x_{i+\frac{1}{2}}} \left[\frac{\partial S_w}{\partial t} + \frac{\partial f(S_w)}{\partial x}\right] = 0 \qquad (47)$$

The second integral form of the conservation law (Eq. 36) can then be rewritten using cells from this discretised domain as

$$Q_i^{n+1} - Q_i^n + \int_{t_n}^{t_{n+1}} \left[f\left(S_w\left(x_{i+\frac{1}{2}}, t\right)\right) - f\left(S_w\left(x_{i-\frac{1}{2}}, t\right)\right)\right] dt = 0 \qquad (48)$$

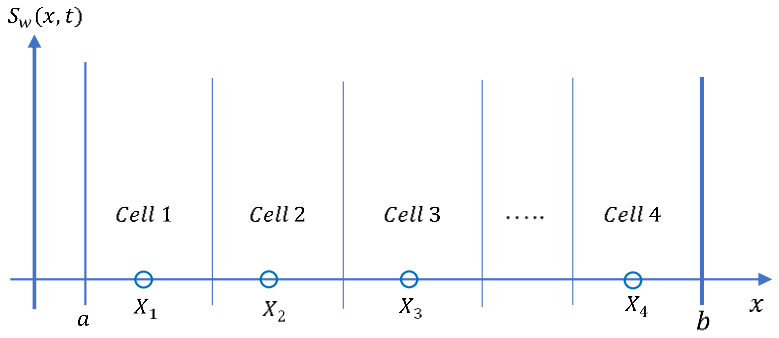

Figure 3.5: Finite volume discretisation (modified after De Sterck and Ullrich, 2009).

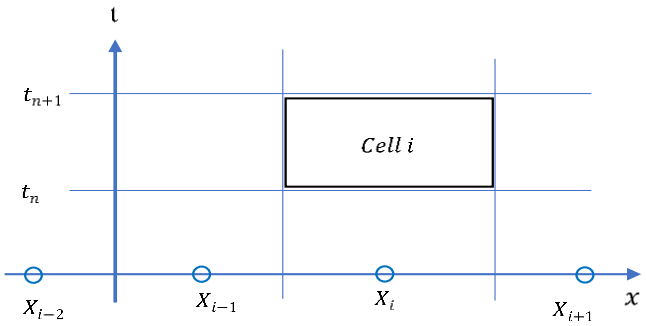

Figure 3.6: Time-discretisation in finite volume methods (modified after De Sterck and Ullrich, 2009).

with

$$Q_i^n = \int_{x_{i-\frac{1}{2}}}^{x_{i+\frac{1}{2}}} S_w(x, t_n)dx \tag{49}$$

where,

$$\int_{x_{i-\frac{1}{2}}}^{x_{i+\frac{1}{2}}} \int_{t_n}^{t_{n+1}} \frac{\partial S_w}{\partial t} dtdx = \int_{x_{i-\frac{1}{2}}}^{x_{i+\frac{1}{2}}} \{S_w(x, t_{n+1}) - S_w(x, t_n)\} dx = Q_i^{n+1} - Q_i^n \tag{50}$$

We now define $\bar{S}_{w_i}^{\ n}$, the average value of $S_w(x, t)$ in cell i at time t_n, by

$$\bar{S}_{w_i}^{\ n} = \frac{Q_i^n}{\Delta x} \tag{51}$$

and $\bar{f}_{i+\frac{1}{2}}^{n+\frac{1}{2}}$, the average value of $f(S_w)$ at the interface $i + \frac{1}{2}$ between t_n and t_{n+1}, by

$$\bar{f}_{i+\frac{1}{2}}^{n+\frac{1}{2}} = \frac{\int_{t_n}^{t_{n+1}} f\left(S_w\left(x_{i+\frac{1}{2}}, t\right)\right) dt}{\Delta t} \tag{52}$$

Divide Eq. [48] by Δx, and substitute Eq. [51], giving

$$\bar{S}_{w_i}^{\ n+1} - \bar{S}_{w_i}^{\ n} + \frac{1}{\Delta x} \int_{t_n}^{t_{n+1}} \left[f\left(S_w\left(x_{i+\frac{1}{2}}, t\right)\right) - f\left(S_w\left(x_{i-\frac{1}{2}}, t\right)\right)\right] dt = 0$$

Using the third integral form of the conservation law and dividing by Δt, the Buckley-Leverett equation becomes

$$\frac{\overline{S_{w_i}}^{n+1} - \overline{S_{w_i}}^{n}}{\Delta t} + \frac{\bar{f}_{i+\frac{1}{2}}^{n+\frac{1}{2}} - \bar{f}_{i-\frac{1}{2}}^{n+\frac{1}{2}}}{\Delta x} = 0 \tag{53}$$

Eq. [53] is an exact equation, since it follows from rewriting the (exact) second integral form. Then, Eq. [53] is discretised by making the approximations

$$\overline{S_{w_i}}^{n} \approx S_{w_i}^{\ n}, \qquad \bar{f}_{i+\frac{1}{2}}^{n+\frac{1}{2}} \approx f^*\left(S_{w_i}^{\ n}, S_{w_{i+1}}^{\ n}\right) \tag{54}$$

Here, $f^*\left(S_{w_i}^{\ n}, S_{w_{i+1}}^{\ n}\right)$ is called the numerical flux function, and is often denoted in shorthand by $f^*\left(S_{w_i}^{\ n}, S_{w_{i+1}}^{\ n}\right) = f_{i+\frac{1}{2}}^{*n}$. This approximation assumes that the flux through the interface $i + \frac{1}{2}$ can be calculated using the state of the system in cells i and $i + 1$. To define an explicit scheme for the Buckley-Leverett equation (assuming no capillary pressure), we take the following form using Eqs. [53] and [54]

$$\frac{S_{w_i}^{n+1}-S_{w_i}^{n}}{\Delta t}+\frac{f^*(S_{w_i}^{n},S_{w_{i+1}}^{n})-f^*(S_{w_{i-1}}^{n},S_{w_i}^{n})}{\Delta x} \tag{55}$$

To define f^*, we reconsider the 1-D Buckley-Leverett model, rewritten in the following form

$$\frac{\partial S_w}{\partial t}+\frac{\partial f_n(S_w)}{\partial x}=0 \Leftrightarrow \frac{\partial S_w}{\partial t}+\frac{q}{A\phi}\frac{df_w(S_w)}{dS_w}\frac{\partial S_w}{\partial x}=0 \tag{56}$$

Taking $\frac{\partial P_c}{\partial x}=0$ in Eq. [10] gives

$$f_w=\left(\frac{1}{1+\frac{k_{ro}\mu_w}{k_{rw}\mu_o}}\right) \tag{57}$$

From Eq. [56], we define

$$\lambda(S_w)=\frac{q}{A\phi}\frac{df_w(S_w)}{dS_w}=f_n{}'(S_w)$$

So, Eq. [56] can be written as

$$\frac{\partial S_w}{\partial t}+\lambda(S_w)\frac{\partial S_w}{\partial x}=0 \tag{58}$$

In Eq. [58], $\lambda(S_w)$ represents the slope of the characteristics, since S_w is constant along characteristic curves. This function, $\lambda(S_w)$, motivates us to define the flux function for the Buckley-Leverett model. The local Lax-Friedrichs flux function is defined by

$$f^*\left(S_{w_i}{}^{n},S_{w_{i+1}}{}^{n}\right)=\frac{f_n(S_{w_i}^{n})+f_n(S_{w_{i+1}}^{n})}{2}-\frac{1}{2}\left|\lambda\left(\frac{S_{w_i}^{n}+S_{w_{i+1}}^{n}}{2}\right)\right|\left(S_{w_{i+1}}{}^{n}-S_{w_i}{}^{n}\right) \tag{59}$$

$$f^*\left(S_{w_{i-1}}{}^{n},S_{w_i}{}^{n}\right)=\frac{f_n(S_{w_{i-1}}^{n})+f_n(S_{w_i}^{n})}{2}-\frac{1}{2}\left|\lambda\left(\frac{S_{w_{i-1}}^{n}+S_{w_i}^{n}}{2}\right)\right|\left(S_{w_i}{}^{n}-S_{w_{i-1}}{}^{n}\right) \tag{60}$$

Here,

$$f_n(S_w)=\frac{q}{A\phi}\left(\frac{1}{1+\frac{k_{ro}\mu_w}{k_{rw}\mu_o}}\right)=\frac{q}{A\phi}\left(\frac{1}{1+M}\right) \tag{61}$$

$$\lambda(S_w)=\frac{q}{A\phi}\left(\frac{df_w(S_w)}{dS_w}\right) \tag{62}$$

From Appendix – A, Eq. [58] can be written as (Eq. [A-15])

$$\lambda(S_w)=\frac{q}{A\phi}\left(\frac{\mu_w}{\mu_o}\frac{a_2}{a_1}\right)\frac{S_{wn}^3(S_w)}{\left(S_{wn}^4(S_w)+\frac{\mu_w a_2}{\mu_o a_1}\left(1-S_{wn}(S_w)\right)^2\right)^2}\left(\frac{4-6S_{wn}(S_w)+2S_{wn}^2(S_w)}{1-S_{wi}-S_{or}}\right) \tag{63}$$

Now, using MATLAB programming, we use Eq. [55] to get the solution for $S_{w_i}{}^{n+1}$ for the new time steps (Figure 3.11), while the remaining parameters are known.

3.3.3.1. Consistency Analysis

For a finite volume scheme, the definition of consistency (De Sterck and Ullrich, 2009) is that

$$f^*(v, v) = f(v), \quad \forall\, v \in \mathbb{R} \tag{64}$$

For the Buckley-Leverett equation the flux function needs to satisfy this consistency requirement in the following form

$$f^*\left(S_{w_i}{}^n, S_{w_i}{}^n\right) = f_n\left(S_{w_i}{}^n\right) \tag{65}$$

This naturally follows from the Lax-Friedrichs form in Eq. [59]. Recalling Eqs. [30, 42, 43, and 44], we get the solution for $S_{w_i}{}^{n+1}$ for the new time step through MATLAB programming (Figure 3.7), while the remaining parameters are known. From simple explicit scheme form, we get

$$S_{w_i}{}^{n+1} = S_{w_i}{}^n - \frac{\Delta t}{\Delta x}\left[f_n\left(S_{w_i}{}^n\right) - f_n\left(S_{w_{i-1}}{}^n\right)\right] \tag{66}$$

Figure 3.7 represents the consistency of proposed numerical scheme when there is no capillary pressure and gravitational force. The solution is similar to the local Lax-Friedrichs method solution, which demonstrates that the proposed method for the simple governing equation is consistent. This technique applies to a linearised 1-D system of equations, and the complete solution (including capillary effect) will achievable only using a computational method.

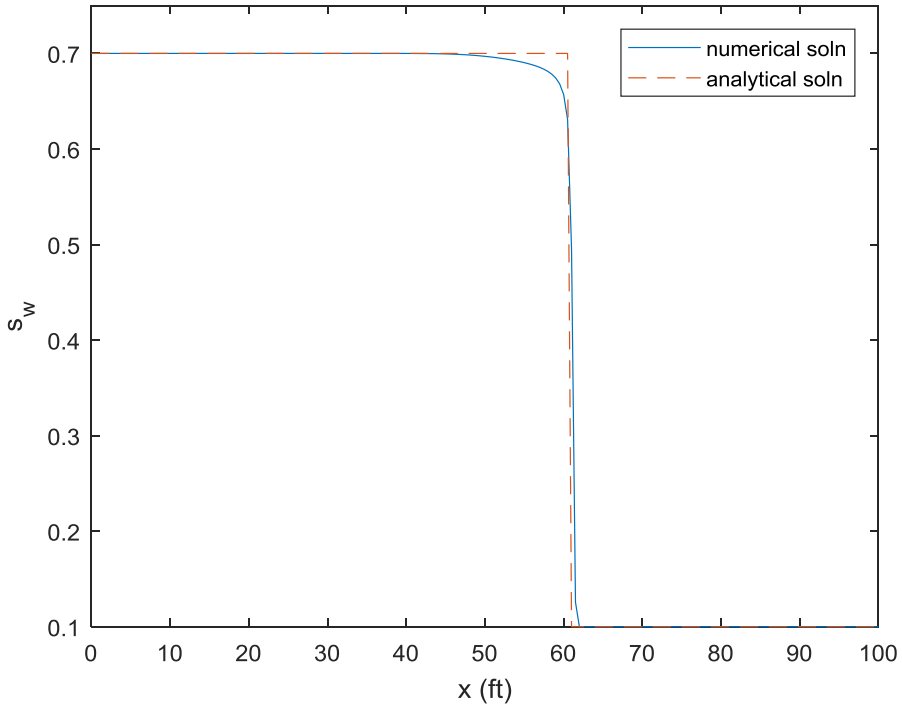

Figure 3.7: Consistency check of the Buckley-Leverett equation.

3.4. RESULTS AND DISCUSSIONS

Consider a reservoir with initial water saturation of 18% with water injected into the reservoir with a linear flow rate of 1 ft^3/day. The water and oil viscosities are 0.52 cp and 1.73 cp, respectively. The residual oil saturation is 10% along with an absolute permeability of 10 mD and porosity of 25%. To analyse the Buckley-Leverett equation numerically, the local Lax-Friedrichs finite volume method is used. This method has proven to be consistent with the simple form of that model (assuming capillary and gravitational forces are negligible). From the local Lax-Friedrichs method, the solution of water saturation is generated for the new time steps using Eq. [55]. We analyse the shock behaviour and shock position by changing the water saturation values that are injected from the injection well. Here we take small time steps to ensure stability of the explicit form. The spatial domain of [0,100] is divided into 200 cells, while the temporal domain of [0, 10] is divided into 1,000 cells. Using MATLAB programming, we change the value of injected water saturation, S_{wl}, and observe the behaviour of the analytical and numerical solutions. In Figure 3.11(a-c), it is demonstrated that the numerical solution converges with the analytical solution at $S_{wl} = 0.70$ (Figure 3.11-a). After the simulation run, we get the shock position at 64.68 ft while the shock speed is 6.468 ft/day for $S_{wl} = 0.70$. The saturation front is smeared in the numerical solution for that amount of water injection. In contrast, the saturation front is sharp in the analytical solution and we were able to validate the simulation code at lower values of S_{wl}. When S_{wl} is larger than 70%, the analytical solution technique used here breaks down incorrectly predicting the shock speed and position. We are aware that we took too simplistic an approach to writing out the analytical solution, and our approach to doing this fails when S_{wl} is larger than about 70%. In addition, when injected water saturation reaches 70%, the relative permeability of oil is decreased and the relative permeability of water is increased, which directly reduces the oil recovery in waterflooding technique. This condition can be easily illustrated by the water-oil relative permeability curves shown in Figure 3.8.

If we draw a tangent line from the point of residual water saturation to the fractional flow curve (Figure 3.9), the point indicates the water saturation percentage that was being injected and represents the corresponding fractional flow. The tangent line also depicts that for the value of $S_{wl} = 0.72$, the maximum amount of oil will displace from the reservoir. This calculation was done when there are no capillary forces in the waterflooding technique. Later, the breakthrough time is calculated by considering the same condition, shown in Figure 3.10. Oil is produced

continually for various S_{wl} and when the value of S_{wl} is 72%, the breakthrough time (Figure 3.10) is steady for the rest of the injected water saturation percentage. Here, the breakthrough time is approximately 15.14 days. The characteristic velocity of water and the amount of oil production is higher, before reaching this time. To find accurate breakthrough timing, we extend the temporal domain to a suitable length. For any injected water saturation percentage, this breakthrough means the time when that saturation is breaking at the outlet side. Moreover, the breakthrough time indicates the level of water saturation, from where the estimation of oil recovery needs to start and calculates the average water saturation percentage behind the shock front. The shock velocity also calculates from the fractional water flow rate curve (Figure 3.9). Since the present research is conducted for a one-dimensional (1-D) medium, we are assuming that the water is injected through the injection well and oil is produced through the production well of that medium. There are no other sources or sinks between the injection and production well in the medium.

For different values of S_{wl}, the shock wave is exhibited in the Buckley-Leverett equation along with their shock position (Figure 3.11(a-c)). Figures 3.11(b-c) depicts the changing of saturation profiles when S_{wl} is larger than 70%. Above this value, the analytical method provides various shock positions, while the numerical method gives a common position for all injected saturation values. This condition reveals that the fractional water flow rate (or, water cut) moves slowly (Figure 3.9) and increases the cost of displacing oil from the reservoir. The breakthrough time is also at a steady rate for those S_{wl} values (Figure 3.10). Only the numerical

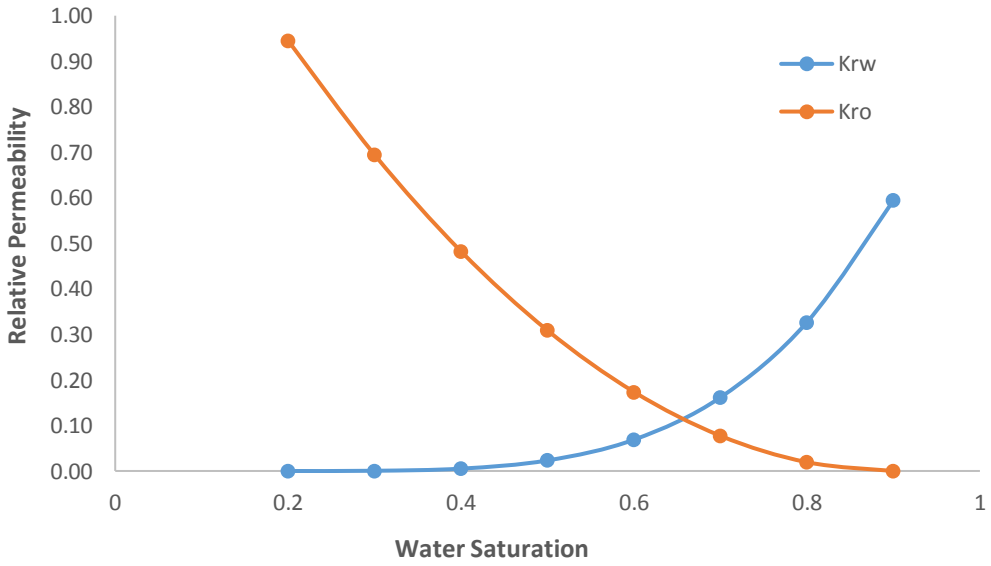

Figure 3.8: Water-oil relative permeability curves.

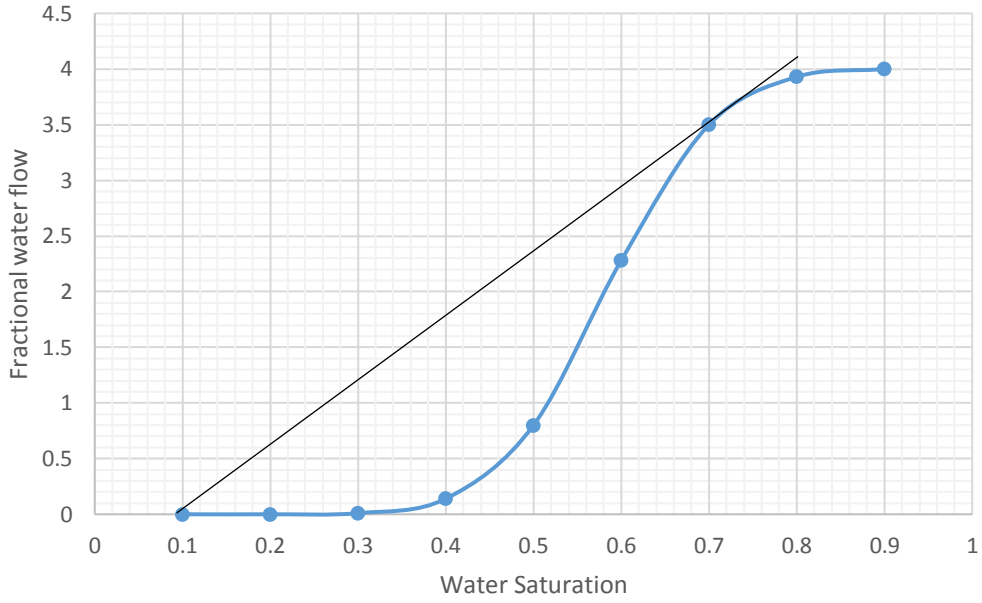

Figure 3.9: The fractional water flow rate with the water saturation.

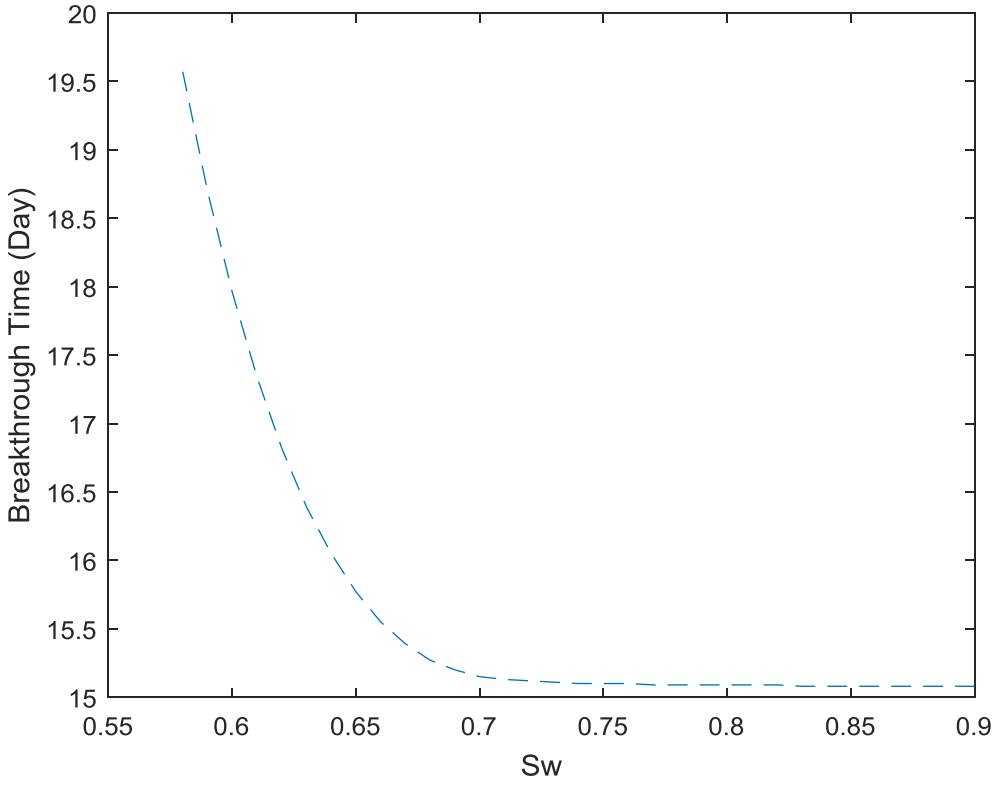

Figure 3.10: Breakthrough time calculation (No capillary).

methods properly illustrate the frontal advancement of saturation profiles and explain the nature of the Buckley-Leverett equation. If we compare the numerical solutions (Figure 3.11(a-c)) with fractional water flow (f_w) profile (Figure 3.9), we see that, after reaching a particular

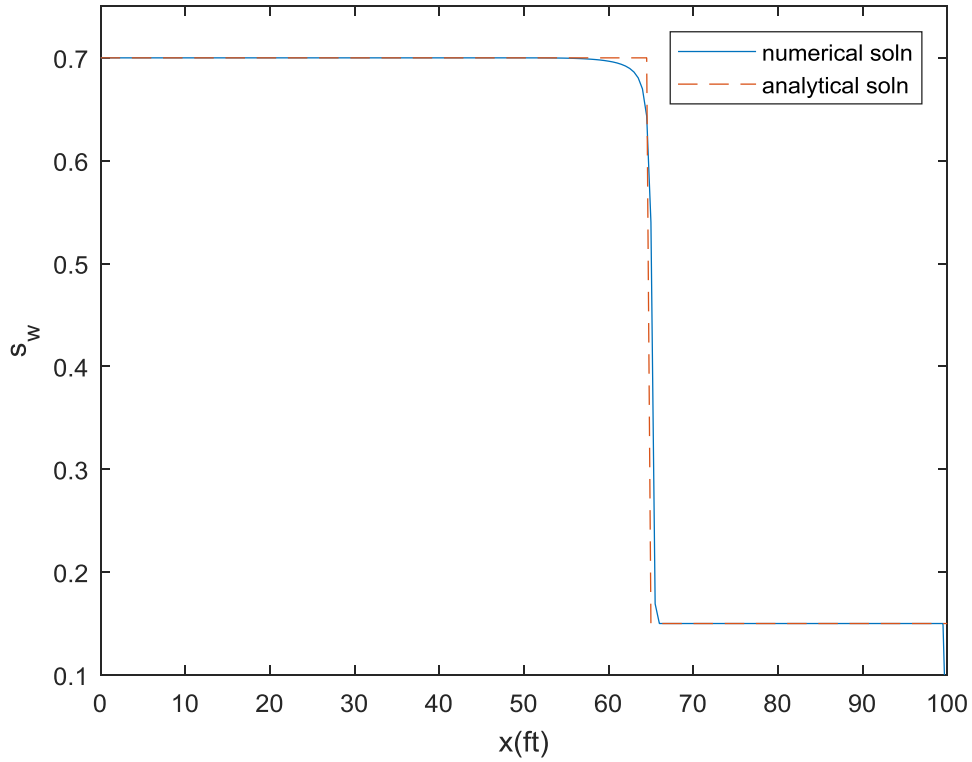

(a): at $S_w = 0.70$

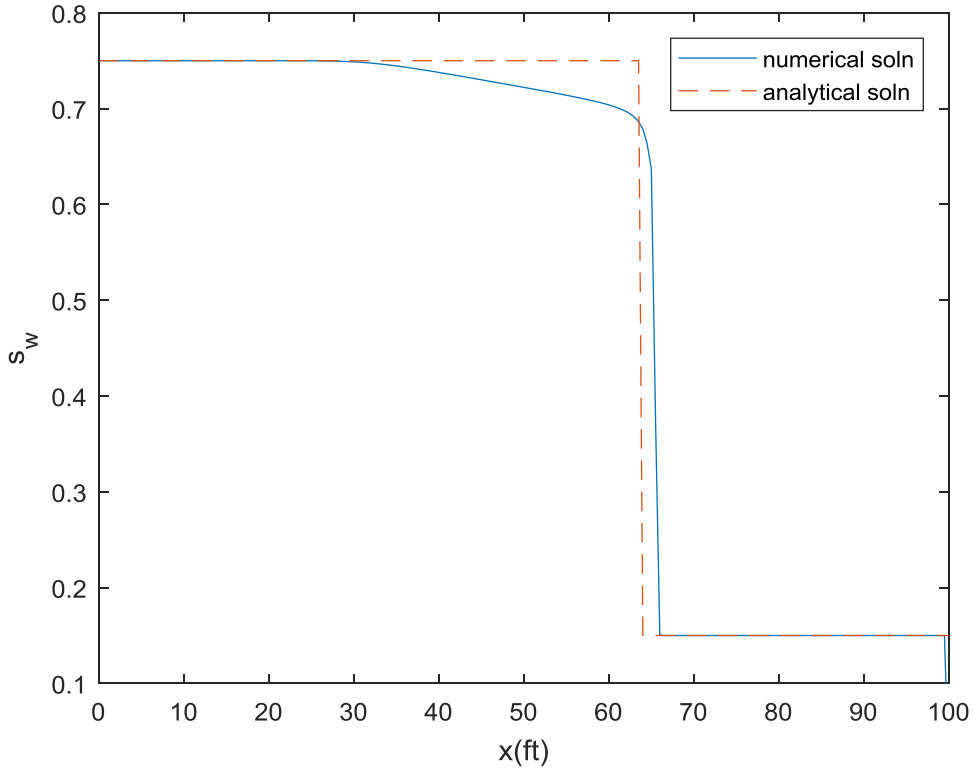

(b): at $S_w = 0.75$

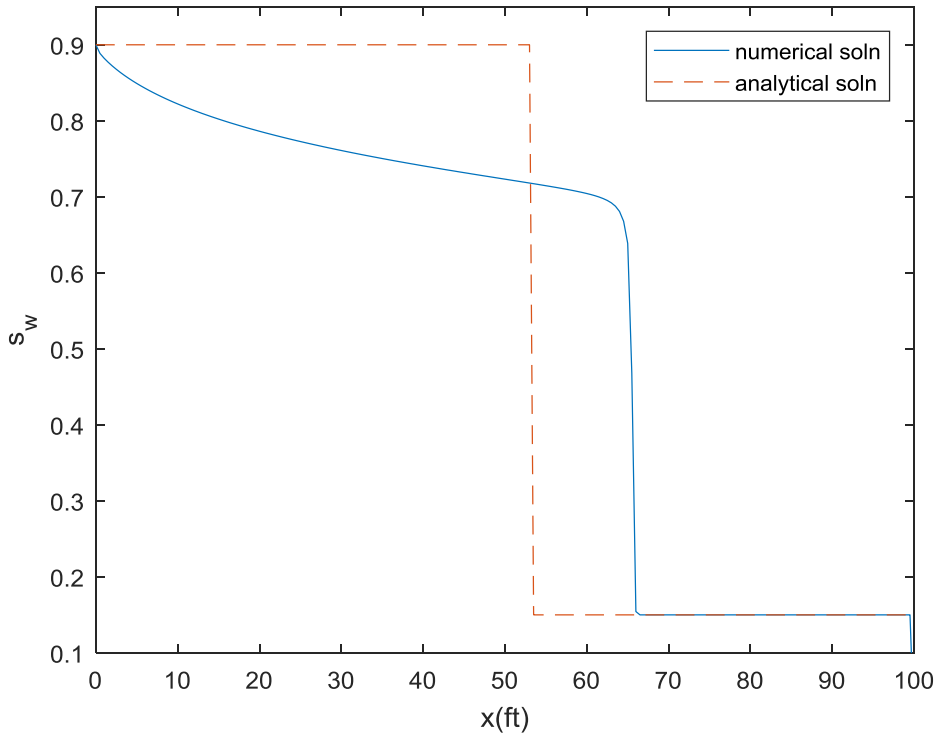

(c): at $S_w = 0.9$

Figure 3.11(a-c): Numerical solution of the Buckley-Leverett equation using local Lax-Friedrichs finite volume method (No capillary).

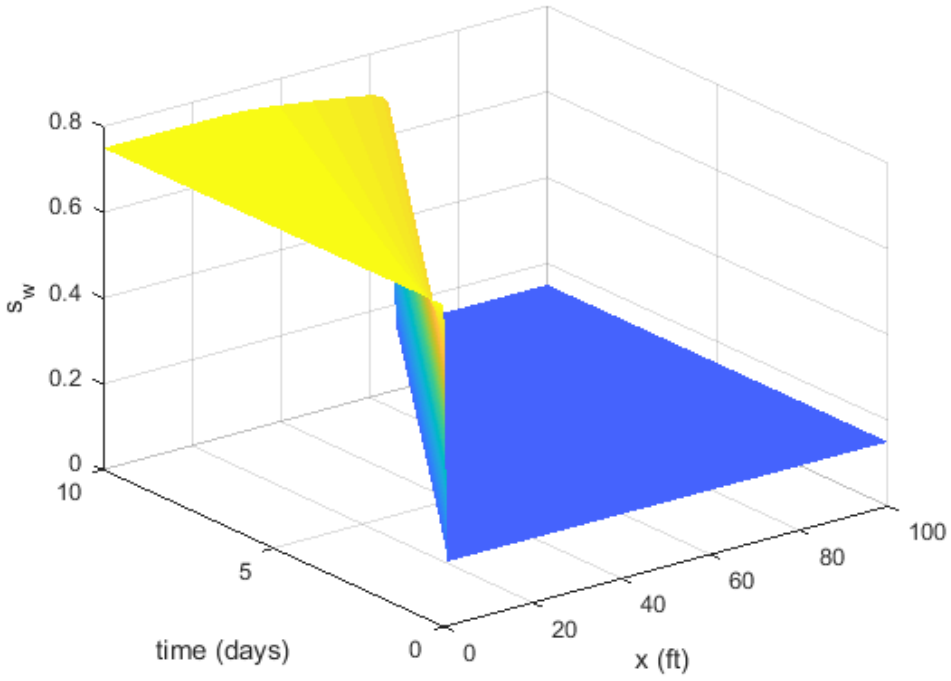

Figure 3.12: Saturation profile (3-D view) at different days (No capillary).

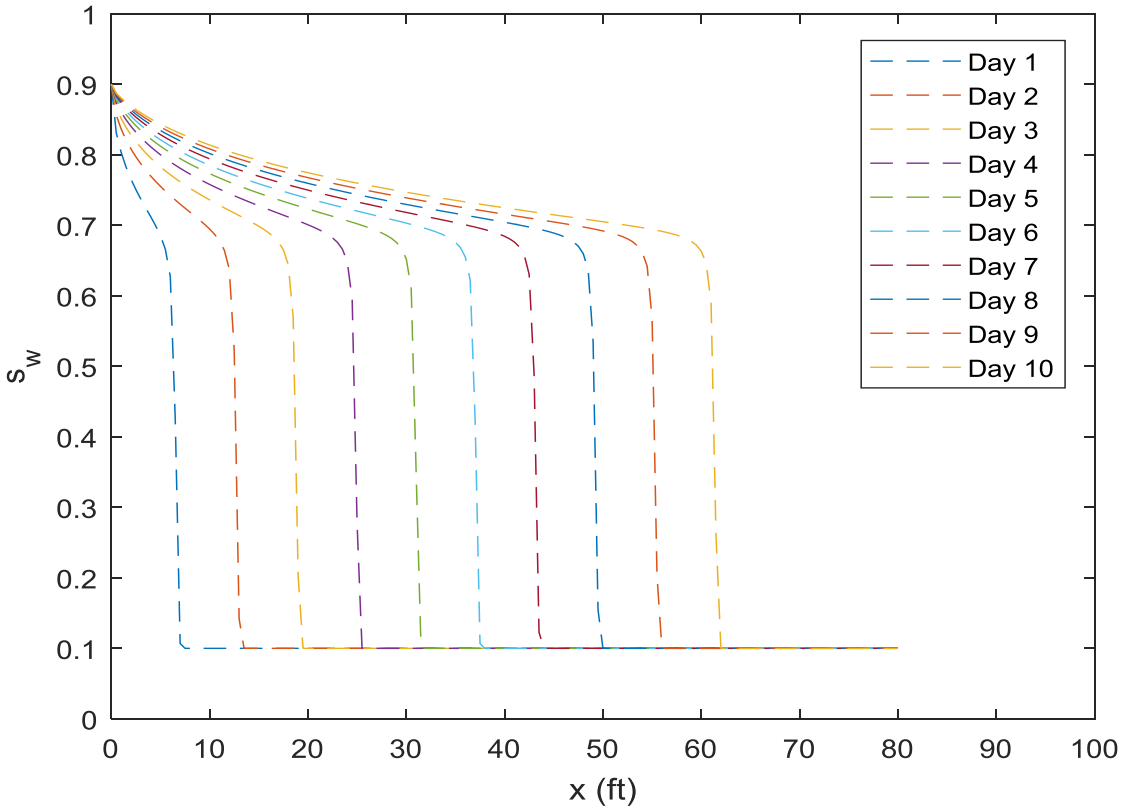

Figure 3.13: Saturation profile (2-D view) at different days (No capillary).

position, the front advancement of f_w is flat rather than steep, and the possibility of recovery is also minimised. Further, the conventional analysis (Figure 3.4) provides double-valued water saturation percentages for position and time. However, the present numerical scheme explains the water saturation profiles by generating shock fronts, and we will use this analysis for the Buckley-Leverett equation including the capillary term. Here, the shock position indicates that oil may yet be recovered by injecting large volumes of water through the reservoir. The region above 90% water saturation depicts that the oil is not recoverable since residual oil saturation is 10%. We also present the saturation profiles for different days after assuming a shock front, shown in Figures 3.12 and 3.13. The physical solution of the Buckley-Leverett equation is obtained here for various timesteps. These figures depict the saturation frontal advancement, where saturation fronts move forward with a definite speed at specific time and distance. The injected water saturations are varying behind the front, while it is constant ahead of the front. At the end of the injection time, the shock fronts provide the exact shock position along with the breakthrough time and water cut percentage. This water cut represents the water saturation percentage that is injected into the injection well and the oil production is economically viable up to that saturation level.

3.5. CONCLUSIONS

The analytical and numerical solution of the Buckley-Leverett equation has been developed for a linear 1-D (one dimensional) immiscible displacement process. Both of these solutions provide an approximately discontinuous single-valued solution, which gives an indication of the shock characteristics for that governing model. The method of characteristics helps to define the nature of the model equation and can reduce the PDEs (Partial differential equation) to a family of ODEs (Ordinary differential equation) along which the solution can be integrated based on some initial data. The solution of ODEs along the characteristics curve is a transform solution of the original PDEs. This analytical solution technique is only reasonable when the injected water saturation is lower than 70% and converges with numerical solutions perfectly. Above this injected water saturation, the analytical solutions fail to compute the saturation front and the numerical solution is capable of representing those shock fronts and explaining the behaviour. On the contrary, the local Lax-Friedrichs finite volume scheme is a good choice for hyperbolic PDEs, using explicit, implicit, or semi-implicit form. To avoid the complexity and maintain the efficiency of the present study, we have used only the explicit form for the local Lax-Friedrichs scheme. It is difficult to get saturation shock characteristics in the reservoir by considering capillary terms. However, numerically it is possible to find the real shock scenario for different saturation values, considering capillary pressure gradients will ensure if a shock has appeared or not. Hence, future research will include advanced numerical techniques for accurately tracking breakthrough time, saturation fronts and their shock characteristics without distorting the physics.

ACKNOWLEDGEMENT

The authors would like to thank the Natural Sciences and Engineering Research Council of Canada (NSERC); Research & Development Corporation of Newfoundland and Labrador (RDC), funding no. 210992; and Statoil Canada Ltd., funding no. 211162 for providing financial support to accomplish this research under the Statoil Chair in Reservoir Engineering at the Memorial University of Newfoundland, St. John’s, NL, Canada.

DECLARATIONS OF INTEREST

All authors have seen and approved the final version of the manuscript being submitted. We warrant that the article is original work, has not received prior publication and is not under consideration for publication elsewhere. Finally, the authors have no conflict of interest.

REFERENCES

Al-Mutairi, S.M., Abu-khamsin, S.A., and Hossain, M.E., (2012, January), A Novel approach to handle continuous wettability alteration during immiscible CO_2 flooding process. In Abu Dhabi International Petroleum Conference and Exhibition. Society of Petroleum Engineers.

Arabzai, A., and Honma, S., (2013), Numerical simulation of the Buckley–Leverett problem. Proceedings of School of Engineering of Tokai University, 38, 9-14.

Buckley, S.E., and Leverett M.C., (1942), Mechanism of fluid displacement in sands, Trans. AIME, 146:187–196.

Chen, Z.X., (1988), Some invariant solutions to two-phase fluid displacement problems including capillary effect (includes associated papers 18744 and 19037). SPE Reservoir Engineering, 3(02):691-700.

Codreanu, D., Hauer, R., and Vernescu, A., (1966), Displacement of oil by water in heterogeneous rocks and evaluation of heterogeneity in reservoir engineering calculations. Revue de L'Institut Français du Pétrole, 21(1):57-80.

Craft, B.C., and Hawkins, M.F., (1991), Applied Petroleum Reservoir Engineering, Second ed. Prentice Hall Inc., USA.

De Sterck, H., and Ullrich, P., (2009), Introduction to Computational PDEs. Course Notes for Amath, 442.

Deb, P.K., Akter, F., Imtiaz, S.A., and Hossain, M.E., (2017), Nonlinearity and solution techniques in reservoir simulation: A review. Journal of Natural Gas Science and Engineering, 46, 845-864.

Fayers, F.J., and Sheldon, J.W., (1959), The effect of capillary pressure and gravity on two-phase fluid flow in a porous medium.

Helvig, O. S. (2013). Models for water flooding, imbibition and coupled fracture-matrix flow in a fractured reservoir (Master's thesis, University of Stavanger, Norway).

Holmgren, C.R., and Morse, R.A., (1951), Effect of free gas saturation on oil recovery by water flooding. J. Pet. Tech. 3(05):135-140.

Hovanessian, S.A., and Fayers, F.J., (1961), Linear water flood with gravity and capillary effects. Soc. Pet. Eng. J. 1(01):32-36.

Islam, M.R., and Nandakumar, K., (1986), Multiple solution for buoyancy-induced flow in saturated porous media for large Peclet numbers. Trans. ASME, Ser. C. J. Heat. Transf. 108 (4):866-871.

Islam, M.R., and Nandakumar, K., (1990), Transient convection in saturated porous layers with internal heat sources. Intl. J. Heat. Mass Transf. 33(1):151-161.

Islam, M.R., Hossain, M.E., Mousavizadeghan, H., Mustafiz, S., and Abou-kassem, J.H., (2016), Advanced Reservoir Simulation: Towards Developing Reservoir Emulators, Second ed. Scrivener-Wiley, p. 592.

Johansen, T.E., (2008), Principles of Reservoir Engineering, Memorial University of Newfoundland, Canada. (Unpublished)

Jordan, A.J., (2006), Linearization of non-linear state equation. Bull. Pol. Ac. Sci.: Tech. Sci. 54(1):63-73.

Koch, M., (1992, June), Numerical solution of the Buckley–Leverett equation by means of a new mesh-adaptive collocation technique. In International Conference on Computational Methods in Water Resources, Denver, Co. pp. 149-156.

Leverett, M. (1941). Capillary behavior in porous solids. Transactions of the AIME, 142(01), 152-169.

McWhorter, D.B., and Sunada, D.K., (1990), Exact integral solutions for two-phase flow. Water Resources Research, 26(3):399-413.

Mustafiz, S., Moussavizadeghan, H., and Islam, M.R., (2008b), Adomian decomposition of Buckley-Leverett equation with capillary effects. J. Pet. Sci. Technol., Taylor Francis 26 (15):1796-1810. doi: 10.1080/10916460701426049.

Mustafiz, S., Moussavizadeghan, S.H., and Islam, M.R., (2008a), The effects of linearization on solutions of reservoir engineering problems. J. Pet. Sci. Technol., Taylor Francis 26, 1224e1246. http://dx.doi.org/10.1080/10916460701833905.

Sheldon, J.W., and Cardwell, Jr, W.T., (1959), One-dimensional, incompressible, noncapillary, two-phase fluid flow in a porous medium.

Singh, K.K., (1970), Comparison of the Buckley-Leverett technique with a numerical simulation model containing heterogeneity and capillary pressure, Masters Theses, Missouri University of Science and Technology. (Unpublished result)

Welge, H.J., (1952), A simplified method for computing oil recovery by gas or water drive. J. Pet. Tech. 4(04):91-98.

White, R.E., and Subramanian, V.R., (2010), Computational methods in chemical engineering with maple, Springer-Verlag. doi: 10.1007/978-3-642-04311-6

Wu, Y.S., Pruess, K., and Chen, Z.X., (1993), Buckley-Leverett flow in composite porous media. SPE Advanced Technology Series, 1(02):36-42.

Yortsos, Y.C., and Fokas, A.S., (1983), An analytical solution for linear waterflood including the effects of capillary pressure. Society of Petroleum Engineers Journal, 23(01):115-124.

Chapter 4

Finite Volume Solution of the Buckley-Leverett Equation including Capillary Pressure

[1]Pulok Kanti Deb, [2]Scott MacLachlan, [1]Syed Ahmad Imtiaz and [1]M. Enamul Hossain

[1]Department of Process Engineering, Memorial University of Newfoundland, NL, Canada
[2]Department of Mathematics and Statistics, Memorial University of Newfoundland, NL, Canada

Abstract

The Buckley-Leverett equation is one of the simplest waterflooding methods to estimate the fluid front advancement and its effect in an immiscible displacement process. In this chapter, we present the Buckley-Leverett equation including capillary pressure and solve it by a numerical technique, the cell-centred finite volume method. A fixed-point iteration is applied to solve the nonlinear equations in an implicit scheme. These calculations provide stable solution for waterflooding against diffusive forces (capillary pressure) in an immiscible displacement process. Saturation profiles are generated where shock solutions form without capillary pressure, showing how smoothly the method handles diffusion properties near a shock position. Moreover, the implicit form is used to achieve better stability and accuracy in this research. The current numerical method will help future researchers to utilise the solution in field-scale models and accurately track saturation fronts without distorting their physics.

Keywords: The Buckley-Leverett equation, cell-centred finite volume, fixed-point iteration, reservoir simulation.

4.1. INTRODUCTION

The petroleum industry looks to maximise the recovery performance from their oil/gas fields. It is essential to maintain the economic value of oil/gas resources, and difficult to discover new hydrocarbon fields. Except for remote and environmentally sensitive areas, most petroleum basins are explored, and huge volumes of hydrocarbons are produced globally. Many unconventional hydrocarbons (shale gas/oil, gas hydrates and heavy viscous oils) are produced by exploiting advanced technologies (e.g., hydraulic fracturing, steam injection) to meet the present demands for hydrocarbons. Sometimes, production from those reservoirs is not possible, due to political unrest or environmental sensitivity. Apart from this issue, there are other technical and economic challenges that need to be addressed before maximising petroleum recovery (Muggeridge et al., 2014). To mitigate these constraints, researchers need to develop more effective recovery processes by addressing all complexities. These

complexities are presented by some inherent assumptions along with the governing equations that are used in the different cases. The mathematical models are based on the theory behind fluid flow through porous media, and their prediction process can mislead the petroleum industry's development. Therefore, advanced numerical tools are needed to predict exact solutions for multivariable problems with solutions that are realistic rather than impractical (Deb et al., 2017).

The Buckley-Leverett equation is a reliable model for waterflooding prediction to understand immiscible displacement processes. Here, the saturation profiles are used to describe frontal displacement theory in petroleum engineering. However, the application of that theory is limited, since it requires certain assumptions and related conditions (Deb et al., 2017). In this research, the capillary pressure effect is included in the Buckley-Leverett equation using a numerical tool. This effect influences the interfacial and surface tension of the rock and fluids, the geometry and pore sizes, and the wetting characteristics in a petroleum system (Helvig, 2013).

We focus on the Buckley-Leverett equation that is used in secondary recovery techniques for petroleum fields. Capillary pressure is considered in the model equation as a function of normalised water saturation, and later this developed equation is solved through a cell-centred finite volume approximation. The stability of the proposed solution is attained using a fixed-point iteration. This computational calculation will certainly help to optimise field recovery processes and mitigate all constraints effectively.

4.2. Development of the Buckley-Leverett Equation Including Capillary Pressure

From Buckley-Leverett's theory (1942), the equation can be written as:

$$\frac{\partial S_w}{\partial t} + \frac{q}{A\varphi}\frac{\partial f_w}{\partial x} = 0 \tag{1}$$

where,

$$f_w = \left(\frac{1}{1+\frac{k_{ro}\mu_w}{k_{rw}\mu_o}}\right)\left(1 + \frac{Akk_{ro}}{q\mu_o}\left[\frac{\partial P_c}{\partial x} - (\rho_w - \rho_o)gsin\alpha\right]\right) \tag{2}$$

Eqs. [1 and 2] are nonlinear PDEs. The relative permeability of oil and water are a function of normalised water saturation and can be expressed in the following form:

$$k_{rw} = 0.59439(S_{wn})^4 \tag{3}$$

$$k_{ro} = (1 - S_{wn})^2 \tag{4}$$

where the normalised water saturation (Al-Mutairi et al., 2012; Islam et al., 2016) is defined as:

$$S_{wn} = \frac{S_w - S_{wi}}{1 - S_{wi} - S_{or}} \tag{5}$$

Differentiating both sides with respect to S_w, gives

$$\frac{\partial S_{wn}}{\partial S_w} = \frac{1}{1 - S_{wi} - S_{or}} \tag{6}$$

For immiscible displacement, capillary pressure is a function of normalised water saturation (Leverett, 1941). The relationship is written in the following form:

$$P_c = P_c(S_{wn}) \tag{7}$$

In Eq. [1], f_w is a function of S_w, but not derivatives of S_w.

Let, $$f = \left(\frac{1}{1 + \frac{k_{ro}\mu_w}{k_{rw}\mu_o}}\right) \tag{8}$$

Rewrite Eq. [2] (considering a horizontal reservoir, $sin\alpha = 0$) to get

$$f_w = f\left(1 + \frac{Ak}{q\mu_o} k_{ro}(S_w) \frac{\partial P_c}{\partial x}\right) \tag{9}$$

$$\Rightarrow f_w = f\left(1 + \frac{Ak}{q\mu_o} k_{ro}(S_w) \frac{\partial P_c}{\partial S_{wn}} \frac{\partial S_{wn}}{\partial S_w} \frac{\partial S_w}{\partial x}\right) \tag{10}$$

where f_w depends on both S_w and $\frac{\partial S_w}{\partial x}$

Substituting these into Eq. [1], we obtain

$$\frac{\partial S_w}{\partial t} + \frac{q}{A\phi} \frac{\partial}{\partial x}\left[f\left(1 + \frac{Ak}{q\mu_o} k_{ro}(S_w) \frac{\partial P_c}{\partial S_{wn}} \frac{\partial S_{wn}}{\partial S_w} \frac{\partial S_w}{\partial x}\right)\right] = 0 \tag{11}$$

$$\Rightarrow \frac{\partial S_w}{\partial t} + \frac{q}{A\phi} \frac{\partial}{\partial x}\left[f + f \frac{Ak}{q\mu_o} k_{ro}(S_w) \frac{\partial P_c}{\partial S_{wn}} \frac{\partial S_{wn}}{\partial S_w} \frac{\partial S_w}{\partial x}\right] = 0 \tag{12}$$

$$\Rightarrow \frac{\partial S_w}{\partial t} + \frac{q}{A\phi} \frac{\partial f}{\partial x} + \frac{q}{A\phi} \frac{\partial}{\partial x}\left[f \frac{Ak}{q\mu_o} k_{ro}(S_w) \frac{\partial P_c}{\partial S_{wn}} \frac{\partial S_{wn}}{\partial S_w} \frac{\partial S_w}{\partial x}\right] = 0 \tag{13}$$

$$\Rightarrow \frac{\partial S_w}{\partial t} + \frac{q}{A\phi} \frac{\partial f}{\partial S_w} \frac{\partial S_w}{\partial x} = \frac{\partial}{\partial x}\left[\left(-\frac{q}{A\phi} \frac{Ak}{q\mu_o} f k_{ro}(S_w) \frac{\partial P_c}{\partial S_{wn}} \frac{\partial S_{wn}}{\partial S_w}\right) \frac{\partial S_w}{\partial x}\right] \tag{14}$$

$$\Rightarrow \frac{\partial S_w}{\partial t} + \frac{q}{A\phi} \frac{\partial f(S_w)}{\partial x} = \frac{\partial}{\partial x}\left[N \frac{\partial S_w}{\partial x}\right] \tag{15}$$

where, N is introduced for notational convenience as

$$N = -\frac{q}{A\phi}\frac{Ak}{q\mu_o} f k_{ro}(S_w)\frac{\partial P_c}{\partial S_{wn}}\frac{\partial S_{wn}}{\partial S_w} \tag{16}$$

Considering the integrated form of the conservation law in Chapter 3, Eq. [15] gives

$$Q_i^{n+1} - Q_i^n + \int_{t_n}^{t_{n+1}} \left[f\left(S_w\left(x_{i+\frac{1}{2}}, t\right)\right) - f\left(S_w\left(x_{i-\frac{1}{2}}, t\right)\right)\right] dt =$$

$$\int_{t_n}^{t_{n+1}} \left[N\frac{\partial S_w}{\partial x}\left(x_{i+\frac{1}{2}}, t\right) - N\frac{\partial S_w}{\partial x}\left(x_{i-\frac{1}{2}}, t\right)\right] dt \tag{17}$$

Dividing Eq. [17] by Δx gives

$$\frac{1}{\Delta x}(Q_i^{n+1} - Q_i^n) + \frac{1}{\Delta x}\left[\int_{t_n}^{t_{n+1}} \left[f\left(S_w\left(x_{i+\frac{1}{2}}, t\right)\right) - f\left(S_w\left(x_{i-\frac{1}{2}}, t\right)\right)\right] dt\right] =$$

$$\frac{1}{\Delta x}\left[\int_{t_n}^{t_{n+1}} \left[N\frac{\partial S_w}{\partial x}\left(x_{i+\frac{1}{2}}, t\right) - N\frac{\partial S_w}{\partial x}\left(x_{i-\frac{1}{2}}, t\right)\right] dt\right] \tag{18}$$

From Chapter 3, we write

$$\bar{S_w}_i^{\,n} = \frac{Q_i^n}{\Delta x} \text{ and,}$$

$$\bar{f}_{i+\frac{1}{2}}^{n+\frac{1}{2}} = \frac{\int_{t_n}^{t_{n+1}} f\left(S_w\left(x_{i+\frac{1}{2}}, t\right)\right) dt}{\Delta t} \tag{19}$$

Dividing Eq. [18] by Δt, substituting into Eq. [19] and taking the approximation,

$$\frac{{S_w}_i^{n+1} - {S_w}_i^n}{\Delta t} + \frac{1}{\Delta x}\left[f^*\left({S_w}_i^n, {S_w}_{i+1}^n\right) - f^*\left({S_w}_{i-1}^n, {S_w}_i^n\right)\right]$$

$$= \frac{1}{\Delta x}\left[N\frac{\partial S_w}{\partial x}\left(x_{i+\frac{1}{2}}, t\right) - N\frac{\partial S_w}{\partial x}\left(x_{i-\frac{1}{2}}, t\right)\right] \tag{20}$$

Rearranging Eq. [20], we write

$${S_w}_i^{n+1} - {S_w}_i^n + \frac{\Delta t}{\Delta x}\left[f^*\left({S_w}_i^n, {S_w}_{i+1}^n\right) - f^*\left({S_w}_{i-1}^n, {S_w}_i^n\right)\right]$$

$$= \frac{\Delta t}{\Delta x}\left[N\frac{\partial S_w}{\partial x}\left(x_{i+\frac{1}{2}}, t\right) - N\frac{\partial S_w}{\partial x}\left(x_{i-\frac{1}{2}}, t\right)\right] \tag{21}$$

Consider the term $\frac{\partial}{\partial x}\left[N\frac{\partial S_w}{\partial x}\right]$ and integrating this term from $x_{i-\frac{1}{2}}$ to $x_{i+\frac{1}{2}}$ gives

$$-\left(NS_{w_x}\right)\left(x_{i+\frac{1}{2}}\right) + \left(NS_{w_x}\right)\left(x_{i-\frac{1}{2}}\right) \tag{22}$$

If we knew $S_w\left(x_{i+\frac{1}{2}}\right)$, we could approximate this as

$$\left(N\frac{\partial S_w}{\partial x}\right)\left(x_{i+\frac{1}{2}}\right) = N_{i+\frac{1}{2}} = N_i \frac{S_{w\,i+\frac{1}{2}} - S_{w\,i}}{\frac{h}{2}} \tag{23}$$

Requiring consistent fluxes from both sides leads to

$$S_{w\,i+\frac{1}{2}} = \frac{S_{w\,i+1}N_{i+1} + S_{w\,i}N_i}{N_{i+1}+N_i} \tag{24}$$

which, in turn, allows us to give an expression for the approximation, $N_{i+\frac{1}{2}}$, of $N\frac{\partial S_w}{\partial x}\left(x_{i+\frac{1}{2}}\right)$ as

$$N_{i+\frac{1}{2}} = \tau_{i+\frac{1}{2}}\left(S_{w\,i+1} - S_{w\,i}\right) \tag{25}$$

for $$\tau_{i+\frac{1}{2}} = \frac{2N_iN_{i+1}}{hN_{i+1}+hN_i} \tag{26}$$

Using Eq. [25], we write

$$N_{i+\frac{1}{2}} = \frac{2N_iN_{i+1}}{h(N_{i+1}+N_i)}\left(S_{w\,i+1} - S_{w\,i}\right) \tag{27}$$

Eq. [27] represents the formulation for $N\frac{\partial S_w}{\partial x}\left(x_{i+\frac{1}{2}}, t\right)$. Similarly, we obtain the other terms $N\frac{\partial S_w}{\partial x}\left(x_{i-\frac{1}{2}}, t\right)$.

Substituting this into Eq. [15] and rearranging, we obtain

$$\frac{\partial S_w}{\partial t} + \frac{q}{A\phi}\frac{\partial f(S_w)}{\partial x} = \frac{2N_iN_{i+1}}{h(N_{i+1}+N_i)}\left(S_{w\,i+1} - S_{w\,i}\right) - \frac{2N_iN_{i-1}}{h(N_i+N_{i-1})}\left(S_{w\,i} - S_{w\,i-1}\right) \tag{28}$$

Using MATLAB programming, the left-hand side of Eq. [28] is calculated using the local Lax-Friedrichs scheme, shown in Chapter 3, and the right-hand side of Eq. [28] is added to that calculation to find the saturation for the new time step.

4.3. Implicit Scheme using Fixed-Point Iteration

A fixed-point iteration determines the roots of a given function by converting the function into an iteration form. For a given function f and point x_0, the fixed-point iteration can be written as

$$x_{n+1} = f(x_n), \qquad n = 0,1,2,\ldots \tag{29}$$

Sometimes it is easier to analyse the fixed-point of the model problem in certain ranges. Moreover, it is locally convergent (Chang et al., 1998). An implicit scheme can solve the full

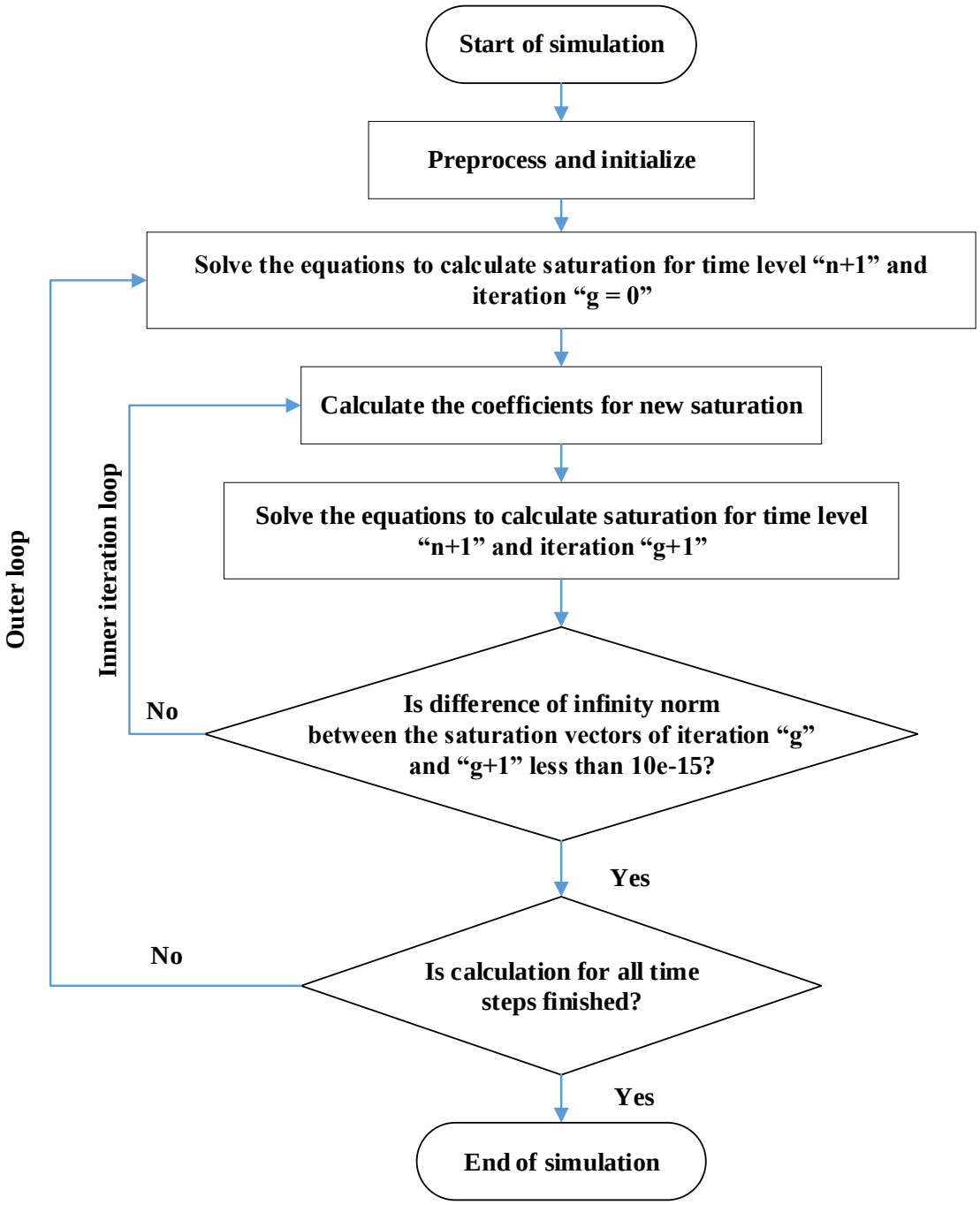

Figure 4.1: Computational algorithm for solving the Buckley-Leverett equation using a fixed-point iteration.

mesh for each time step and solutions obtained by solving simultaneous equations of each grid. Larger time-steps can be implemented here, which makes the solution more stable than the explicit scheme. In this research, we studied the one-dimensional Buckley-Leverett equation in a heterogeneous medium. The computational algorithm for solving the Buckley-Leverett equation using the fixed-point iteration is illustrated in Figure 4.1. This method generates the saturation profiles using an iteration process and helps to find a stable solution for large time-

steps. The computation time of this calculation is also captured for better simulation of water flooding. From Fig. 1, the saturation profile is first calculated for time-level $n+1$ and iteration $g=0$. Using the prior time-step (i.e., explicitly), this step will provide a new saturation profile that is used to calculate further saturation at iteration, $g+1$. This step is repeated until consecutive solutions agree to high tolerance when all conditions are met, then the simulation will provide the stable solution for the governing equation.

4.4. Oil Production Calculation

In accordance with the proposed numerical solution, we tried to calculate the oil production from the water-oil formation. By injecting water into the injection well, the formulation will tell us the recoverable amount of oil based on the provided data parameters. For a particular time and position, the cumulative oil recovery at the production end, (x_{end}) is defined by

$$Q(t) = \int_0^t q(x_{end}, t)dt \tag{30}$$

Recall the Darcy flux (for any position and time) (Yortsos and Fokas, 1983),

$$\text{(For Oil)} \qquad q_0(x,t) = -k\frac{k_{ro}}{\mu_o}\frac{\partial P_o}{\partial x} \tag{31}$$

$$\text{(For water)} \qquad q_w(x,t) = -k\frac{k_{rw}}{\mu_w}\frac{\partial P_w}{\partial x} \tag{32}$$

Based on the conservation law, we write –

$$\frac{d}{dt}\int_0^{x_{end}} S_w(x,t)dx = q_w(x_{end},t) - q_w(0,t) \tag{33}$$

$$\Rightarrow q_w(x_{end},t) = q_w(0,t) + \frac{d}{dt}\int_0^{x_{end}} S_w(x,t)dx \tag{34}$$

Here,

$$q_w(0,t) = Constant\ Injection\ rate = Inlet\ flow$$

$$q_w(x_{end},t) = Outlet\ flow$$

On the other hand, the total amount of water and oil are defined by

$$\text{Total water} = \left[\int_0^{x_{end}} S_w(x,t)dx\right] * Area * Porosity \tag{35}$$

$$\text{Total oil} = Volume * Porosity - Total\ water \tag{36}$$

Again, the oil flux can be defined as

$$\text{Oil Flux} = Oil\ out - Oil\ in \tag{37}$$

$$= \frac{d}{dt}(Total\ oil) = \frac{d}{dt}\left(-Area * Porosity * \left[\int_0^{x_{end}} S_w(x,t)dx\right]\right) \tag{38}$$

where, oil out or oil production for any time (t) can be written as

$$Oil\ out(t) = Oil\ in(t) - \frac{d}{dt}\left(Area * Porosity * \left[\int_0^{x_{end}} S_w(x,t)dx\right]\right) \quad (39)$$

or,

$$Oil\ out = Oil\ in + \frac{d}{dt}(Total\ oil) \quad (40)$$

Here, the amount of oil at initial time $(t = 0)$ is

$$Oil\ in = q_{inj} * (1 - S_{wl}) \quad (41)$$

From the finite volume approximation, we have

$$\int_0^{x_{end}} S_w(x,t_n)dx = \sum_{i=1}^{N_x}(\Delta x) * {S_w}_i^n \quad (42)$$

Differentiating Eq. [42] with respect to time,

$$\frac{d}{dt}\int_0^{x_{end}} S_w(x,t_n)dx = \frac{1}{\Delta t}\left[\int_0^{x_{end}} S_w(x,t_n)dx - \int_0^{x_{end}} S_w(x,t_{n-1})dx\right] \quad (43)$$

$$= \frac{1}{\Delta t}\sum_{i=1}^{N_x}(\Delta x) * \left({S_w}_i^n - {S_w}_i^{n-1}\right) \quad (44)$$

$$= \frac{1}{\Delta t}\left[\sum_{i=1}^{N_x}(\Delta x) * {S_w}_i^n - \sum_{i=1}^{N_x}(\Delta x) * {S_w}_i^{n-1}\right] \quad (45)$$

From Eq. [45], we compute the saturations for any time and position and, later, we calculate the oil production from Eq. [39] using MATLAB programming.

4.5. RESULTS and DISCUSSION

Consider a reservoir with initial water saturation of 18%, where water is injected into the reservoir with a linear flow rate of $1 ft^3/day$. The water and oil viscosities are $0.52\ cp$ and $1.73\ cp$, respectively. The residual oil saturation is 10% along with an absolute permeability of $10\ mD$ and porosity of 25%. The capillary pressure data used in this calculation is shown in Table 4.1 and graphically represented in Figure 4.2. To capture the capillary pressure effects and converge the diffusion coefficient in the Buckley-Leverett equation, the cell-centred finite volume scheme is followed. The spatial domain of [0, 100] is divided into 200 cells, while the temporal domain of [0, 10] is divided into 1000 cells. For every new time-step, the saturation front is calculated from Eq. [28] using MATLAB programming. This saturation front creates a shock wave, and for a certain value of water saturation (S_{wl}) that are injected from the injection well, the shock position is obtained from the shock wave travelling. Due to stability criterion in explicit formulation, we are taking small time-steps for our calculations. As a result, the changing of capillary pressure gradients $\left(\frac{\partial P_c}{\partial x}\right)$ has less effects on the Buckley-Leverett

equation. Theoretically, the capillary pressure values tend to infinity when the water saturation approaches the initial water saturation. For different S_{wl} values, the numerical solution deviates from analytical solution due to shock behaviour. In Figure 4.3(a-b), the numerical solution matches at $S_{wl} = 0.70$ (Figure 4.3a). For that S_{wl}value, the shock position is $64.67\ ft$ while the shock speed is $6.47\ ft/day$. Increasing the values of S_{wl}, the numerical solution deviates clearly from analytical solution and, the shock position is firm for all numerical solutions instead of the analytical solution shock position, shown in Figure 4.3b. We took too simplistic an approach to writing out the analytical solution, and our approach to doing this fails when S_{wl} is larger than about 70%. Besides, the water cut (or, the fractional flow of water) is highly increased and displaces lower amounts of oil from the reservoir. As a result, the cost of recovery will increase through the waterflooding process. This situation is also illustrated through the calculation of breakthrough time, shown in Figure 4.4. The breakthrough time is constant while water saturation is 70% or higher. Later, we compared the breakthrough time by considering with and without capillary, as shown in Figure 4.5. The breakthrough time is same for both capillary conditions. This time will help us to find average water saturation in waterflooding technique and gives an idea if it will be economical to continue the production or not. Considering different times, the saturation profiles are shown in Figure 4.6, and the saturation front moves forward using a shock wave.

The saturation profiles are now calculated using a fixed-point iteration method, shown in Figure 4.7(a-c). This method represents how the successive iterations come with a solution. By following the computational algorithm (Figure 4.1), this method applied the basic upwind and Lax-Friedrichs schemes. For 1,000 time-steps and tolerance 10^{-15}, this method took 26 iterations per time-step on average (maximum 28 iterations at some time-steps) in the explicit and local

Table 4.1: Capillary pressure data (Retrieved from Islam et al., 2016)

S_{wn}	$P_c(atm)$	S_{wn}	$P_c(atm)$	S_{wn}	$P_c(atm)$	S_{wn}	$P_c(atm)$
0	3.99	0.11	1.20	0.30	0.36	0.65	0.06
0.01	3.59	0.15	0.87	0.36	0.27	0.72	0.04
0.02	3.20	0.18	0.70	0.42	0.20	0.87	0.01
0.05	2.26	0.21	0.57	0.48	0.15	0.95	0.003
0.08	1.62	0.25	0.46	0.56	0.09	1	0

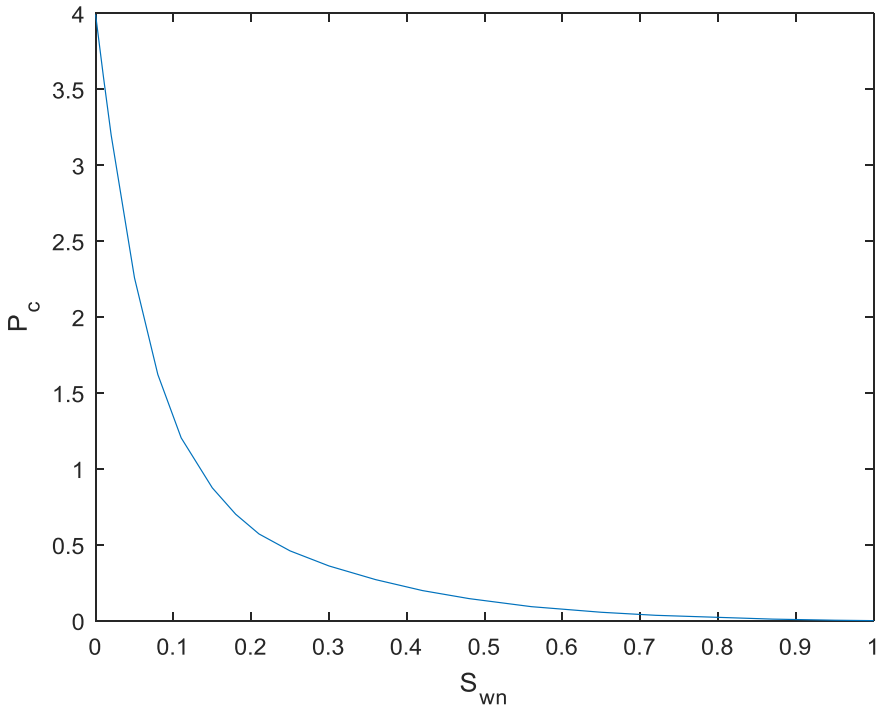

Figure 4.2: Variation of capillary pressure with respect to normalized water saturation.

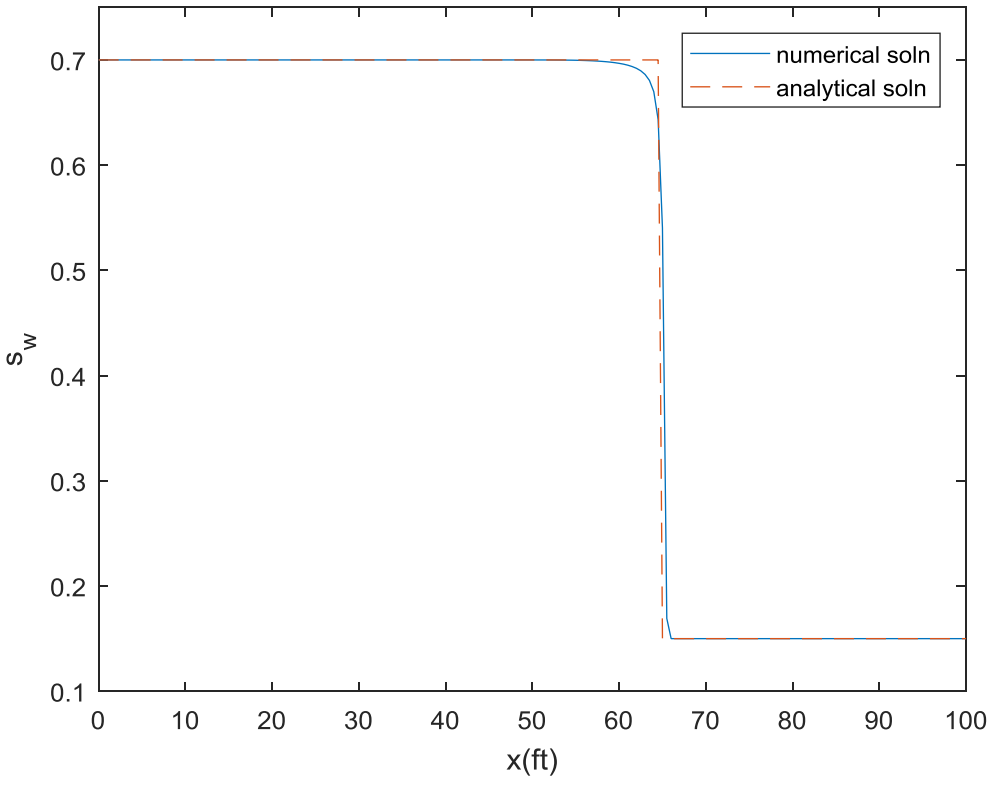

(a): at $S_w = 0.70$

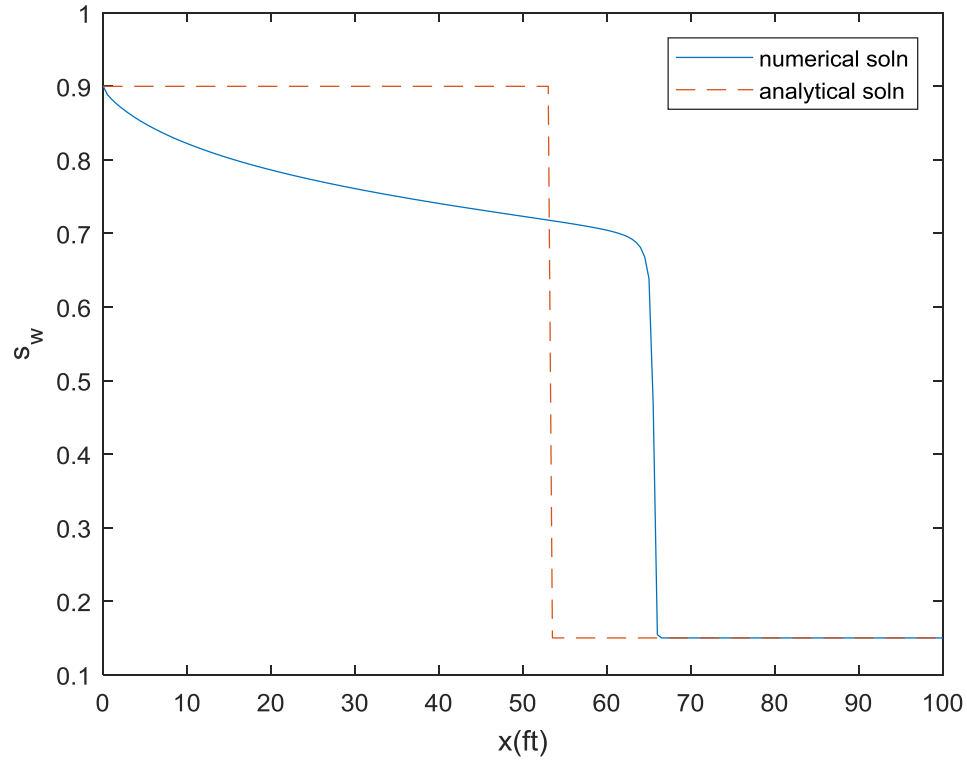

(b): at $S_w = 0.90$

Figure 4.3 (a-b): Saturation profiles including capillary pressure.

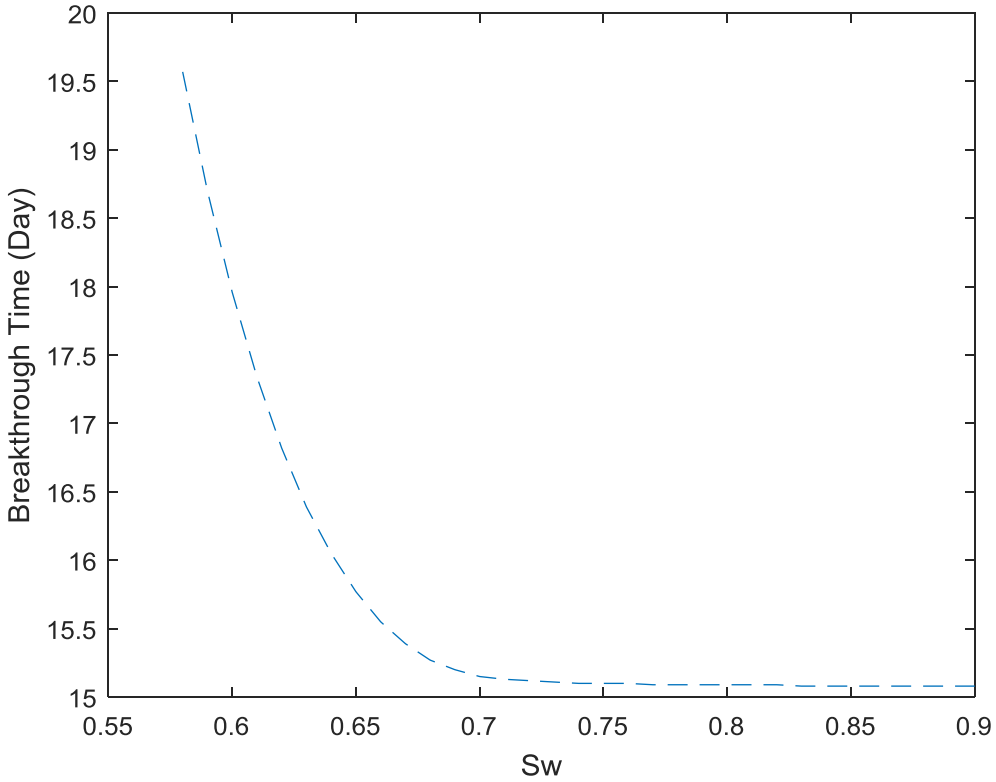

Figure 4.4: Breakthrough time calculation (with capillary)

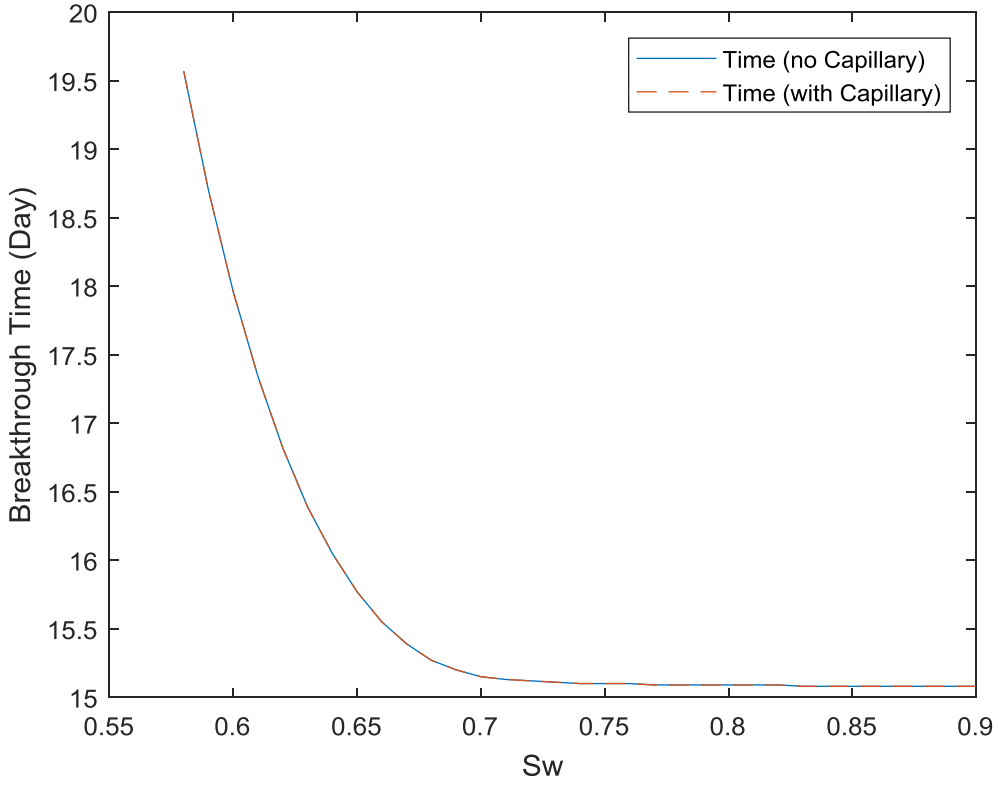

Figure 4.5: Comparison of breakthrough time with water saturation.

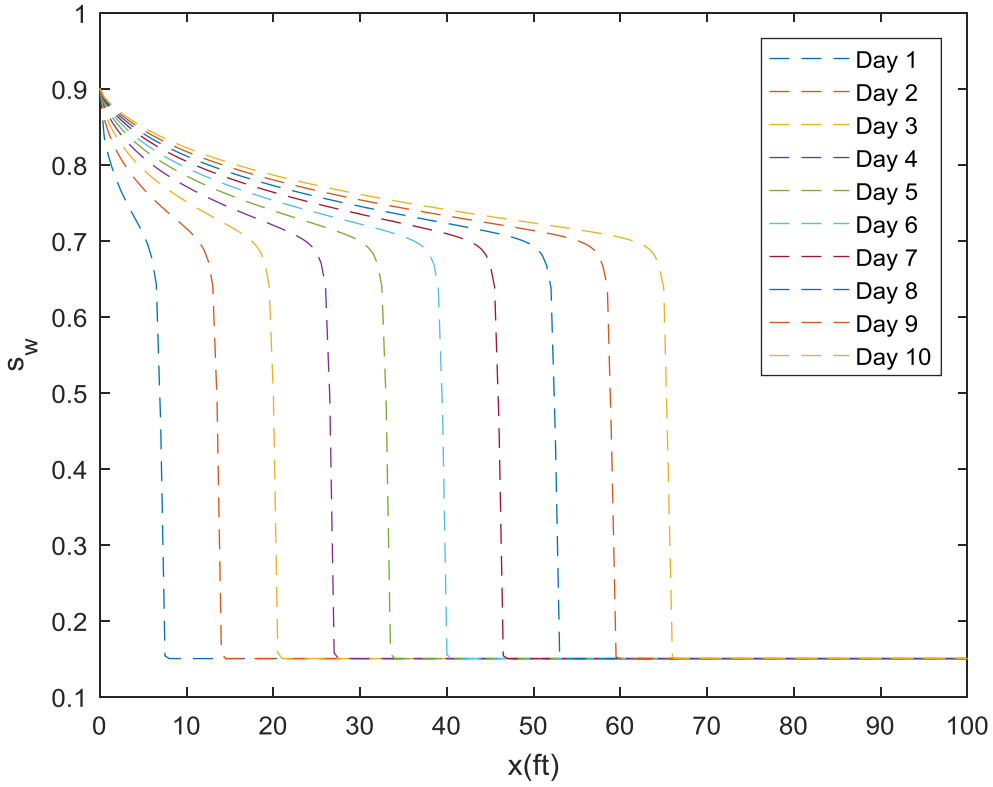

Figure 4.6: Saturation profile at different days (with capillary)

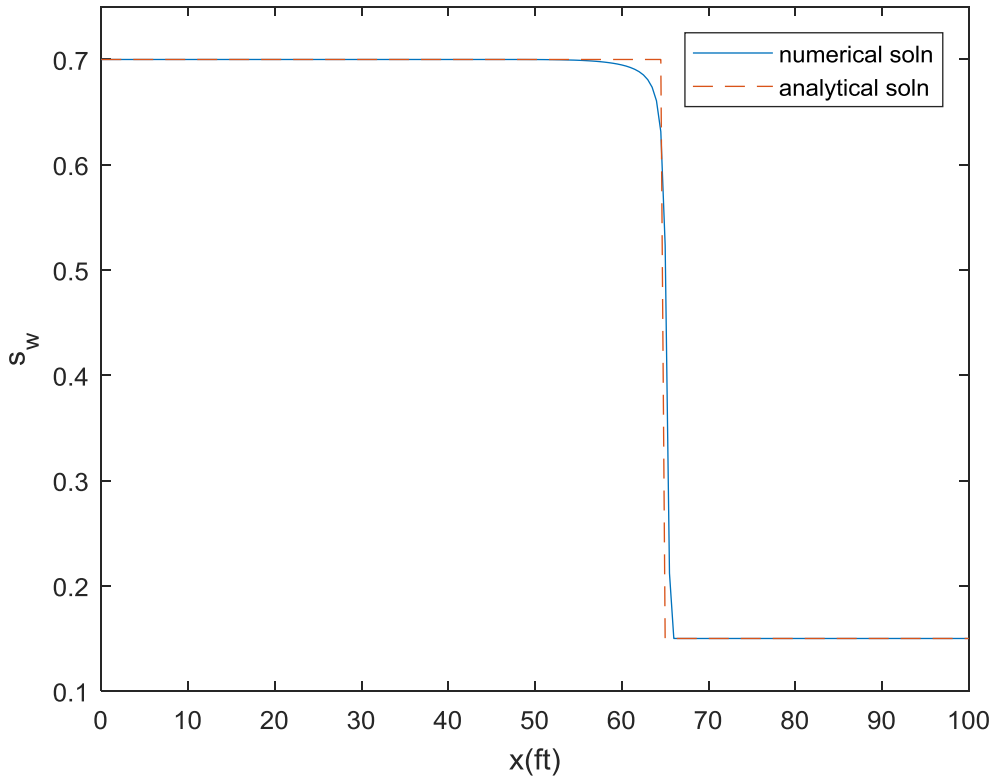

(a) For simple explicit form (no capillary)

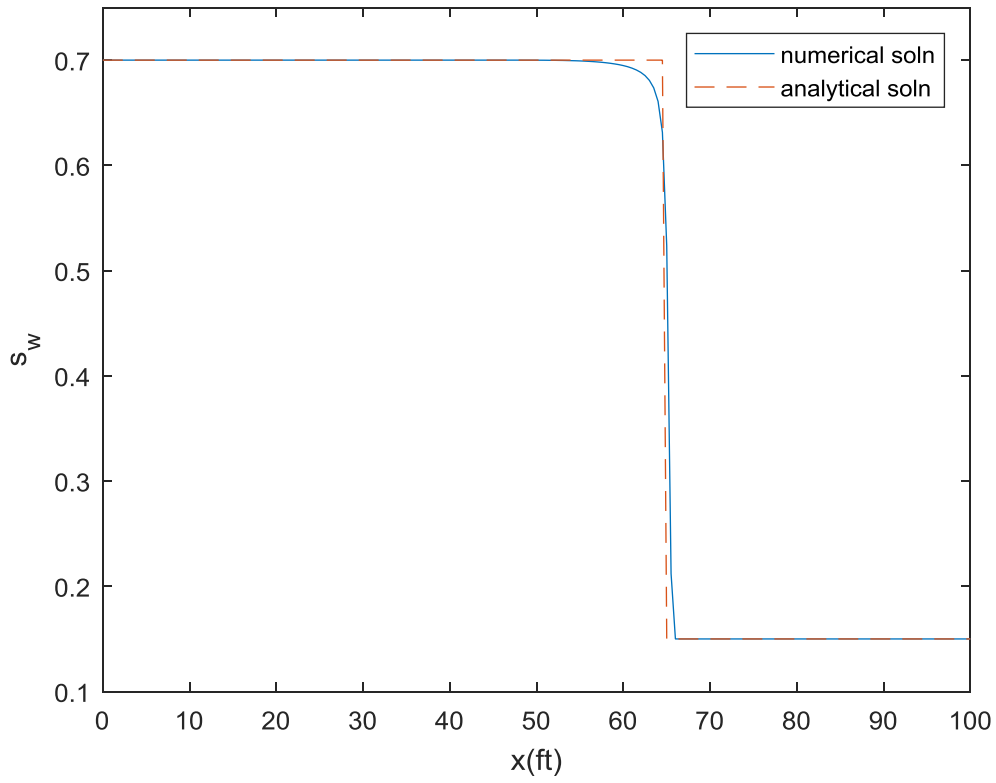

(b) For local Lax-Friedrichs scheme in explicit form (no capillary).

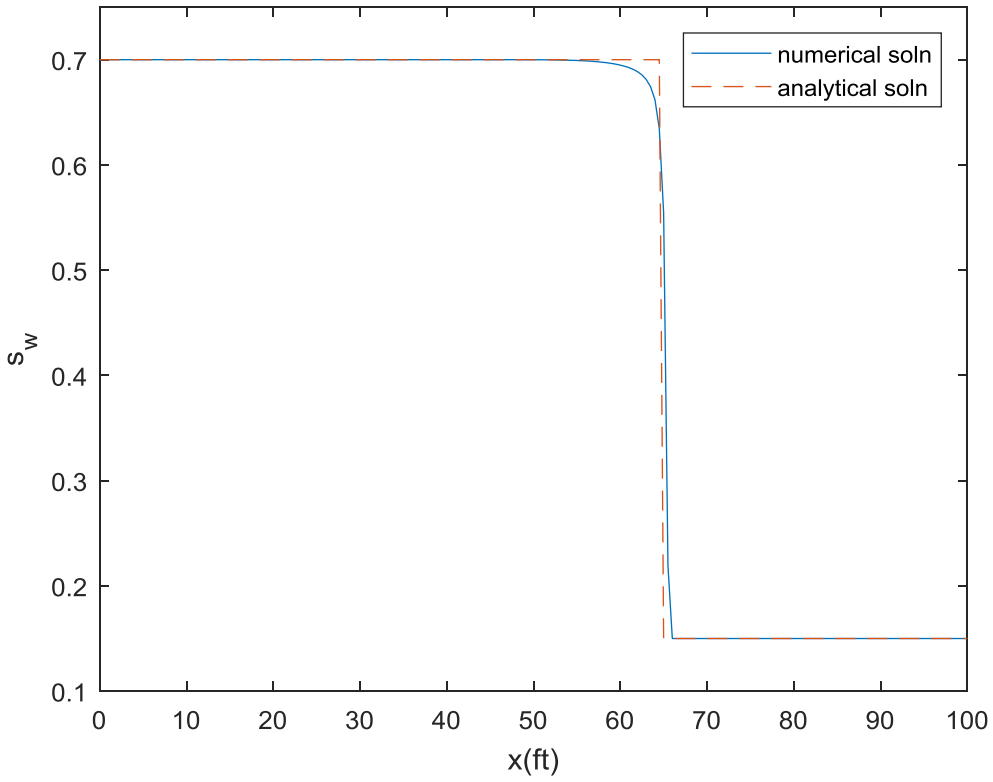

(c) Cell-centered finite volume scheme (with capillary)

Figure 4.7 (a-c): Development of saturation profiles using fixed-point iteration scheme.

Lax-Friedrichs scheme, while 29 iterations per time-steps on average (maximum 31 iterations at some time-steps) for a basic upwind scheme. The numerical and analytical solutions are converged at shock position $64.67\ ft$ (Figure 4.7). This result means the solutions are stable and convergent through the proposed numerical scheme. Finally, to check the validity of all those mathematical schemes, we do a case study using real field data in the later section.

If we compare our results with those of Mustafiz et al., (2008), they solved the Buckle-Leverett equation using the ADM (Adomian decomposition method), where the capillary pressure effects were addressed using a cubic spline method. They claimed that their solution converged rapidly and provided single-value saturation at each point. Regarding consistency, the ADM (Adomian decomposition method) calculation was cumbersome and failed to provide a stable solution. In contrast, the proposed numerical method in our research is consistent and provides a stable solution in detail. Even the proposed solution offers realistic saturation values without distorting their physics. The saturation profiles change mildly along the length and generate smoothed fronts here based on the presented rock and fluid properties.

4.5.1. Effects of Capillary Pressure

The capillary pressure is the ratio of viscous and capillary forces and the gradient received from the capillary curve drives the saturation profile in waterflooding mechanism. The capillary effect governs the fluid phase motion in a porous medium and may happen due to decreasing the relative permeability in the pore volume or the pressure difference as a result of surface tension. The effect is generated by the relative permeability related to the capillary forces and, finally, effects on the cumulative oil production when injecting water in the injection well. Yortsos and Fokas (1983) presented an analytical solution briefly and show the effects of capillary pressure in the Buckley-Leverett equation for changing the viscosity ratio and injection rates. The oil recovery is decreased by increasing the capillary forces. And by changing the viscosity ratio, the saturation profiles give smooth distribution during the shock front advancement. In the present study, a comparison between numerical solutions (with and without capillary) is shown in Figure 4.8. The simulation is running for 70% injected water saturation and observed very little change in saturation profiles. Based on shock position, the saturation front generated with capillary pressure is ahead of the front without capillary pressure, and the profiles are smoother along the position with time. Numerically, the

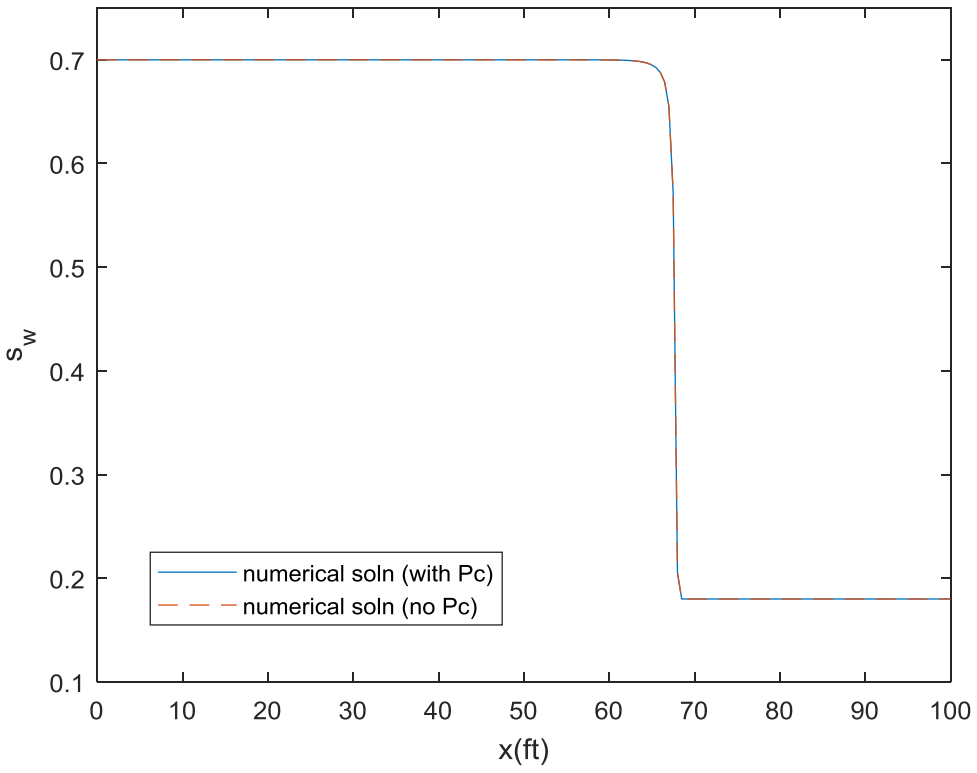

Figure 4.8: Comparison of numerical solutions (with and without capillary) at $S_{wl} = 0.70$

difference between shock positions is less than $0.0001\ ft$. More likely, though, this small change happens due to lower injection rates, or smaller viscosity ratio. To capture the more realistic scenarios in water flooding mechanism, future researchers could use exact field data and simulate all numerical calculations.

4.5.2. Impact on Oil Production

The oil production for a given reservoir formation is calculated using Eq. [39]. Both conditions (with and without capillary forces) are considered during calculation and illustrated in Figure 4.9(a-b). For a certain amount of water injection in the injection well, oil is produced at a steady rate, except the first time-step of the simulation. Here, a small oscillation spike is observed in Figure 4.9(a-b) which occurs due to rapidly changing the injected water saturation (increases from 40 to 70%). Mathematically, we can define the reason for the oscillation in the following form

$$Water\ Volume|_{t=0} = \sum(\Delta x)A\phi S_w|_{t=0} \approx \int_0^{Length} A\phi S_w dx \qquad (46)$$

For time difference (Δt), changing the water volume is expressed by

$$Water\ Volume|_{t=\Delta t} - Water\ Volume|_{t=0} \approx \Delta x A\phi(S_w|_{t>0} - S_w|_{t=0}) \qquad (47)$$

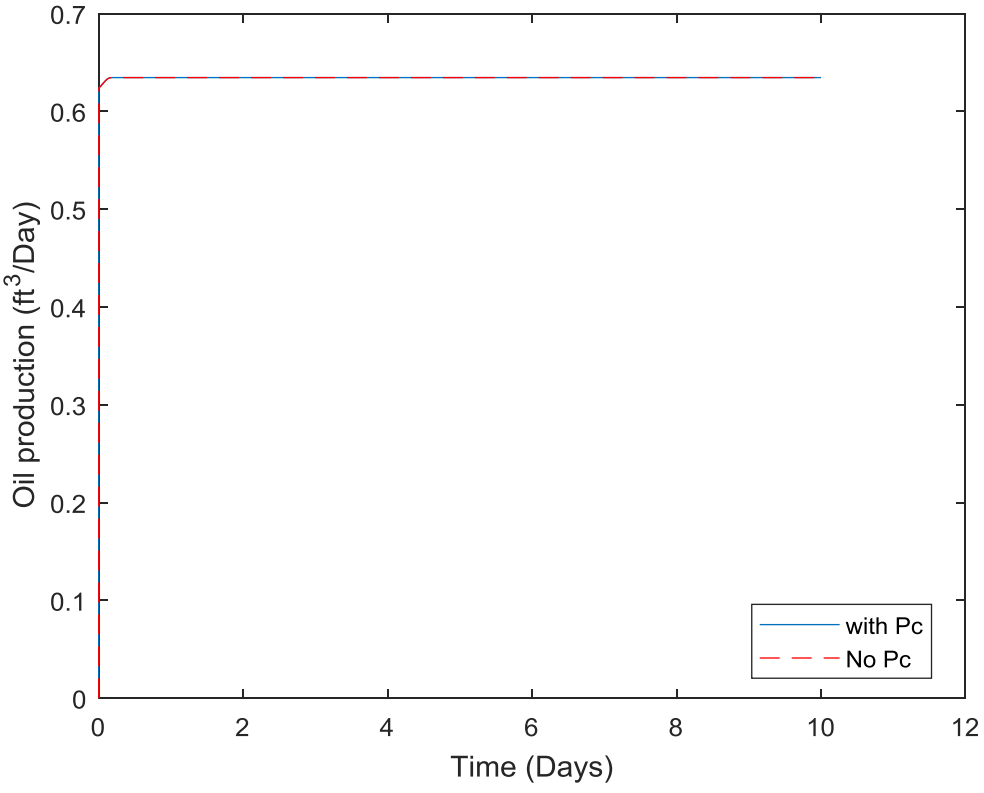

(a) For $S_{wl} = 0.40$

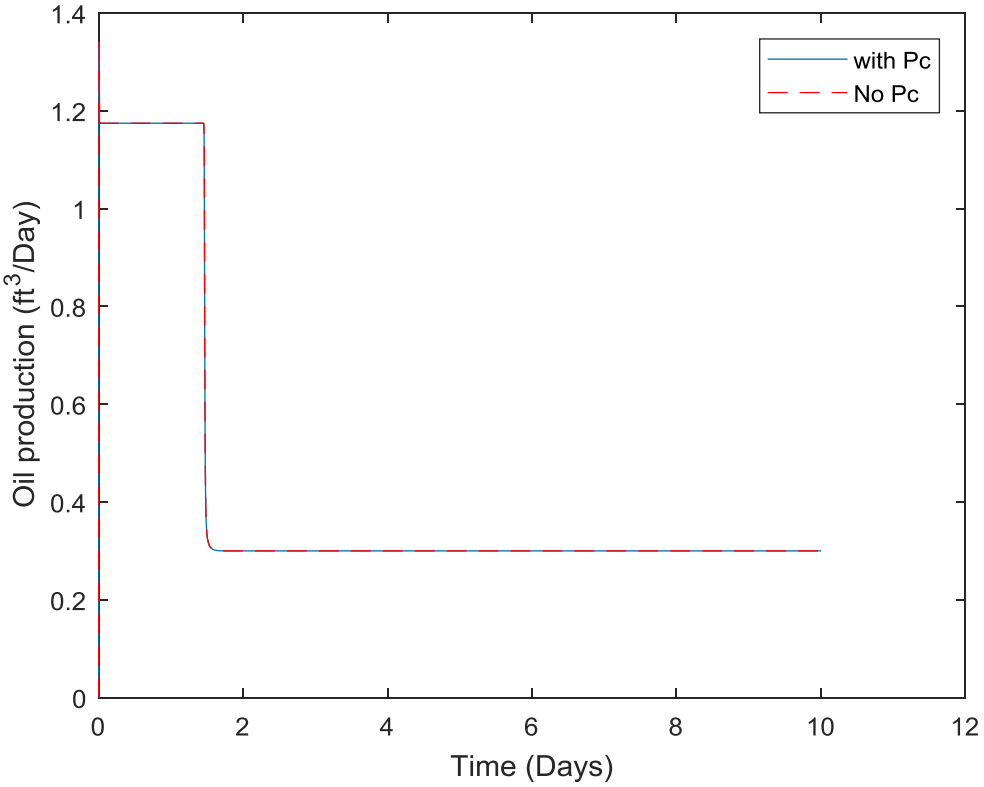

(b) For $S_{wl} = 0.70$

Figure 4.9(a-b): Comparison of oil production (with and without capillary)

In Eq. [47], small changes in the water saturation or spatial values can bring about a significant change in the water volume and, later, will influence the amount of oil production. This change of water saturation creates the spike at the beginning, shrinks oil production from the waterflooding mechanism and, after that, the production goes on at a steady state rate. For injected water saturation (S_{wl}) 70%, the oil production against time are shown in Figure 4.9b. Here, the oscillation spike for oil production reaches approximately $1.40\ ft^3$ per day at the first timestep, then decreases slightly and, from the second day onwards, the oil is produced at a steady rate in the amount of $0.30\ ft^3$ per day. On the other hand, there are no spike or oscillation observed when the injected water saturation is 40%. The oil is produced at a steady rate in the amount of approximately $0.63\ ft^3$ per day from the first day to the end (Figure 4.9a). If we compare these results (Figure 4.9(a-b)), there is no significant changes in oil production rate with or without capillary pressure and simulations are quite stable, while the spatial and temporal dimensions are same, except for changes in the "spike" of first-day production when S_{wl} is 70%. This oscillation may come from grid effects or lower injection

rates, or the viscosity ratio in our presented simulation case study. We validated this calculation by another case study in the next section.

4.6. VALIDATION OF THE PROPOSED MATHEMATICAL SCHEME

In this section, we run a standard case study for validating the stability and consistency of our proposed mathematical schemes. Here, we choose a reservoir formation where water is injected at a rate of $900\ stb/day$, porosity is 25%, the cross-sectional area is $26{,}400\ square\ ft$, initial water saturation is 20%, residual oil saturation is 20%, the viscosity of oil and water are $2\ cp$ and $1\ cp$ respectively. The absolute permeability is $10\ mD$. The value of Corey indices is taken as 2.0 here. The values of the two constants ($a1$ and $a2$) are 0.2 and 0.8 respectively. The mesh size is taken to be 512 for this problem. The capillary pressure data is also presented in Table 4.2. The spatial domain [0, 10] is divided into 200 cells, while the and temporal domain of [0, 10] is divided into 1,000 cells. At first, the local Lax-Friedrichs scheme is used for the simplified Buckley-Leverett equation (assuming zero gravitational forces and neglecting capillary pressure gradients), and later we applied the cell-centred finite volume method to check the capillary pressure effects in the Buckley-Leverett equation. Both of these calculations are run using the explicit form of discretisation. Each of these solutions is represented in Figures 4.12 and 4.13. The consistency of this study is also checked and presented in Figure 4.11. For different values of S_{wl}, the shock position is changed, and the numerical solution provides the exact shock position according to the breakthrough time, shown in Figure 4.14. The Buckley-Leverett equation with capillary provides more reasonable breakthrough time and water saturation percentage rather than the equation without capillary. Future researchers can further explore the more accurate approximation of water saturation percentage to make the oil recovery economically feasible.

For $S_{wl} = 0.75$, the shock position after 10 days is $2.35\ ft$ (Figures 4.11, 4.12). The breakthrough time (Figure 4.10) indicates the point of fractional flow curve for water saturation, where the tangent line meets if drawn from the point of residual water saturation (Figure 4.10). This point of fractional flow provides the average water saturation value for the waterflooding mechanism, from where the economical production is viable. If we compare these results with our base case study, the analytical and numerical solutions are matched closely here for all values of S_{wl}. The possibility of oil recovery is also lower after $S_{wl} = 0.75$. During the local Lax-Friedrichs scheme simulation, the slope of the characteristics $\lambda(S_w)$, is written from Appendix – B [Eq. B-15]

$$\lambda(S_w) = \frac{q}{A\phi}\left(\frac{\mu_w}{\mu_o}\frac{a_2}{a_1}\right)\frac{S_{wn}(S_w)}{\left(S_{wn}^2(S_w)+\frac{\mu_w a_2}{\mu_o a_1}\left(1-S_{wn}(S_w)\right)^2\right)^2}\left(\frac{2-2S_{wn}(S_w)}{1-S_{wi}-S_{or}}\right) \quad (48)$$

Later, we determined the gradients of capillary pressure from Table 2 and utilized into the cell-centred finite volume numerical simulation. During this simulation, we captured all capillary pressure gradients, which ensure that our mathematical scheme is accurate for the entire range. The results generated from this method are illustrated in Figure 4.13, and the shock position is 2.35 ft for S_{wl} is 70%, which means that there are no observable capillary effects.

Table 4.2: Capillary pressure data.

S_{wn}	$P_c(psi)$	S_{wn}	$P_c(psi)$	S_{wn}	$P_c(psi)$	S_{wn}	$P_c(psi)$
0	53.47	0.25	11.80	0.50	3.88	0.75	2.40
0.05	30.20	0.30	9.18	0.55	3.26	0.80	2.24
0.10	24.26	0.35	7.35	0.60	2.85	0.85	1.70
0.15	16.94	0.40	6.12	0.65	2.82	0.90	1.40
0.20	14.29	0.45	5.05	0.70	2.80	0.90	1.22
						1.00	1.02

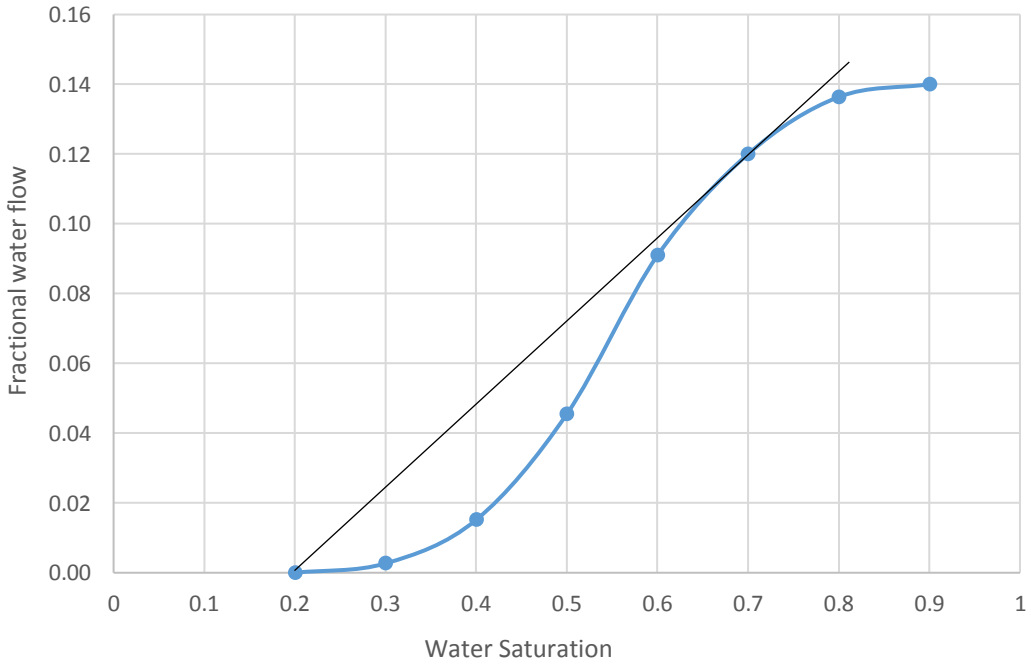

Figure 4.10: The fractional water flow rate with the water saturation.

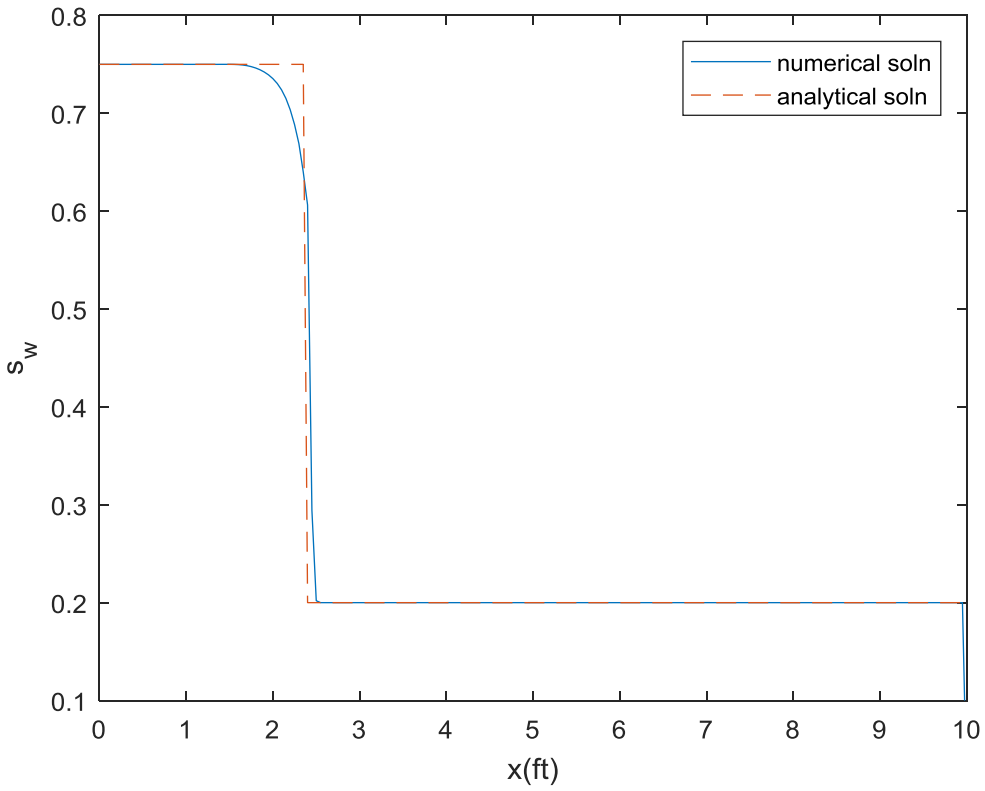

Figure 4.11: Saturation profiles during simple explicit-form (at $S_{wl} = 0.75$)

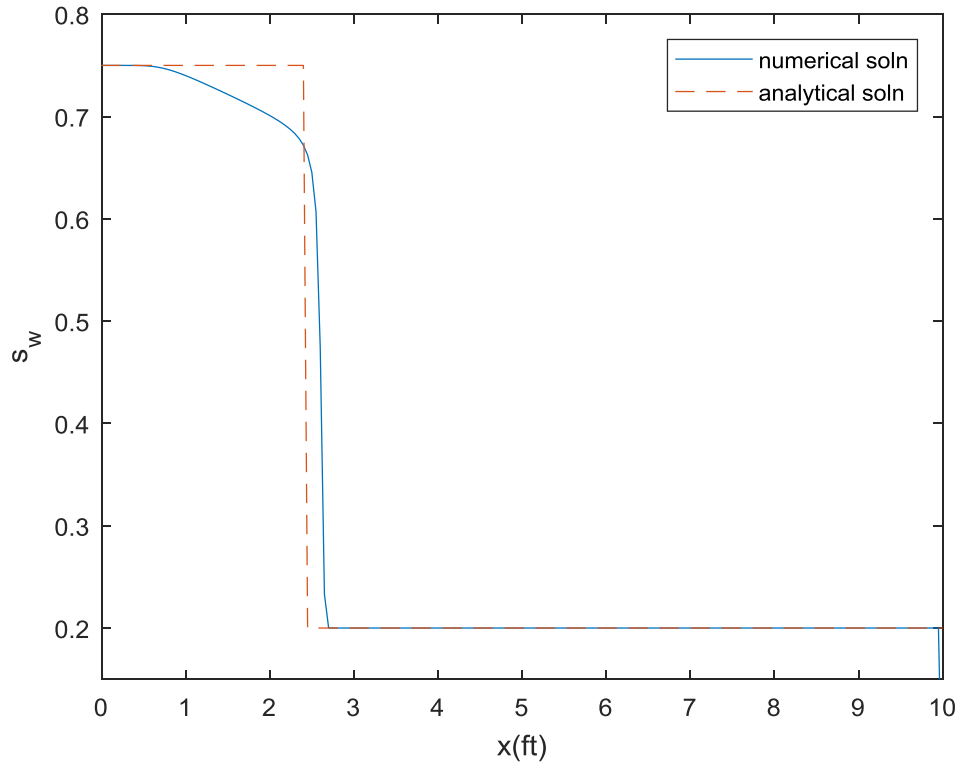

Figure 4.12: Saturation profiles during the local Lax-Friedrichs scheme (at $S_{wl} = 0.75$)

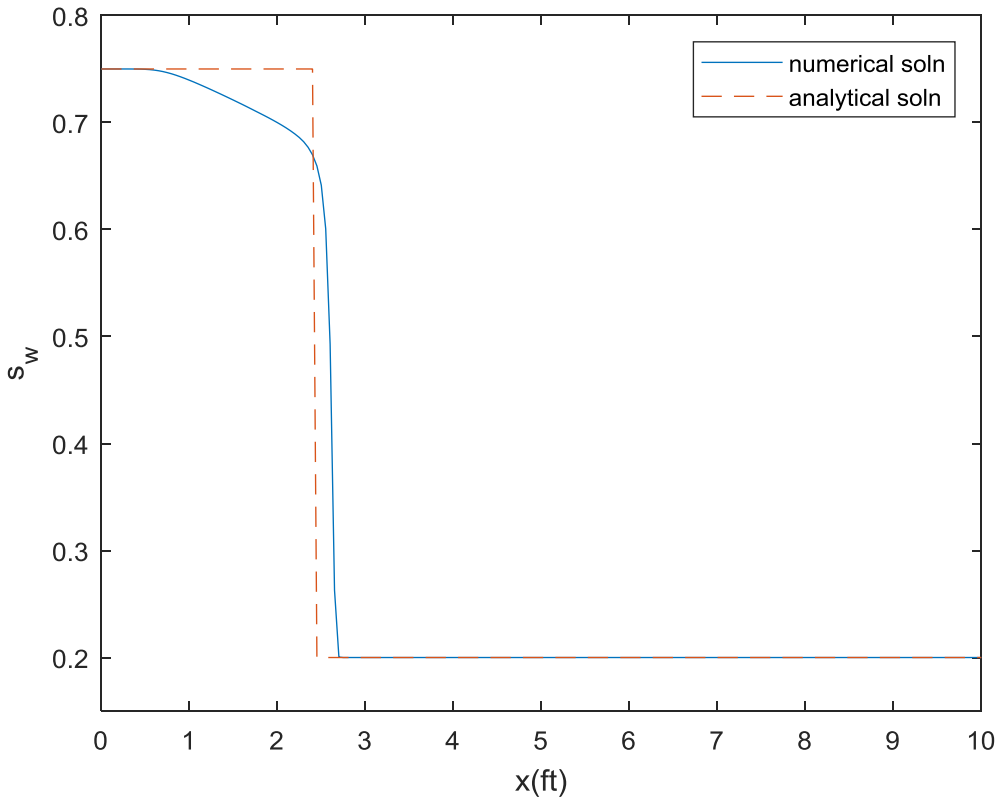

Figure 4.13: Saturation profiles during Cell-centered finite volume scheme (at $S_{wl} = 0.75$)

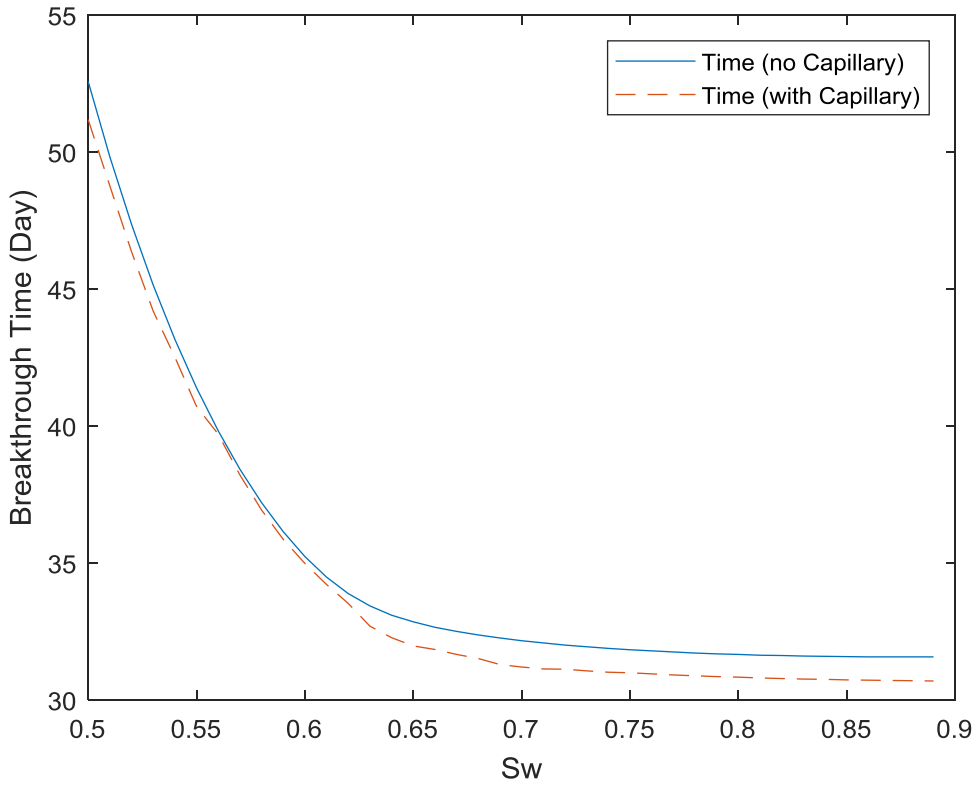

Figure 4.14 : Comparison of breakthrough time with water saturation

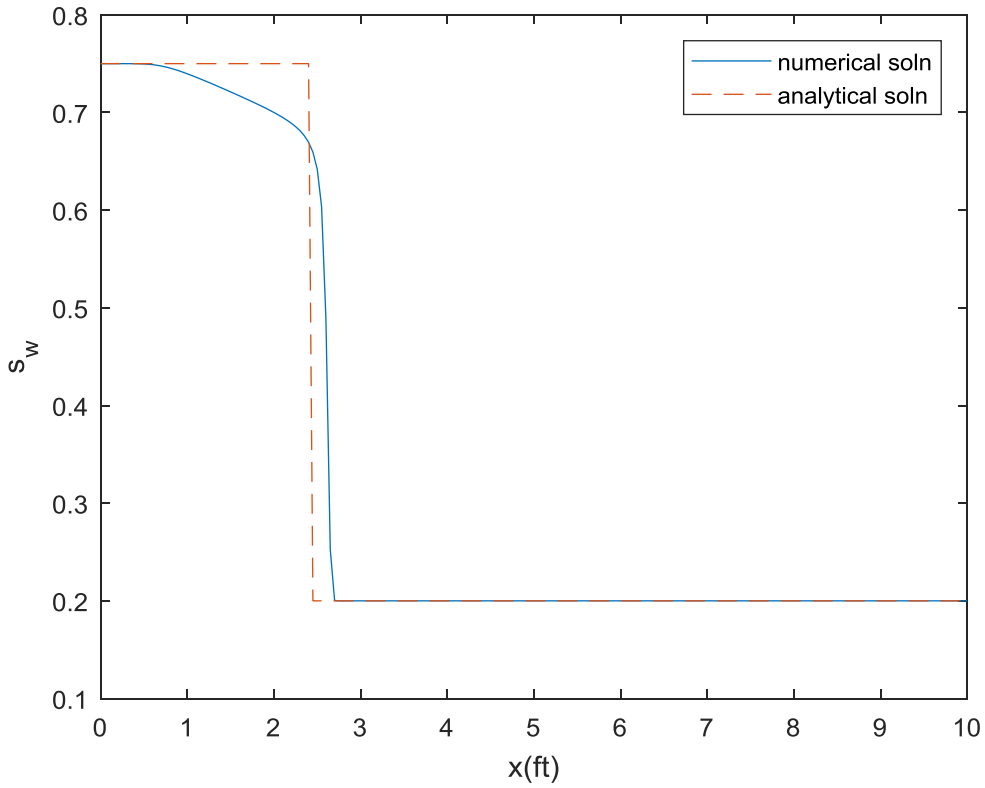

(a) For local Lax-Friedrichs scheme at $S_w = 0.75$

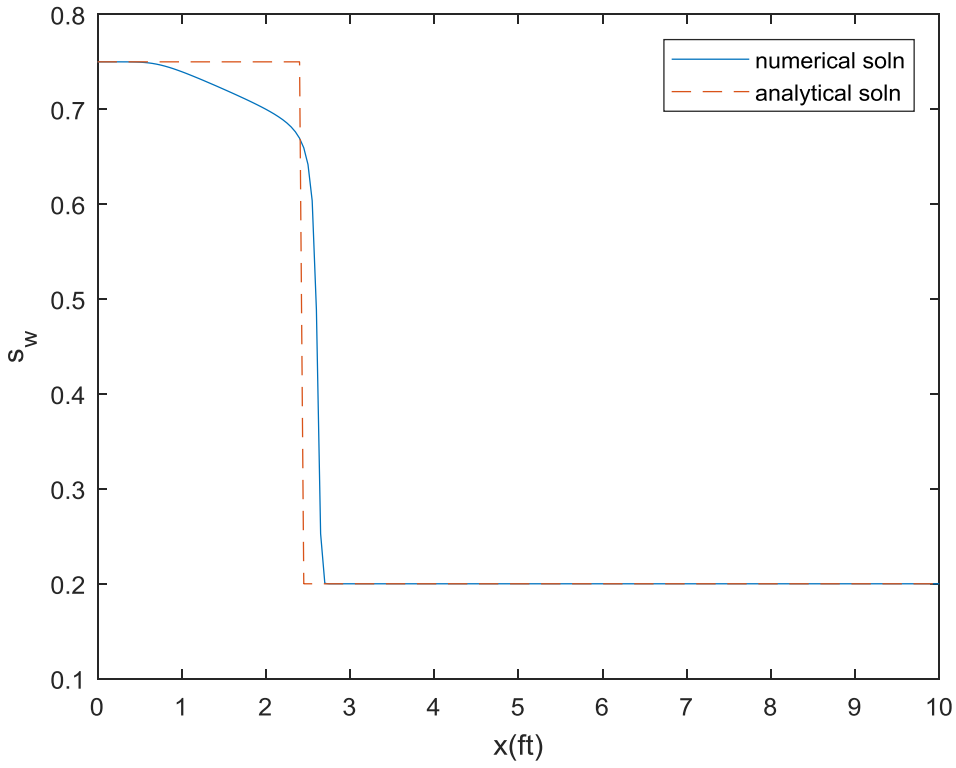

(b) For cell-centered FVM at $S_w = 0.75$

Figure 4.15(a-b): Saturation profiles during the Fixed-Point Iteration

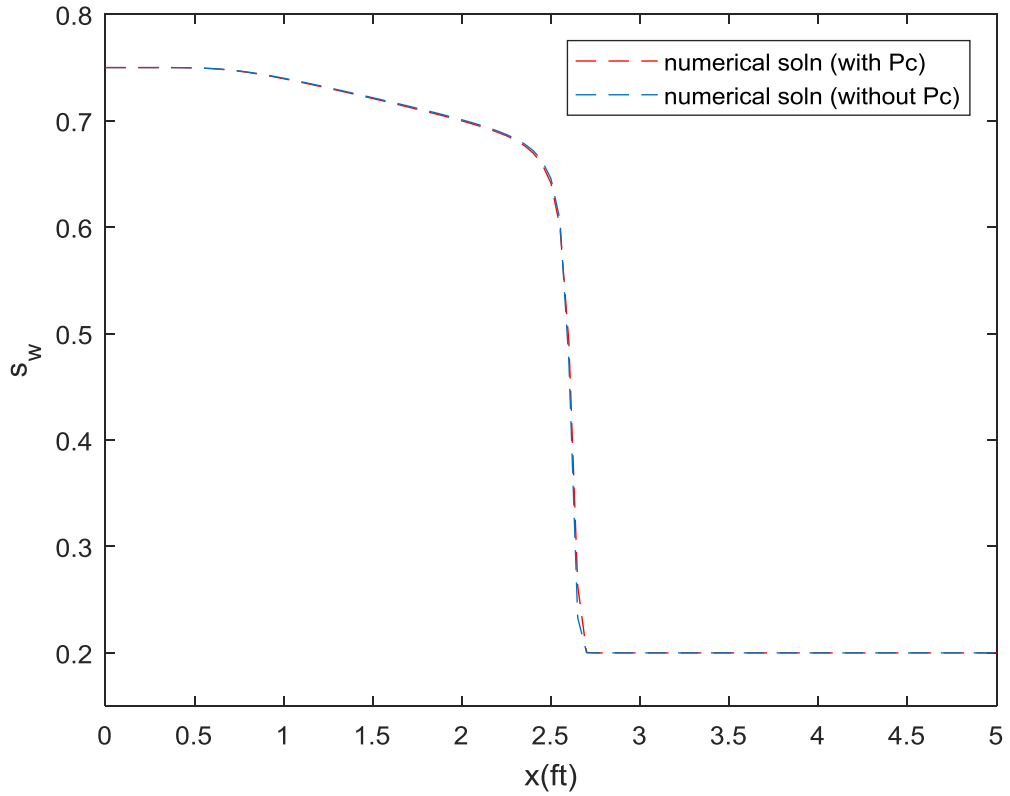

Figure 4.16: Comparison of saturation profiles with and without capillary pressure.

After this, the fixed-point iteration is used to check stability by following the implicit formulation and computing the number of iterations (average and maximum) at each solution. In Figure 4.15a, the average number of fixed point iterations is 48 per time-step, while the maximum number is 52 per time-step, assuming there are no capillary pressure gradients. In contrast, including the capillary gradients through the cell-centred finite volume scheme, the solution iterates more than with the local Lax-Friedrichs scheme. The maximum number of fixed point iterations is 58 per time-step, and the average number is 49 per time-step (Figure 4.15b). During this implicit calculation, the analytical and numerical solutions are matched, and there is no deviation, like in the base case study of this research. The numerical solution provides the exact shock position for every solution. Finally, we compare both numerical solutions by considering and neglecting capillary forces, shown in Figure 4.16. The shock front is a little bit ahead when considering the capillary term than the shock front without capillary effects. Numerically, the difference between the shock fronts is $0.025\ ft$, which is remarkably small. This may happen due to the lower oil flowrate per day, or lower viscosity ratio or the lower capillary force. However, the capillary force still affects the solution during the waterflooding mechanism, and the effects are soluble through the proposed numerical schemes. This solution ensures that the proposed mathematical scheme in this research is stable for field

cases and will absorb the capillary effects during the waterflooding mechanism. Finally, the capture of capillary effects will help to improve the estimation of oil recovery calculation and core floods experimentation.

4.6.1. Impact of Oil Production

In this study, the calculation of oil production gives an idea about changing the injected water saturation and the effects of capillary pressure on oil production. All simulations are run for 10 days, and the results are summarised in Figure 4.17(a-b). At injected water saturation (S_{wl}) of 40%, the oil is produced at a steady rate from the beginning of the injection, and the amount is approximately $550\ STB\ per\ day$ at zero capillary forces (Figure 4.17a). When the injected water saturation increases to 70%, there is a small spike created at the first timestep, and after that, the oil is produced on a steady rate in the amount of $420\ STB\ per\ day$ approximately (Figure 4.17b). This oscillation may happen due to the rapid change in water saturation, which is explained earlier in Eq. [47]. The same things happen when we consider capillary forces in the numerical calculation, shown in Figure 4.17(a-b). Here, the oscillation is a little bit larger, but the oil production is at a steady rate after the first day onwards. We compare the results and observe the effect of capillary forces on oil production (Figure 4.17). The production decreases

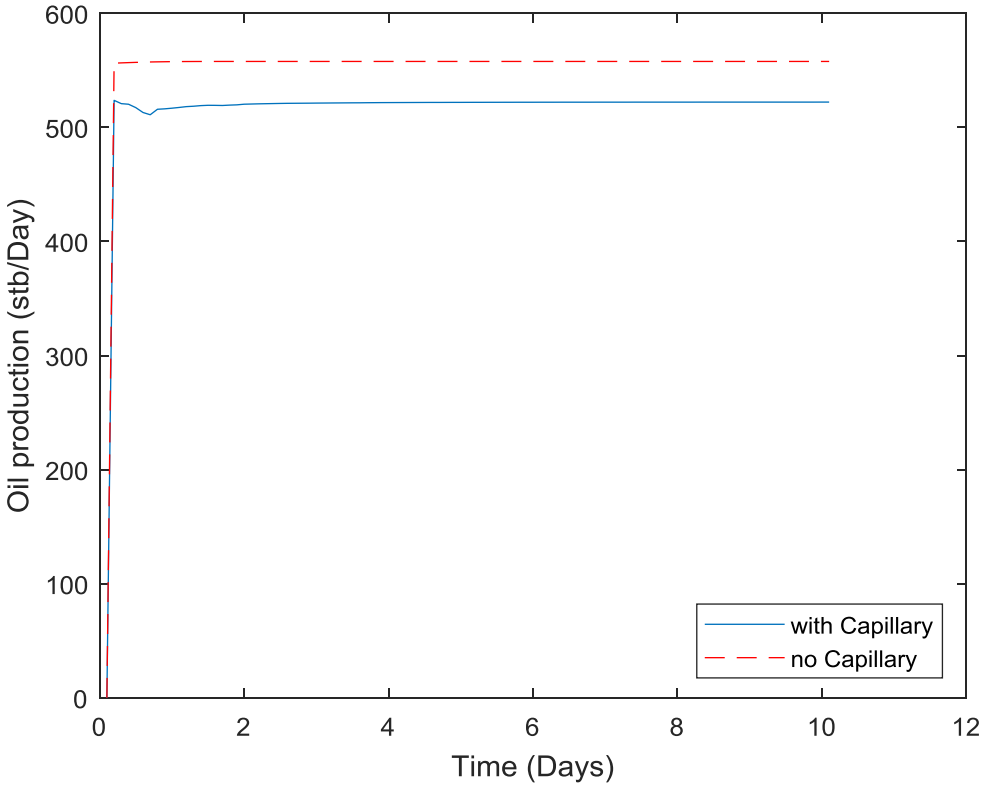

(a) For $S_{wl} = 0.40$

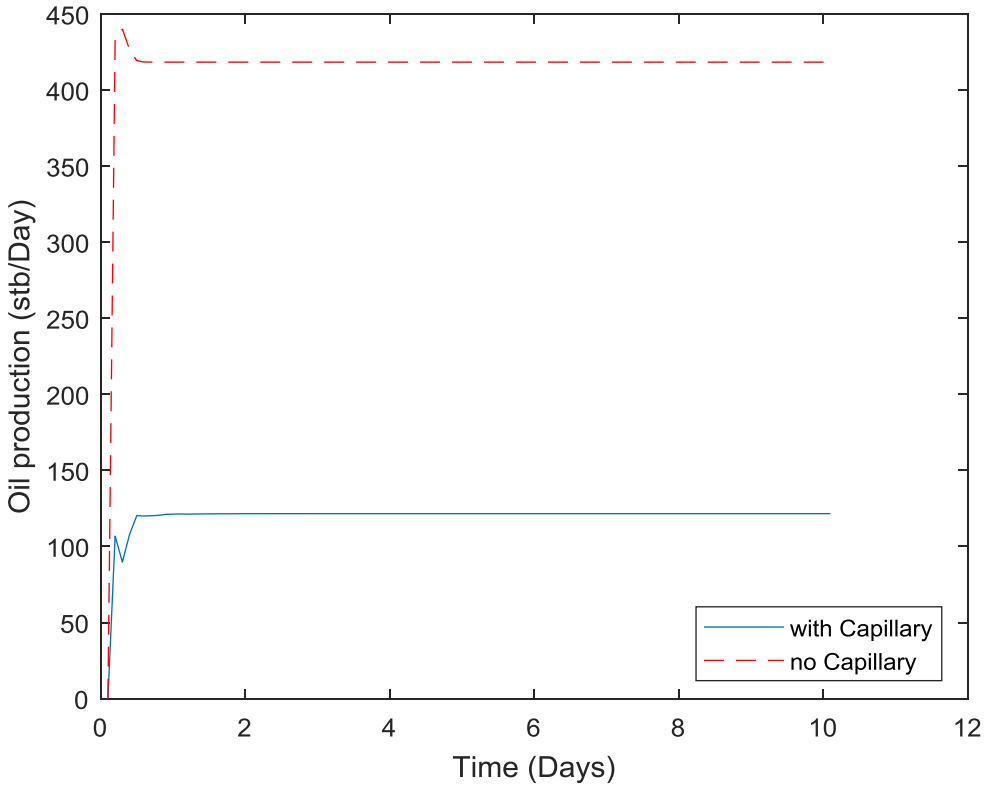

(b) For $S_{wl} = 0.70$

Figure 4.17(a-b): Comparison of oil production (with and without capillary)

due to the influence of capillary forces and the difference in oil production is highly observable when the water saturation front is 70% (Fig.17-b), more so than when the water saturation front is 40% (Fig.17-a).

4.6.2. Effect of the Viscosity Ratio and Permeability

The saturation profiles are influenced by the ratio of water (μ_w) to oil viscosity (μ_o). The solution has a shock front behaviour when the viscosity ratio is greater than one. In contrast, the saturation profiles are smoother for the frontal advancement when the viscosity ratio is lower than one (Yortsos and Fokas, 1983). We considered this in our study, and the results are illustrated in Figure 4.18(a-c). Figure 4.18a represents the base study $(\mu_o = 2cp;\ \mu_w = 1cp)$ where the shock position is approximately 2.70 ft. If we consider heavy oil $(\mu_o = 10cp)$, the saturation profiles move forward, and the shock position is approximately 3.50 ft (Figure 4.18b). In contrast, if we consider light oil $(\mu_o = 0.1cp)$, the shock position is approximately 2.0 ft due to saturation front movement, shown in Figure 4.18c. Moreover, for all cases, the numerical solution considering capillary pressure is a little bit ahead of the solution without capillary pressure. Similarly, changing the permeability, the solution with capillary pressure

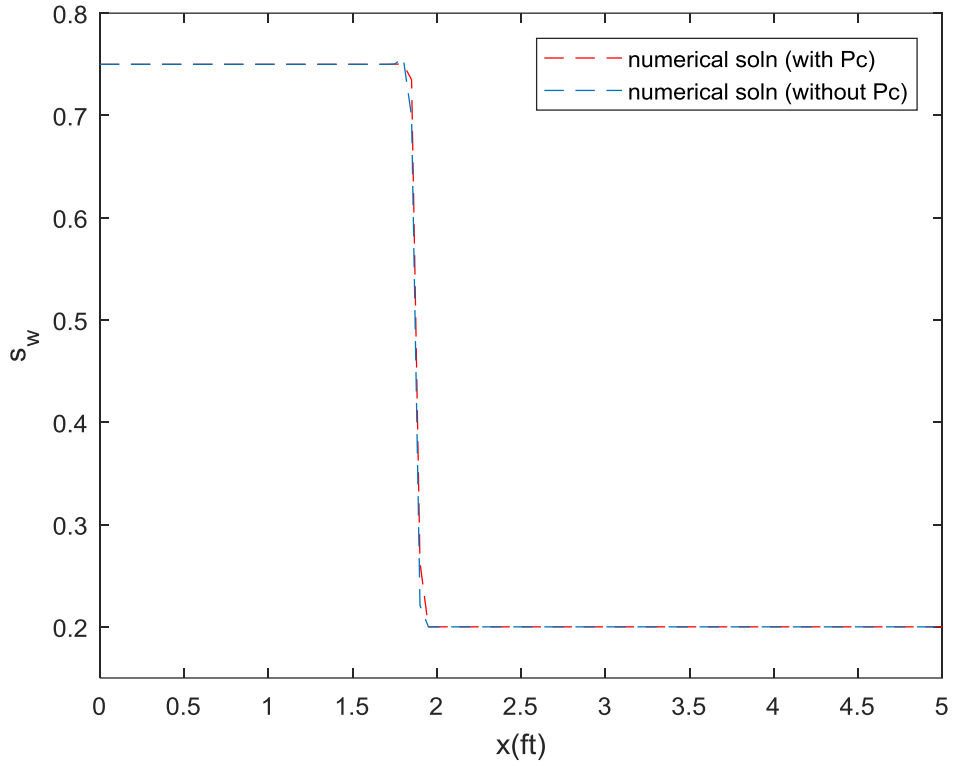

(a) At $\mu_o = 0.1cp \; and \; \mu_w = 1cp$

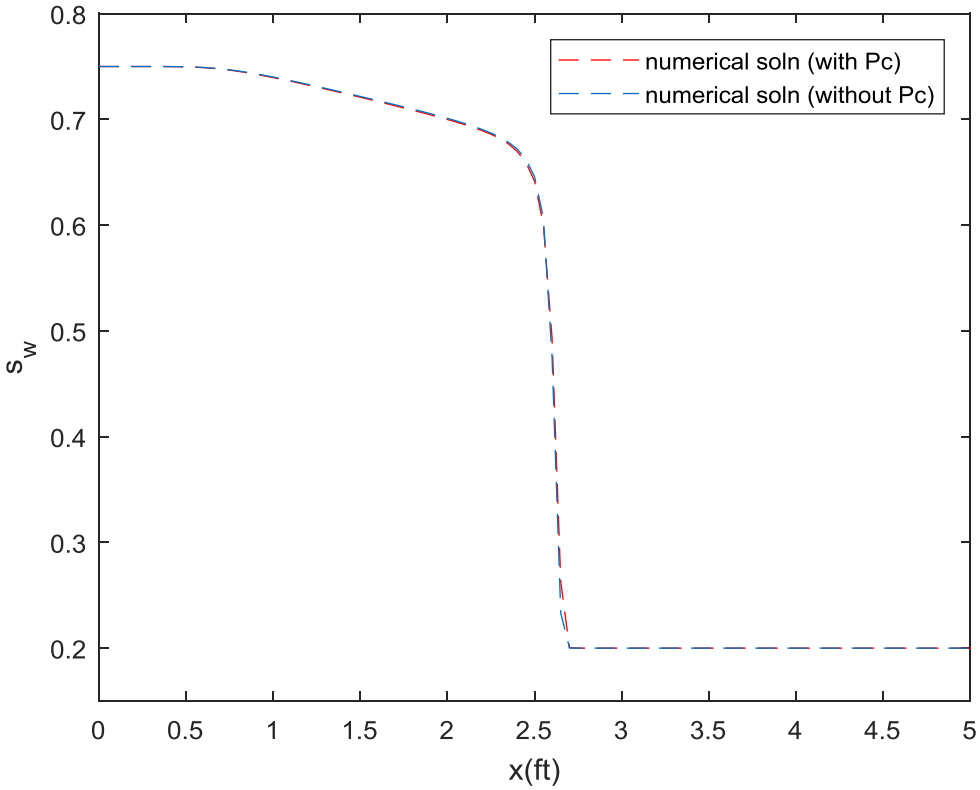

(b) At $\mu_o = 2cp \; and \; \mu_w = 1cp$

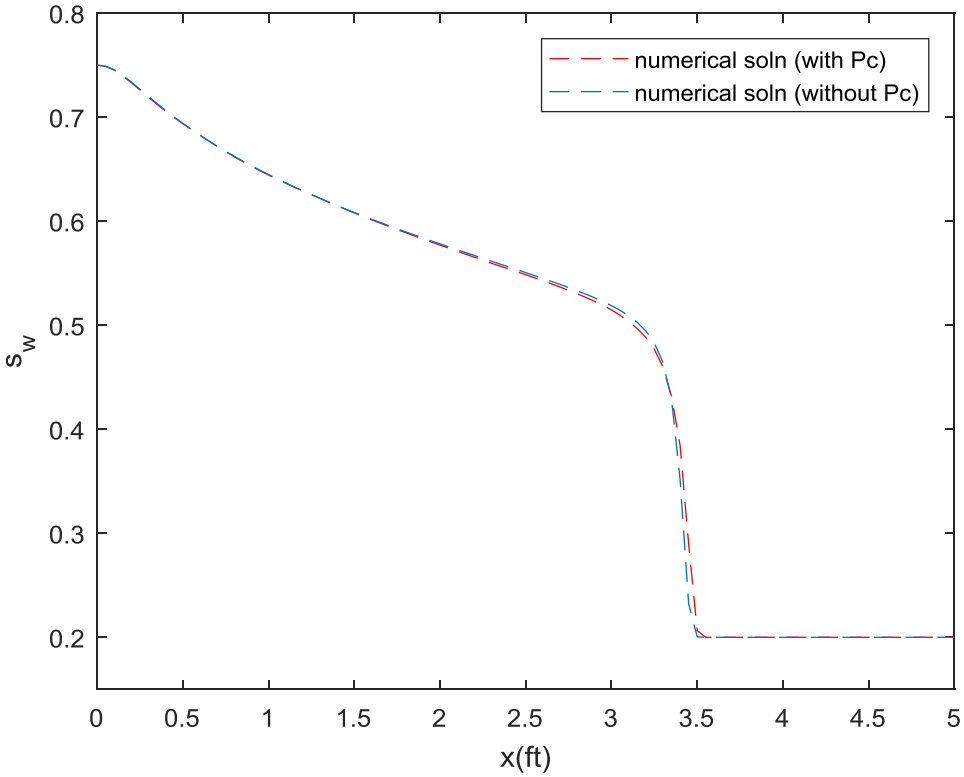

(c) At $\mu_o = 10cp \; and \; \mu_w = 1cp$

Figure 4.18(a-c): Effect on saturation profiles when changing the viscosity ratio.

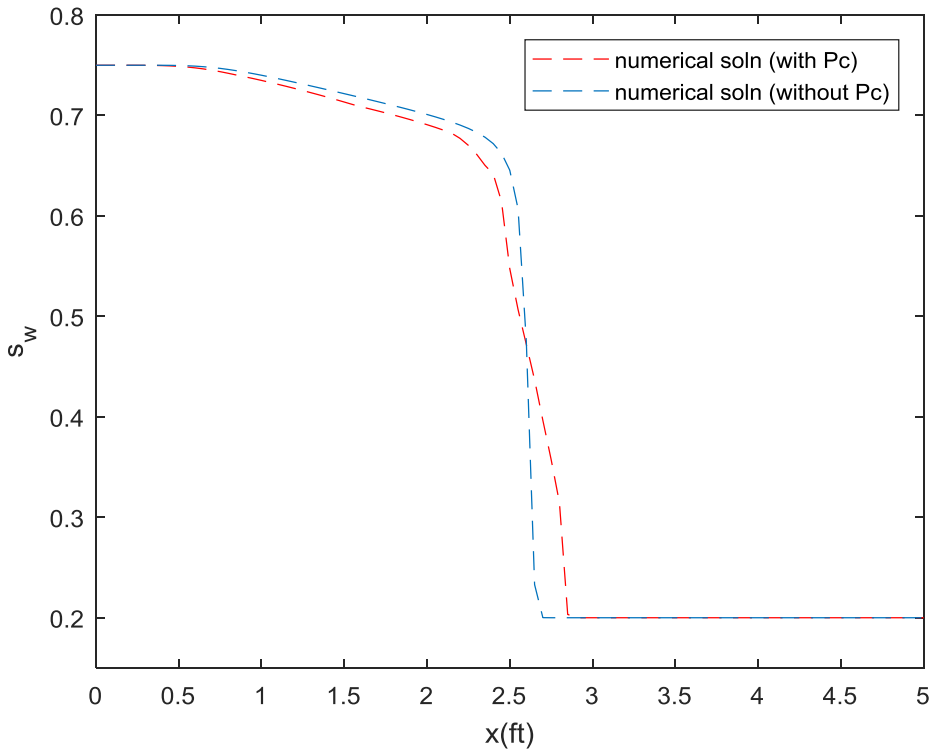

Figure 4.19: Effect on saturation profiles when changing the permeability.

significantly changes in comparison to the solution without capillary pressure. The numerical solution with capillary pressure is moved ahead with time when the reservoir formation is highly permeable ($K = 100mD$), shown in Figure 4.19. With higher permeability, the oil flows more smoothly through the production well.

4.7. CONCLUSION

Water flooding is relatively cheap, especially for offshore fields because of the ready availability of seawater, although care has to be taken to ensure that the injected water does not result in unwanted, adverse reactions in the reservoir. To increase petroleum recovery, engineers should increase the microscopic displacement efficiency by reducing capillary effects.

In this research, we develop a nonlinear solver to find single-valued solutions for the immiscible oil displacement application. The cell-centred finite volume scheme is used to capture the capillary effects in the Buckley-Leverett equation. The saturation profiles are generated following a shock wave mechanism. Smooth frontal advancement of saturation profiles indicates that there is little capillary pressure as well as diffusion forces in effect in the displacement process. Later, the fixed-point iteration scheme is applied to check the stability of the proposed finite volume schemes. However, these simulations are checked using lab scale data and might be wrong. In addition, we run another case study based on standard field data to validate the proposed numerical schemes and found that there are small capillary effects on saturation frontal advancement based on their shock position difference. The shock front with capillary effects is advanced in comparison to the shock front without capillary effects.

Since the saturation wave propagates from the injecting well to the producing well, the solution should be consistent for different time-steps. The choice of proper time-steps and capillary pressure gradients will help to minimise the possibility of shock wave oscillation during saturation profile movement. This might happen due to an explicit formulation or the limitations of rock and fluid properties data. Moreover, this research provides an idea that how the oil production is affected by the presence of capillary effects. Further, we changed the other parameters (i.e., viscosity, permeability) in the numerical calculation and captured their behaviours through several plots. Nevertheless, we have tried to present detailed solution steps for the Buckley-Leverett equation including capillary term, and these solution procedures will help future researchers to find precisely the capillary effects on saturation profiles for oil

reservoirs. The present research finds consistent solution techniques for lab-scale simulation models, and future researchers can develop it for field scale simulations by simulating with more experimental results.

ACKNOWLEDGEMENT

The authors would like to thank the Natural Sciences and Engineering Research Council of Canada (NSERC); Research & Development Corporation of Newfoundland and Labrador (RDC), funding no. 210992; and Statoil Canada Ltd., funding no. 211162 for providing financial support to accomplish this research under the Statoil Chair in Reservoir Engineering at the Memorial University of Newfoundland, St. John's, NL, Canada.

DECLARATIONS OF INTEREST

All authors have seen and approved the final version of the manuscript being submitted. We warrant that the article is original work, has not received prior publication and is not under consideration for publication elsewhere. Finally, the authors have no conflict of interest.

REFERENCES

Al-Mutairi, S.M., Abu-khamsin, S.A., and Hossain, M.E., (2012, January), A Novel approach to handle continuous wettability alteration during immiscible CO_2 flooding process. In Abu Dhabi International Petroleum Conference and Exhibition. Society of Petroleum Engineers.

Buckley S.E., and Leverett M.C., (1942), Mechanism of Fluid Displacement in Sands, Trans. AIME, 146:187–196.

Chang, S.S., Cho, Y.J., Lee, B.S., Jung, J.S., and Kang, S.M., (1998), Iterative approximations of fixed points and solutions for strongly accretive and strongly pseudo-contractive mappings in Banach spaces. Journal of Mathematical Analysis and Applications, 224(1), 149-165.

Deb, P.K., Akter, F., Imtiaz, S.A., and Hossain, M.E., (2017), Nonlinearity and solution techniques in reservoir simulation: A review. Journal of Natural Gas Science and Engineering, 46, 845-864.

Goumiri, I. R., Prévost, J. H., & Preisig, M. (2012). The effect of capillary pressure on the saturation equation of two-phase flow in porous media. International Journal for Numerical and Analytical Methods in Geomechanics, 36(3), 352-361.

Helvig, O.S., (2013), Models for water flooding, imbibition and coupled fracture-matrix flow in a fractured reservoir (Master's thesis, University of Stavanger, Norway).

Islam M.R., Hossain M.E., Mousavizadeghan H., Mustafiz S., and Abou-kassem J.H., (2016), Advanced Reservoir Simulation: Towards Developing Reservoir Emulators, Scrivener-Wiley, 2nd Ed., 592 pp.

Leverett, M. (1941), Capillary behavior in porous solids. Transactions of the AIME, 142(01), 152-169.

Muggeridge, A., Cockin, A., Webb, K., Frampton, H., Collins, I., Moulds, T., and Salino, P., (2014), Recovery rates, enhanced oil recovery and technological limits. Phil. Trans. R. Soc. A, 372(2006), 20120320.

Yortsos, Y.C., and Fokas, A.S., (1983), An analytical solution for linear waterflood including the effects of capillary pressure. Society of Petroleum Engineers Journal, 23(01), 115-124.

CHAPTER – 5

CONCLUSION

5.1 Conclusion

This thesis focuses on mathematical techniques for solving nonlinear governing equations in petroleum engineering. Especially in reservoir engineering, the Buckley-Leverett equation is solved for a one-dimensional (1-D) immiscible displacement process, where the capillary pressure gradient term is included. Finding a stable and efficient scheme which can solve the model equation consider any parameters is a great challenge in this research area.

The goal of this study is to develop a computational scheme which provides a realistic physical solution by generating sharp displacement fronts and accurately includes diffusion processes due to capillary pressure. In this research, the author applied the method of characteristics (MOC) and the local Lax-Friedrichs scheme to solve the Buckley-Leverett equation assuming there is no capillary pressure gradient and zero gravitational force for the 1-D immiscible process. Here, the MOC is used to define the Buckley-Leverett equation analytically, whether it is hyperbolic or not, and the solution is discontinuous or not. The flux function is considered for solution of the model equation and exhibits the shock wave characteristics and shock position owing to water saturation. The curves generated from the MOC are known as the characteristic curves for the Buckley-Leverett equation and the saturation front is moved forward with a definite speed. Also, conservation laws help the computational method to generate correct physical solutions where discontinuities are present, and the solution is converged. If this condition is not satisfied by numerical methods, diffusion will generate due to the capillary pressure gradient and make the saturation front smear.

By following the finite-volume approach to conservation laws, water saturation values are advected from an injecting well and moved to the outlet side, while the outflow boundary condition is fixed at a producing well. This fixed boundary condition was used to save time and avoid complexity during the calculation. An explicit form discretisation was followed to make the calculation easier. The solution found from the analytical and numerical analysis are similar and consistent. All calculations are graphically presented using MATLAB programming.

After this, the author applied the cell-centered finite volume technique along with the local Lax-Friedrichs scheme to capture capillary pressure effects on the Buckley-Leverett equation.

Here, the responses of shock waves are similar to previous calculations and exhibited that our proposed technique is well-fitted for that governing equation. There is a position difference between the shock waves that are calculated using both numerical schemes. Most likely, this difference comes from the effects of capillary forces. Capillary effects are most visible during the calculation of cumulative oil production and when changing the permeability of the reservoir formation. Later, the author followed the fixed-point iteration scheme. Though this method is conventional, of results in more stable solution for larger time steps. The solution is also consistent and valid for any mesh sizes and capillary pressure gradients. Finally, the author ran a standard case study to check the consistency of the proposed numerical solution and found that these schemes are best fitted for the Buckley-Leverett equation during water flooding techniques.

In comparison with previous research like Mustafiz et al. (2008), our proposed numerical scheme is better-fitted for the Buckley-Leverett equation (including and excluding capillary pressure) and provides a good solution, matched with the analytical solution. Concerning stability and consistency, the present proposed scheme is better-fitted for the Buckley-Leverett equation.

5.2 Future Directions

The Buckley-Leverett equation is one of the key models for petroleum recovery through waterflooding. Due to the presence of nonlinear parameters, the application of that model equation is limited. Solving the nonlinear complexities is one of the major challenges for reservoir engineers, and this research has addressed this issue by treating real scenarios of petroleum fields. The finite volume methods are used for solving the nonlinear PDE's and the detailed solution steps are presented in this study. We get an accurate solution by simple formulation and flux calculation using each neighbouring domain. Due to limited data sources and stability criterion issues, the present study is conducted using explicit and implicit scheme. This research considered small time steps but provides a stable solution in all cases, which saves computational time.

Future researchers can implement these schemes in an implicit form where large time steps would be considered and validate the solution with real field and experimental data for different reservoirs. Changing the initial and boundary conditions would be another scope of the research. The estimation of oil recovery, analysing the core floods experiment and the

determination of average water saturation percentage from the breakthrough time behaviour and the fractional water flowrate curve would be another milestone for future researchers. They can also compare the present numerical solutions with different ECLIPSE and PETREL model solutions and employ them for industrial purposes.

Appendix – A

The flux function $\left(f_n(S_w)\right)$ in the Buckley-Leverett equation is defined as

$$f_n(S_w) = \frac{q}{A\phi}\left(\frac{1}{1+M}\right) \tag{A-1}$$

Differentiating Eq. [A-1] with respect to water saturation (S_w) gives

$$\frac{\partial f_n(S_w)}{\partial S_w} = -\frac{q}{A\phi}\frac{1}{\left(1+M(S_w)\right)^2}\frac{\partial M(S_w)}{\partial S_w} \tag{A-2}$$

The mobility ratio $\left(M(S_w)\right)$ is defined by

$$M(S_w) = \frac{k_{ro}(S_w)\mu_w}{k_{rw}(S_w)\mu_o} \tag{A-3}$$

Differentiating Eq. [A-3], we get

$$\frac{\partial M(S_w)}{\partial S_w} = \frac{\mu_w}{\mu_o}\left(\frac{k_{rw}(S_w)\frac{\partial k_{ro}(S_w)}{\partial S_w} - k_{ro}(S_w)\frac{\partial k_{rw}(S_w)}{\partial S_w}}{\left(k_{rw}(S_w)\right)^2}\right) \tag{A-4}$$

The variation of relative permeability to water as a function of water saturation can be written in the following form

$$k_{rw}(S_w) = a_1 S_{wn}^4(S_w) \tag{A-5}$$

Differentiating Eq. [A-5],

$$\frac{\partial k_{rw}(S_w)}{\partial S_w} = 4a_1 S_{wn}^3(S_w)\frac{\partial S_{wn}}{\partial S_w} \tag{A-6}$$

Again, the variation of relative permeability to oil as a function of water saturation is defined as

$$k_{ro}(S_w) = a_2\left(1 - S_{wn}(S_w)\right)^2 \tag{A-7}$$

Differentiating Eq. [A-7],

$$\frac{\partial k_{ro}(S_w)}{\partial S_w} = -2a_2\left(1 - S_{wn}(S_w)\right)\frac{\partial S_{wn}}{\partial S_w} \tag{A-8}$$

To calculate the relative permeability, the normalized water saturation defined as –

$$S_{wn}(S_w) = \frac{S_w - S_{wi}}{1 - S_{wi} - S_{or}} \tag{A-9}$$

Differentiating Eq. [A-9] gives

$$\frac{\partial S_{wn}}{\partial S_w} = \frac{1}{1 - S_{wi} - S_{or}} \tag{A-10}$$

Substituting Eqs. [A-6], [A-8], and [A-10] into Eq. [A-4], we obtained

$$\frac{\partial M(S_w)}{\partial S_w} = \frac{\mu_w}{\mu_o}\left(\frac{a_1 S_{wn}^4(S_w)\left(-2a_2\left(1 - S_{wn}(S_w)\right)\right) - a_2\left(1 - S_{wn}(S_w)\right)^2 4a_1 S_{wn}^3(S_w)}{a_1^2 S_{wn}^8(S_w)}\right)\frac{1}{1 - S_{wi} - S_{or}}$$

$$\Rightarrow \frac{\partial M(S_w)}{\partial S_w} = \frac{\mu_w}{\mu_o}\left(\frac{S_{wn}(S_w)\left(-2a_2\left(1 - S_{wn}(S_w)\right)\right) - 4a_2\left(1 - S_{wn}(S_w)\right)^2}{a_1 S_{wn}^5(S_w)}\right)\frac{1}{1 - S_{wi} - S_{or}}$$

$$\Rightarrow \frac{\partial M(S_w)}{\partial S_w} = \frac{\mu_w}{\mu_o}\left(\frac{\left(-2a_2\left(S_{wn}(S_w) - S_{wn}^2(S_w)\right)\right) - 4a_2\left(1 - 2S_{wn}(S_w) + S_{wn}^2(S_w)\right)}{a_1 S_{wn}^5(S_w)}\right)\frac{1}{1 - S_{wi} - S_{or}}$$

$$\Rightarrow \frac{\partial M(S_w)}{\partial S_w} = \frac{\mu_w}{\mu_o}\frac{a_2}{a_1}\left(\frac{-4 + 6S_{wn}(S_w) - 2S_{wn}^2(S_w)}{S_{wn}^5(S_w)}\right)\frac{1}{1 - S_{wi} - S_{or}} \tag{A-11}$$

Incorporating Eq. [A-11] into Eq. [A-2] gives

$$\frac{\partial f_n(S_w)}{\partial S_w} = -\frac{q}{A\phi}\frac{1}{\left(1 + M(S_w)\right)^2}\frac{\partial M(S_w)}{\partial S_w}$$

$$\frac{\partial f_n(S_w)}{\partial S_w} = \frac{q}{A\phi}\frac{1}{\left(1 + M(S_w)\right)^2}\left(\frac{\mu_w}{\mu_o}\frac{a_2}{a_1}\right)\left(\frac{4 - 6S_{wn}(S_w) + 2S_{wn}^2(S_w)}{S_{wn}^5(S_w)}\right)\frac{1}{1 - S_{wi} - S_{or}} \tag{A-12}$$

Again,

$$\frac{1}{\left(1 + M(S_w)\right)^2} = \frac{1}{\left(1 + \frac{\mu_w a_2}{\mu_o a_1}\frac{\left(1 - S_{wn}(S_w)\right)^2}{S_{wn}^4(S_w)}\right)^2} = \frac{S_{wn}^8(S_w)}{\left(S_{wn}^4(S_w) + \frac{\mu_w a_2}{\mu_o a_1}\left(1 - S_{wn}(S_w)\right)^2\right)^2} \tag{A-13}$$

Finally substituting Eq. [A-13] into Eq. [A-12], we obtain

$$\frac{\partial f_n(S_w)}{\partial S_w} = \frac{q}{A\phi}\left(\frac{\mu_w}{\mu_o}\frac{a_2}{a_1}\right)\frac{S_{wn}^8(S_w)}{\left(S_{wn}^4(S_w) + \frac{\mu_w a_2}{\mu_o a_1}\left(1 - S_{wn}(S_w)\right)^2\right)^2}\left(\frac{4 - 6S_{wn}(S_w) + 2S_{wn}^2(S_w)}{S_{wn}^5(S_w)}\right)\frac{1}{1 - S_{wi} - S_{or}}$$

$$\Rightarrow \frac{\partial f_n(S_w)}{\partial S_w} = \frac{q}{A\phi}\left(\frac{\mu_w}{\mu_o}\frac{a_2}{a_1}\right)\frac{S_{wn}^3(S_w)}{\left(S_{wn}^4(S_w)+\frac{\mu_w a_2}{\mu_o a_1}\left(1-S_{wn}(S_w)\right)^2\right)^2}\left(\frac{4-6S_{wn}(S_w)+2S_{wn}^2(S_w)}{1-S_{wi}-S_{or}}\right) \quad \text{(A-14)}$$

Substituting $\frac{\partial f_n(S_w)}{\partial S_w} = \lambda(S_w)$, we obtain

$$\lambda(S_w) = \frac{q}{A\phi}\left(\frac{\mu_w}{\mu_o}\frac{a_2}{a_1}\right)\frac{S_{wn}^3(S_w)}{\left(S_{wn}^4(S_w)+\frac{\mu_w a_2}{\mu_o a_1}\left(1-S_{wn}(S_w)\right)^2\right)^2}\left(\frac{4-6S_{wn}(S_w)+2S_{wn}^2(S_w)}{1-S_{wi}-S_{or}}\right) \quad \text{(A-15)}$$

Appendix – B

The flux function $\left(f_n(S_w)\right)$ in the Buckley-Leverett equation is defined as

$$f_n(S_w) = \frac{q}{A\phi}\left(\frac{1}{1+M}\right) \tag{B-1}$$

Differentiating Eq. [B-1] with respect to water saturation (S_w) gives

$$\frac{\partial f_n(S_w)}{\partial S_w} = -\frac{q}{A\phi}\frac{1}{\left(1+M(S_w)\right)^2}\frac{\partial M(S_w)}{\partial S_w} \tag{B-2}$$

The mobility ratio $\left(M(S_w)\right)$ is defined by

$$M(S_w) = \frac{k_{ro}(S_w)\mu_w}{k_{rw}(S_w)\mu_o} \tag{B-3}$$

Differentiating Eq. [B-3], we get

$$\frac{\partial M(S_w)}{\partial S_w} = \frac{\mu_w}{\mu_o}\left(\frac{k_{rw}(S_w)\frac{\partial k_{ro}(S_w)}{\partial S_w} - k_{ro}(S_w)\frac{\partial k_{rw}(S_w)}{\partial S_w}}{\left(k_{rw}(S_w)\right)^2}\right) \tag{B-4}$$

The variation of relative permeability to water as a function of water saturation can be written in the following form

$$k_{rw}(S_w) = a_1 S_{wn}^2(S_w) \tag{B-5}$$

Differentiating Eq. [B-5],

$$\frac{\partial k_{rw}(S_w)}{\partial S_w} = 2a_1 S_{wn}(S_w)\frac{\partial S_{wn}}{\partial S_w} \tag{B-6}$$

Again, the variation of relative permeability to oil as a function of water saturation is defined as

$$k_{ro}(S_w) = a_2\left(1 - S_{wn}(S_w)\right)^2 \tag{B-7}$$

Differentiating Eq. [B-7],

$$\frac{\partial k_{ro}(S_w)}{\partial S_w} = -2a_2\left(1 - S_{wn}(S_w)\right)\frac{\partial S_{wn}}{\partial S_w} \tag{B-8}$$

To calculate the relative permeability, the normalized water saturation defined as –

$$S_{wn}(S_w) = \frac{S_w - S_{wi}}{1 - S_{wi} - S_{or}} \tag{B-9}$$

Differentiating Eq. [B-9] gives

$$\frac{\partial S_{wn}}{\partial S_w} = \frac{1}{1 - S_{wi} - S_{or}} \tag{B-10}$$

Substituting Eqs. [B-6], [B-8], and [B-10] into Eq. [B-4], we obtained

$$\frac{\partial M(S_w)}{\partial S_w} = \frac{\mu_w}{\mu_o}\left(\frac{a_1 S_{wn}^2(S_w)\left(-2a_2\left(1 - S_{wn}(S_w)\right)\right) - a_2\left(1 - S_{wn}(S_w)\right)^2 2a_1 S_{wn}(S_w)}{a_1^2 S_{wn}^4(S_w)}\right)\frac{1}{1 - S_{wi} - S_{or}}$$

$$\Rightarrow \frac{\partial M(S_w)}{\partial S_w} = \frac{\mu_w}{\mu_o}\left(\frac{S_{wn}(S_w)\left(-2a_2\left(1 - S_{wn}(S_w)\right)\right) - 2a_2\left(1 - S_{wn}(S_w)\right)^2}{a_1 S_{wn}^3(S_w)}\right)\frac{1}{1 - S_{wi} - S_{or}}$$

$$\Rightarrow \frac{\partial M(S_w)}{\partial S_w} = \frac{\mu_w}{\mu_o}\left(\frac{\left(-2a_2\left(S_{wn}(S_w) - S_{wn}^2(S_w)\right)\right) - 2a_2\left(1 - 2S_{wn}(S_w) + S_{wn}^2(S_w)\right)}{a_1 S_{wn}^3(S_w)}\right)\frac{1}{1 - S_{wi} - S_{or}}$$

$$\Rightarrow \frac{\partial M(S_w)}{\partial S_w} = \frac{\mu_w}{\mu_o}\frac{a_2}{a_1}\left(\frac{2S_{wn}(S_w) - 2}{S_{wn}^3(S_w)}\right)\frac{1}{1 - S_{wi} - S_{or}} \tag{B-11}$$

Incorporating Eq. [B-11] into Eq. [B-2] gives

$$\frac{\partial f_n(S_w)}{\partial S_w} = -\frac{q}{A\phi}\frac{1}{\left(1 + M(S_w)\right)^2}\frac{\partial M(S_w)}{\partial S_w}$$

$$\frac{\partial f_n(S_w)}{\partial S_w} = \frac{q}{A\phi}\frac{1}{\left(1 + M(S_w)\right)^2}\left(\frac{\mu_w}{\mu_o}\frac{a_2}{a_1}\right)\left(\frac{2 - 2S_{wn}(S_w)}{S_{wn}^3(S_w)}\right)\frac{1}{1 - S_{wi} - S_{or}} \tag{B-12}$$

Again,

$$\frac{1}{\left(1 + M(S_w)\right)^2} = \frac{1}{\left(1 + \frac{\mu_w a_2}{\mu_o a_1}\frac{\left(1 - S_{wn}(S_w)\right)^2}{S_{wn}^2(S_w)}\right)^2} = \frac{S_{wn}^4(S_w)}{\left(S_{wn}^2(S_w) + \frac{\mu_w a_2}{\mu_o a_1}\left(1 - S_{wn}(S_w)\right)^2\right)^2} \tag{B-13}$$

Finally substituting Eq. [B-13] into Eq. [B-12], we obtain

$$\frac{\partial f_n(S_w)}{\partial S_w} = \frac{q}{A\phi}\left(\frac{\mu_w}{\mu_o}\frac{a_2}{a_1}\right)\frac{S_{wn}^4(S_w)}{\left(S_{wn}^2(S_w) + \frac{\mu_w a_2}{\mu_o a_1}\left(1 - S_{wn}(S_w)\right)^2\right)^2}\left(\frac{2 - 2S_{wn}(S_w)}{S_{wn}^3(S_w)}\right)\frac{1}{1 - S_{wi} - S_{or}}$$

$$\Rightarrow \frac{\partial f_n(S_w)}{\partial S_w} = \frac{q}{A\phi}\left(\frac{\mu_w}{\mu_o}\frac{a_2}{a_1}\right)\frac{S_{wn}(S_w)}{\left(S_{wn}^4(S_w)+\frac{\mu_w a_2}{\mu_o a_1}\left(1-S_{wn}(S_w)\right)^2\right)^2}\left(\frac{2-2S_{wn}(S_w)}{1-S_{wi}-S_{or}}\right) \quad \text{(B-14)}$$

Substituting $\frac{\partial f_n(S_w)}{\partial S_w} = \lambda(S_w)$, we obtain

$$\lambda(S_w) = \frac{q}{A\phi}\left(\frac{\mu_w}{\mu_o}\frac{a_2}{a_1}\right)\frac{S_{wn}(S_w)}{\left(S_{wn}^2(S_w)+\frac{\mu_w a_2}{\mu_o a_1}\left(1-S_{wn}(S_w)\right)^2\right)^2}\left(\frac{2-2S_{wn}(S_w)}{1-S_{wi}-S_{or}}\right) \quad \text{(B-15)}$$